(NASA-CR-158540) EVALUATION AND ANALYSIS OF SEASAT-A SCANNING MULTICHANNEL MICROWAVE RADIOMETER (SMMR) ANTENNA PATTERN CORRECTION (APC) ALGORITH. SUB-TASK 2: T SUB B MEASURED (Environmental Sensing Algorithm HC A07/MF A01 G3/32 N79-24213 Unclas 25162

EVALUATION AND ANALYSIS OF SEASAT-A SCANNING MULTICHANNEL MICROWAVE RADIOMETER (SMMR) ANTENNA PATTERN CORRECTION (APC) ALGORITHM

FINAL REPORT FOR SUB-TASK 2: T_B MEASURED VS. T_B CALCULATED COMPARISON RESULTS

Prepared under JPL contract number 955368 by:

J. L. Kitzis
S. N. Kitzis

Environmental Sensing Algorithm Development Company

8238 Fenwick Street
Sunland, California 91040

April 13, 1979

This work was performed for the Jet Propulsion Laboratory, California Institute of Technology sponsored by the National Aeronautics and Space Administration under Contract NAS7-100.

This report contains information prepared by Environmental Sensing Algorithm Development Company under JPL sub-contract. Its content is not necessarily endorsed by the Jet Propulsion Laboratory, California Institute of Technology, or the National Aeronautics and Space Administration.

ABSTRACT

This report documents the second part of a three-part study whose overall objective is an initial assessment of the accuracy of the SEASAT-A SMMR Antenna Pattern Correction (APC) algorithm. Interim APC brightness temperature measurements for all ten SMMR channels are compared with calculated values generated from surface truth data. Plots and associated statistics are presented for the available points of coincidence between SMMR and surface truth measurements acquired for the Gulf of Alaska SEASAT Experiment (GOASEX). The most important conclusions of the study deal with the apparent existence of different instrument biases for each SMMR channel, and their variation across the scan (i.e., cross-track gradients).

CONTENTS

CONTENTS (Continued)

FIGURE

CONTENTS (Continued)

FIGURE

TABLE

1.0 SUMMARY

This report documents the second part of a three-part study whose overall objective is an initial assessment of the accuracy of the SMMR Antenna Pattern Correction (APC) Algorithm. Interim APC brightness temperature measurements for all ten SMMR channels are compared to model-calculated values. The assumptions used in generating the calculated brightness temperatures include (1) a standard atmospheric profile, (2) a constant integrated water vapor content, and (3) cloud-free conditions. The surface truth data used in this study includes buoy, ship, and radiosonde measurements originally acquired for the Gulf of Alaska SEASAT Experiment (GOASEX). Plots and associated statistics are presented for the available points of coincidence between SMMR and surface truth measurements.

The two most important conclusions of the study are:

(1) There appear to exist significantly different instrument biases for the ten channels of SMMR data output by the interim APC algorithm.

(2) Sizable opposing cross-track gradients are evident in the vertical and horizontal brightness temperatures output by the interim APC for the 6.6, 18, and 21 GHz channels.

2.0 INTRODUCTION

2.1 Problem Statement. The SEASAT-A Scanning Multichannel Microwave Radiometer (SMMR) is designed to make measurements of thermal microwave emission from the Earth for the primary purpose of determining sea surface temperatures, wind speed, and atmospheric water vapor and liquid water parameters. The antenna temperatures measured by the SMMR contain known antenna pattern effects which must be removed before these measurements can be used to derive geophysical parameters. The Antenna Pattern Correction (APC) Algorithm has been designed by E. G. Njoku and coded by R. E. Cofield to remove these effects. In brief summary, the APC algorithm accepts as input SMMR antenna temperature (T_A) measurements and produces corrected brightness temperatures (T_B) as its output. These output brightness temperatures are then used as inputs to the geophysical parameter algorithms. The problem to be addressed here is the evaluation of the accuracy of the APC brightness temperature outputs.

Specifically, this report documents the second part of a three-part study whose overall objective is an initial assessment of the accuracy of the APC algorithm. As the SMMR algorithms mature, and as a larger data set becomes available, it is expected that further studies will refine the results presented here. The three parts of this initial assessment are:

A. <u>6.6 GHz T_B vs. $T_{surface\ truth}$ Comparison</u>

T_B measurements for the SMMR 6.6 GHz channels are compared to surface truth derived sea surface temperatures. The two 6.6 GHz channels are used because they are most sensitive to sea surface temperature (SST) but least sensitive to atmospheric effects. SST measurements are more numerous and more accurate than other types of surface truth measurements. Thus, the comparison of 6.6 GHz T_B with SST under clear atmospheric conditions provides a large, high-quality data set from which to assess the accuracy of the APC algorithm.

B. <u>T_B Measured vs. T_B Calculated Comparison</u>

T_B measurements for all ten SMMR channels are compared with T_B values calculated from geophysical models using surface truth data. Although this task is restricted to a smaller surface truth data set than task A, it assesses the accuracy of all ten SMMR channels rather than only two of them. In addition, this task is less dependent on using clear atmospheric conditions since the models take atmospheric variations into account.

C. <u>T_A vs. T_B Comparison</u>

T_A measurements for all ten SMMR channels are compared with the corresponding T_B outputs. This comparison allows a determination of whether the APC algorithm adequately removes those instrument effects known to be present in the T_A data.

The results obtained for Task A are given in reference 1. The results obtained for Task B are the subject of this document.

2.2 <u>Brief Description of the APC Algorithm</u>. At this time, the APC algorithm has not yet reached its final form. Section 2.2.1 describes the full set of capabilities to be implemented in the final APC algorithm. Section 2.2.2 outlines the subset presently implemented in the interim version of the APC. The results of this study are based only on output obtained from the interim APC. It is expected that a later study will perform a similar evaluation of the final APC.

2.2.1 <u>Final APC Description</u>. The input T_A data to the APC algorithm consists of measurements of microwave emission at ten different channels. Each channel is characterized by one of five frequencies (6.6, 10.69, 18, 21, and 37 GHz) and one of two polarizations (vertical and horizontal). The T_A measurements are sampled at regular time intervals along the SMMR scan, which results however in an irregular spacing of points on the Earth's surface. The APC algorithm outputs T_B data in the form of square arrays of data cells which are uniformly distributed within the SMMR swath. There are four different array sizes which are

referred to as Grids 1, 2, 3, and 4. The ten channels are output on the four grids as shown in Table 1.

The final APC algorithm performs the following operations:

(1) Read SMMR T_A data.

(2) Average T_A data into grid cells.

(3) Correct T_A cells for Faraday rotation.

(4) Correct T_A cells for non-nominal incidence angles.

(5) Correct T_A cells for cross-polarization antenna pattern effects.

(6) Correct T_A cells for polarization rotation effects due to scan motion.

(7) Correct T_A cells for sidelobe contributions from within the SMMR swath, from outside the SMMR swath but on the Earth's surface, and from space.

(8) Output SMMR T_B data and associated quality flags.

2.2.2 Interim APC Description. The interim version of the APC algorithm performs the following subset of the final APC operations:

(1) Read SMMR T_A data.

(2) Average T_A data into grid cells.

(3) Correct T_A cells for cross-polarization antenna pattern effects.

(4) Correct T_A cells for polarization rotation effects due to scan motion.

(5) Correct T_A cells for sidelobe contributions from space.

(6) Output SMMR T_B data.

Note that the interim APC does not include corrections for Faraday rotation, incidence angles, or Earth sidelobe contributions, nor does it calculate data quality flags.

2.3 General Evaluation Approach. In attempting to compare brightness temperatures measured by the SMMR with those calculated from surface truth, we are constrained by the following items:

(1) Since the final APC algorithm is not yet available, the interim APC must be used as the source of measured T_B data.

(2) The immediately available spacecraft data set is limited primarily to that compiled for the Gulf of Alaska SEASAT Experiment (GOASEX), covering the month of September, 1978. Twelve SMMR passes extending from equatorial latitudes through the Gulf of Alaska have been obtained in addition to the original fifteen passes assembled for the first GOASEX workshop.

(3) The usable surface truth data set for the GOASEX region includes measurements made by six NOAA data buoys (46001-46006), the research vessel Oceanographer, and Canadian vessels located at Ocean Station P (PAPA). For the available spacecraft data set, there are only 38 times at which the SMMR swath crosses the location of an operating buoy or ship.

(4) Currently available radiosonde data is limited to that compiled for the first GOASEX workshop. This data set includes only four sets of radiosonde measurements coincident with a SMMR overflight.

(5) It is unlikely that many other points of coincidence between spacecraft data and surface truth data can be acquired within the time span of the present study.

In accordance with the above constraints, the following approach to the problem has evolved over the course of this study:

(1) Due to complexities encountered in manually matching spacecraft and surface truth data, this matching process has been automated with the development of computer software.

(2) Since the available surface wind speed measurements are made at varying heights above sea level and during periods of different atmospheric stability, these measurements have been converted to equivalent wind speeds at a standard reference height of 19.5 meters in a neutral atmosphere. This conversion is accomplished with the use of a program originally developed by I. Halberstam for the first GOASEX workshop.

(3) Calculated brightness temperature values are produced by the use of a program supplied by R. Hofer. The model T_B's are calculated using surface truth derived measurements of sea surface temperature and wind speed, and assuming a standard atmosphere, a constant integrated water vapor content, and cloud-free conditions.

(4) The currently available radiosonde data has been used to determine an appropriate value of integrated water vapor content for calculating model brightness temperatures. Unfortunately, this GOASEX radiosonde data cannot be entered directly into the atmospheric model program since it is not available at all of the pressure levels required by the model.

(5) Software has been developed to produce computer-generated plots of SMMR T_B values versus calculated T_B values and associated statistical information.

(6) In an effort to reduce data scatter attributable to unmodeled variations in atmospheric water vapor content, the observed 21 V brightness temperature values have been used to sort the SMMR T_B data into several water vapor ranges. Separate plots and statistics have been produced for each band of water vapor values.

(7) Software has been developed to produce plots of the T_B cross-track gradients versus latitude in an effort to identify any effects which may vary across the SMMR swath.

3.0 TECHNICAL DISCUSSION

3.1 Reference Models

3.1.1 Calculation of Model Brightness Temperatures. Radiative transfer and the physics of the ocean surface and atmosphere allow T_B to be modeled as a function of various physical parameters. These include sea surface temperature, surface air temperature, surface wind speed, and atmospheric profiles of temperature, pressure, and water content. The particular program employed to generate calculated T_B's for this study is one supplied by R. Hofer.

This program is able to use radiosonde data as well as several "canned" atmospheric profiles in determining the effects of the atmosphere on microwave radiation corresponding to each SMMR channel. When radiosonde data is used, the program requires this data to be available at specific pressure levels and over a large vertical height range. Unfortunately, the GOASEX radiosonde data does not meet these criteria, and therefore, it has been necessary to employ one of the "canned" atmospheric profiles. However, the GOASEX radiosonde humidity profiles have been useful in determining an appropriate integrated water vapor value for use in the model.

The assumptions used in generating calculated T_B values include (1) a global average standard atmosphere, (2) a constant integrated water vapor content (WVC), and (3) cloud-free conditions. These assumptions allow the establishment of reference T_B values against which the actual SMMR measurements may be compared.

A WVC value of 1.0 gram/cm^2 is chosen as a reasonable lower limit to those WVC values actually encountered in the GOASEX region. The integrated radiosonde humidity data indicate that the WVC values actually range between 1.0 and 2.2 g/cm^2 (see Section 3.4.1.2). Brightness temperature values for all ten SMMR channels increase with increasing water vapor content. The frequencies in order of

increasing sensitivity to WVC are 6.6, 10.69, 18, 37, and 21 GHz, and for each frequency the horizontal polarization is more sensitive than the vertical (see Section 3.4.1.3). Therefore, it is expected that measured T_B values will scatter upwards from the calculated reference values due to unmodeled variations in WVC, with the more sensitive SMMR channels showing more scatter than the less sensitive channels.

The assumption of cloud-free conditions is made since no information is available on the actual cloud conditions present at the time of each measurement. Many of the measured T_B values are undoubtedly affected to some degree by clouds. The effect of this unmodeled liquid water is similar to that produced by increased water vapor in that the different SMMR channels will scatter upwards according to their respective sensitivies.

Since unmodeled water vapor and liquid water both increase the measured T_B values, the chosen model should produce calculated T_B values which act as a lower bound for the SMMR data. Under low water vapor, cloud-free conditions, the difference between measured and calculated T_B values should be due primarily to instrument-induced effects. However, these instrument effects are increasingly masked as the environmental conditions deviate from those assumed in the model.

3.1.2 Wind Speed Adjustments. The surface truth wind speed measurements needed to calculate model brightness temperatures are made by ships and buoys with varying anemometer heights and during periods of different atmospheric stabilities. In order to derive a uniform standard of measurement, it is necessary to convert these wind speeds to a standard height and atmospheric stability. During this study, these corrections have been applied with the use of a program supplied by I. Halberstam.

This program was originally developed by Halberstam for use during the first GOASEX workshop (pp. 3-20 to 3-23 of reference 2). It employs a surface layer model which relates winds at various heights and stability conditions to equivalent wind speeds at 19.5 meters in a neutrally stratified atmosphere. Reference 2 gives three alternate equations which relate the surface roughness parameter, z_0, to the frictional wind velocity, u*. Since the Pierson equation (number 3) was used for the first GOASEX workshop, we have decided to also use this equation so as to be compatible with the workshop results. As noted in reference 2, the differences between the three equations are not significant. In addition, the wind speed corrections applied during this study (with only one exception) were always less than one meter/second.

3.2 Data Selection. The major difficulty which plagues an evaluation of this type is that of acquiring spacecraft and surface truth data sets which are matched in location and time. The desirability of cloud-free conditions further compounds this problem. During the first part

of this three-part study (Ref. 1), a search was conducted for clear atmospheric conditions using images produced by the Geostationary Orbiting Environmental Satellites (GOES). As a result, twelve passes of SMMR data through the Gulf of Alaska have been obtained and utilized in this portion of the study as well as the original fifteen passes assembled for the first GOASEX workshop. Unfortunately, out of this combined spacecraft data set, the SMMR swath intersects the location of an operating buoy or ship only 38 times.

3.2.1 Spacecraft Data Set. Only twelve of the original fifteen GOASEX passes contain data useful to a SMMR evaluation study. The remaining three are either over land or contain numerous data gaps. The twelve newly acquired passes cross not only through the Gulf of Alaska but also extend into equatorial latitudes. The equatorial data generally exhibit better atmospheric conditions than that of the GOASEX region. Twenty-two of the buoy and ship "hits" occur for the original twelve GOASEX passes. The twelve new passes have added sixteen additional "hits" and also have provided better weather conditions for investigating possible cross-track gradients in the measured T_B data. Table 2.1 contains an inventory of the SMMR T_B data available for this study.

3.2.2 Surface Truth Data Set. This study makes use of surface truth data in the form of spot reports. The thirty-eight hits compiled for the study consist of twenty-eight measurements made by six NOAA data buoys (46001-46006), nine measurements made by the Oceanographer, and one made by PAPA. The three NOAA buoys 46007, 46008, and 46009 are not used since they lie so close to the Alaskan coastline that corresponding SMMR data would be corrupted by land within the field of view. Although there exist five spot reports from merchant ships which coincide with SMMR overflights, these are not used since the anemometer heights are unknown and sea surface temperature measurements were not always reported. Table 2.2 contains an inventory of the 38 surface truth hits used within this study. Table 2.3 gives the reported accuracies for each type of measurement.

The radiosonde data available within the time span of the study consists of eight sets of PAPA measurements and eight sets of Oceanographer measurements. However, only four of the Oceanographer measurements coincide with SMMR overflights. This radiosonde data was prepared specifically for the first GOASEX workshop and does not contain measurements at all the pressure levels available from fully reduced data. Therefore, it is not suitable as input to the atmospheric model used for this study (Section 3.1.1).

3.3 Software Development. Various pieces of software have been developed in the course of this study. Several of the programs work together as a software system in which the output of one program becomes the input to the next. This section presents a brief description of the development process and the outputs produced by each program.

Several basic principles have been followed during the development of the software:

(1) Existing code should be used whenever possible. Specific examples include Halberstam's wind adjustment model (Section 3.1.2), Hofer's geophysical models (Section 3.1.1), and various plotting and statistical subroutines from JPL libraries.

(2) The software system should consist of independent modules so as to facilitate design, coding, and check-out procedures. Since each module may be executed independently of the others, data can be re-processed through a chosen subset of modules without necessarily accessing the entire system.

(3) All output files should be written in a text editable format. This facilitates the partitioning and/or merging of files as desired.

(4) Each item in an output file should be labeled with an unique identifier. This facilitates the editing of files whose contents must correspond with each other.

A brief description of each subprogram within the software system follows.

3.3.1 <u>Reading IGDR Files</u>. The output T_B data from the APC algorithm are written onto what is called a SMMR IGDR basic sensor file. The data on this file is in a packed format compatible with the JPL IBM 360/75 machine and must be converted into a format compatible with the JPL UNIVAC 1108 computer used for this study. This conversion was accomplished using a set of subroutines developed by W. D. McFaddin and modified by J. Kitzis. The reformatted data for all grids has been written to tape for later use. This procedure is more efficient than reformatting the data each time it is re-processed.

3.3.2 <u>Locating Spacecraft/Surface Truth Data Coincidences</u>. Given a set of surface truth measurements made by buoys or ships, the task of searching the T_B grids for SMMR measurements which most closely coincide with this surface truth data is a laborious procedure. In order to facilitate this process and reduce the chances of human error, a computer program has been developed which identifies the T_B measurements corresponding to a series of surface truth measurements. For each surface truth measurement, the program accepts as input the latitude and longitude of the measurement, and the time tag of the corresponding SMMR basic sensor record to be searched. Once the correct record has been found (based on its time tag), a search is performed on latitude and longitude grids 1, 2, 3, and 4 to determine which T_B grid locations lie closest to the location of the surface truth measurement. Grid 1 locations are searched for the 6.6 GHz channels, grid 2 for the 10.69 GHz channels, grid 3 for the 18 and 21 GHz channels, and grid 4 for the 37 GHz channels.

The equation used to calculate the distance between the location of the two measurements is given below:

$$D = \cos^{-1}\left[\sin \phi_1 \sin \phi_2 + \cos \phi_1 \cos \phi_2 \cos (\lambda_1 - \lambda_2)\right]*111$$

where

D = distance in kilometers between the location of the surface truth measurement and that of the T_B measurement.

ϕ_1 = latitude of the T_B measurement

λ_1 = longitude of the T_B measurement

ϕ_2 = latitude of the surface truth measurement

λ_2 = longitude of the surface truth measurement

111 = arc length (km) on the surface of the Earth subtended by an angle of one degree at the Earth's center.

Once the minimum distance D has been found for each grid, the program outputs the desired brightness temperature values, the cell numbers in which these occur, and the approximate time at which the SMMR passed over the surface truth site. In addition to printed output, the program produces a file of SMMR measured T_B values and cell numbers which is read by the plotting and statistics program to be discussed in Section 3.3.5. This software has greatly reduced the problem of matching surface truth and T_B measurements.

3.3.3 Surface Truth Data Interpolation. The NOAA buoys stationed in the Gulf of Alaska make measurements of sea surface temperature, wind speed, and air temperature at regular time intervals, usually every hour. Rarely does the time of one of these measurements coincide exactly with the time of a SMMR overflight. A small program has been developed to perform a linear interpolation on the buoy measurements made before and after the time of the SMMR overflight. This interpolation produces slightly more accurate surface truth values for use in generating calculated brightness temperatures. In addition to printed output, this program also produces a file of interpolated surface truth measurements which is read by the geophysical model program to be discussed next in Section 3.3.4.

3.3.4 Wind Height Adjustment and Calculation of Model Brightness Temperatures. The primary purpose of this study is to compare SMMR measured T_B values with corresponding model calculated values. The program which produces calculated T_B values incorporates the models supplied by I. Halberstam and R. Hofer which have been previously discussed in Section 3.1. This program reads the file of surface truth data produced by the interpolation program described above in Section 3.3.3. The surface truth wind speed measurements are adjusted for anemometer height and atmospheric stability by a subroutine created from Halberstam's program. These

adjusted surface truth measurements, along with parameters defining an atmospheric model, are then used in a second subroutine created from Hofer's program to calculate model brightness temperatures. In addition to printed output, this program produces a file of model T_B values which is read by the plotting and statistics program to be discussed next in Section 3.3.5.

3.3.5 <u>T_B Measured vs. T_B Calculated Plots and Statistics.</u> The primary software analysis tool developed for this study produces plots of measured brightness temperatures versus corresponding calculated brightness temperatures for all ten SMMR channels, as well as associated statistics. Printed statistics and 15 plots are produced each time the program is executed. Examples of all these outputs may be found in Table 7 and Figures 7.1 through 7.15.

In the first plot produced, as shown in Figure 7.1, each vertical T_B measured-T_B calculated pair is plotted as a single Arabic numeral (1, 2, 3, 4, or 5). Each numeral indicates the frequency of the measurement as shown below.

Plotted Numeral	Frequency
1	6.6
2	10.69
3	18.0
4	21.0
5	37.0

This plot also contains two curves. The curve marked with the letter "V" represents the first-order polynomial which fits all the V data points best in a least squares sense. The unmarked curve is simply the line of unit slope through the origin along which all the points would lie if there were perfect agreement between the measured and calculated T_B values.

The second plot produced (Figure 7.2) contains information similar to that of the first plot, but for horizontal rather than vertical data. Note that the curve fitted to the H data points is marked with the letter "H".

The third plot (Figure 7.3) repeats the curve fitted to the V data, the curve fitted to the H data, and the line of unit slope through the origin. In addition, it displays a curve representing the first-order polynomial which fits all the data points best in a least squares sense. This curve is marked with the letter "A". Note that the individual data points are not displayed in this plot.

The next two plots (Figures 7.4 and 7.5) display curve fits for each channel of V data and H data respectively. The curve for each of the five frequencies is labeled with an Arabic numeral from 1 to 5

as before; the curves for all V data and all H data are respectively labeled with "V" or "H". The unmarked curve is the line of unit slope through the origin.

The remaining ten plots (Figures 7.6 through 7.15) display the T_B measured-T_B calculated pairs for each of the ten SMMR channels. Each pair is plotted as a single alphanumeric character indicating the grid cell from which the measured T_B value is drawn. The correspondence between plotted characters and cell numbers is shown below.

Grid	Cell Number	Plotted Character
1	1-4	1-4
2	1-7	1-7
3	1-9	1-9
	10-11	A-B
4	1-9	1-9
	10-22	A-M

Each of these ten plots also contains two curves. The curve marked with plus ("+") signs represents the curve fit for all data of the given channel, and the unmarked curve is once again the line of unit slope through the origin.

These last twelve plots were generated in hopes of gaining more insight into the behavior of the SMMR data on a channel-by-channel basis. Unfortunately, there were too few surface truth hits available to make these plots particularly meaningful. Although they are included here for completeness, they will not be discussed further in this report.

The printed statistical output (Table 7) is divided into two sections. The upper section contains the two polynomial coefficients and the root-mean-square (RMS) statistic for the least squares fitted curves for (1) each of the ten channels taken individually, (2) all V channels taken together, (3) all H channels taken together, and (4) all ten channels taken together. The RMS statistic is calculated according to:

$$\mathrm{RMS} = \sqrt{\frac{\sum_{i=1}^{N} \left(T_{B_i} - p\left(\text{Calculated } T_{B_i}\right)\right)^2}{N}}$$

where

$$T_{B_i} = i^{th} \text{ measured } T_B \text{ value}$$

$$\text{Calculated } T_{B_i} = i^{th} \text{ calculated } T_B \text{ value}$$

$$p\left(\text{Calculated } T_{B_i}\right) = \text{fitted polynomial evaluated for the } i^{th} \text{ calculated } T_B \text{ value}$$

$$N = \text{total number of data points}$$

The lower section of the printout contains a bias and an RMS statistic around a biased line of unit slope for the thirteen data groups represented by (1) each of the ten individual channels, (2) all the vertically polarized data, (3) all the horizontally polarized data, and (4) all the data taken as a whole. This bias is calculated according to:

$$\text{Bias} = \frac{\sum_{i=1}^{N}\left(T_{B_i} - \text{Calculated } T_{B_i}\right)}{N}$$

where T_{B_i}, Calculated T_{B_i}, and N are as defined above.

The corresponding RMS statistic is calculated according to:

$$\text{RMS} = \sqrt{\frac{\sum_{i=1}^{N}\left(T_{B_i} - \text{Bias} - \text{Calculated } T_{B_i}\right)^2}{N}}$$

where T_{B_i}, Calculated T_{B_i}, and N are as defined above, and the bias is as defined above for the appropriate data group.

3.3.6 Cross-Track Gradients vs. Latitude. A secondary software analysis tool developed as a supplement to the primary study produces a plot (see Figures 15.1 through 15.5) of the T_B gradient across the SMMR swath versus latitude for each SMMR channel, and also associated statistics (Tables 15.1 through 15.5). A first-order polynomial is fitted in a least squares sense to each row of T_B values in the grid appropriate for each frequency. (Grid 1 is used for 6.6 GHz, grid 2 for 10.69 GHz, grid 3 for 18 and 21 GHz, and grid 4 for 37 GHz.) The slope of the fitted line for each row (expressed as degrees per cell) is plotted against the average latitude for the row. The character "V" is plotted for V data, and the character "H" for H data.

The printed statistical output includes the average latitude, the two polynomial coefficients, and the RMS statistic for each row of T_B data for both polarizations of each frequency.

The RMS is calculated according to:

$$\text{RMS} = \sqrt{\frac{\sum_{i=1}^{N} \left(T_{B_i} - p(i)\right)^2}{N}}$$

where

T_{B_i} = i^{th} measured T_B value in a grid row

N = number of cells in the grid row

$p(i)$ = fitted polynomial evaluated for cell number i

Note that the calculated slopes for each SMMR channel must be scaled to take into account the fact that the different T_B grids contain different numbers of cells per row. For instance, a cross-track gradient of one degree per cell would represent a total variation across the swath of 4 degrees for the 6.6 GHz channels, 7 degrees for the 10.69 GHz channels, 11 degrees for the 18 and 21 GHz channels, and 22 degrees for the 37 GHz channels.

3.3.7 Calculation of Integrated Water Vapor Content from Radiosonde Humidity Data. A small program has been developed in the course of this study to produce an integrated water vapor content from radiosonde relative humidity measurements. The total water vapor content is calculated by use of a crude Riemann sum:

$$\text{IWC} = \sum_{i=2}^{N} (z_i - z_{i-1}) \left[\frac{h_i S(t_i) + h_{i-1} S(t_{i-1})}{2}\right]$$

where

IWC = integrated water vapor content

z_i = height at which the i^{th} measurement was made

t_i = air temperature at the i^{th} height level

$S(t_i)$ = maximum amount of water that can be held by air at temperature t_i

h_i = relative humidity at the i^{th} height level expressed as a percentage of $S(t_i)$.

The subroutine needed to calculate the function S for each temperature t_i was supplied by R. Hofer. We felt that a more sophisticated integration technique was not warranted by the quality of the available radiosonde data.

3.4 Discussion of Results. Most of the results of this study are drawn from computer-generated plots and statistics produced by the software described in the previous sections. A summary of the computer runs made for the study may be found in Table 3. Runs 1 through 8 are executions of the measured versus calculated T_B software package. These are designated as Type A runs in Table 3, and were made for the purpose of identifying possible instrument-induced biases in the SMMR data. Runs 9 through 12 are executions of the T_B cross-track gradient program, and are designated as Type B runs in Table 3. These runs were made for the purpose of gaining further insight into the cross-track gradients discovered for the 6.6 GHz channels during the first part of this study (Reference 1). The output from each run consists of one or more tables of statistics and several plots, each of which is labeled with the appropriate run number. The table and figure numbers corresponding to the output from each run are indicated in Table 3.

The following sections contain discussions of the results of all these runs as well as discussions of radiosonde-derived integrated water vapor content and the expected variation in brightness temperatures due to atmospheric water.

3.4.1 Instrument Bias Estimation

3.4.1.1 Approach. The numbers contained in the final column of Table 4.3 represent our best estimates of the instrument-induced biases in the T_B data for each SMMR channel. The general approach used in obtaining these estimates is outlined below:

(1) Partition the 38 available "hits" into several groups or bands based on the 21 V T_B value observed for each "hit."

(2) Execute the measured versus calculated T_B software for each band separately. This produces observed T_B biases corresponding to each band.

(3) Estimate a mean value of integrated WVC for each band of "hits."

(4) Calculate predicted environmental biases for each band based on the above WVC values.

(5) Calculate an instrument bias for each channel by subtracting the predicted environmental biases from the corresponding observed biases.

The subsequent paragraphs explain the rationale behind this approach in greater detail.

3.4.1.2 <u>Radiosonde-Derived Integrated Water Vapor Contents</u>. The attempt to accurately estimate instrument-induced biases in the SMMR data is severely constrained by the lack of an accurate estimate of total atmospheric water content present at the time of each SMMR measurement. Total atmospheric water content is a combination of water vapor, and liquid water in the form of rain and/or clouds.

Currently available radiosonde data provides an estimate of atmospheric water content for only 4 of the 38 data points assembled. No measurements are available for the remaining 34 points. This deficiency is critical since the radiosonde data does show that water content is a parameter which varies significantly from point to point, and therefore must be accurately modeled.

The program described in Section 3.3.7 has been used to calculate WVC values for each of the 20 available radiosonde measurement sets. These 20 WVC values are displayed in Table 5. These 20 values are representative of the weather conditions encountered during the GOASEX period, although only four of them (as shown in Table 5) actually coincide with SMMR overflights. Note that the WVC values range from .93 to 2.2 g/cm^2.

This degree of variation, if unmodeled, would result in a corresponding variation in calculated T_B's ranging from .5°K for the least sensitive channel (6.6 V) to 28°K for the most sensitive (21 H). Since radiosonde measurements are not available to model the variation in WVC for all 38 "hits," the total data set has been partitioned into five bands. Each band encompasses a smaller range of WVC than the total data set, thus reducing the data scatter due to water content variability.

3.4.1.3 <u>Model T_B Variation with Integrated Water Vapor Content</u>. Table 6 contains model-calculated T_B's for all 10 SMMR channels corresponding to WVC values ranging from .5 to 2.4 g/cm^2. These T_B's are calculated assuming a constant sea surface temperature of 15°C, wind speeds below 7 meters/sec, and cloud-free conditions. Several observations are made regarding Table 6:

(1) For each frequency, the H channel is more sensitive to WVC variations than the V channel.

(2) The frequencies in order of increasing sensitivity are 6.6, 10.69, 18, 37, and 21 GHz.

(3) For any given channel, the increase in T_B corresponding to a .1 g/cm^2 increase in WVC is almost constant, indicating a nearly linear relationship over the range of WVC included in Table 6.

(4) For the more sensitive channels, the increase in T_B corresponding to a .1 g/cm^2 increase in WVC diminishes slightly with increasing WVC.

Thus, it is possible to use a mean 21 V value to estimate a WVC value for each band.

3.4.1.4 Calculation of Instrument Biases. Our initial attempts to compare measured and calculated brightness temperatures (runs 6 and 7) do not adequately account for the variation in atmospheric water content. The model-calculated T_B values corresponding to all 38 "hits" are produced using a single constant value for integrated WVC. Because of the resulting data scatter (Figures 12.1, 12.2, 13.1 and 13.2), we have decided to use the 21 V measured T_B values as an indicator of the atmospheric water present at the time of each measurement. This decision is based on two observations: (1) the two 21 GHz channels are the most sensitive to variations in atmospheric water, and (2) the lowest observed 21 V values consistently fall closer to the model-predicted values (using WVC = 1.0 g/cm^2) than do the lowest 21 H values. Thus, the 21 V channel appears to be the more reliable indicator of atmospheric water content.

Using the 21 V T_B values as a filter, the 38 "hits" are partitioned into five bands as follows:

Band No.	21 V Range (K)
1	180-185
2	185-190
3	190-195
4	195-200
5	>200

The measured versus calculated T_B software has been executed for each band separately (runs 1-5). The data scatter observed in each of these runs is significantly less than that observed in the initial runs (runs 6 and 7) which combine all 38 hits together. Table 4.1 contains the observed biases for each of these 7 runs. The individual plots and statistics for these runs may be found in Tables and Figures 7 through 13.

The next step in calculating instrument biases involves the estimation of a mean water vapor content for each band. As described in Section 3.4.1.3, Table 6 defines a unique, nearly linear relationship between the brightness temperature for each channel and atmospheric water vapor content. The estimation of a mean WVC value for each band has been accomplished by choosing the WVC value in Table 6 whose corresponding 21 V value is closest to the mean 21 V value for the band. We have taken this mean 21 V value to be the midpoint of each band's 21 V range.

This method yields WVC values to a resolution of .1 g/cm^2. We do not feel that the quality of the current data set justifies the interpolation of WVC values to achieve better numerical resolution. The estimated values for WVC corresponding to bands 1 through 4 are listed below. Band 5 has not been included in this analysis because the 21 V range for this band is much wider than that for the other four.

Band	Mean 21 V Value	Estimated WVC (grams/cm^2)
1	182.5	1.0
2	187.5	1.4
3	192.5	1.8
4	197.5	2.2

Note that the above WVC values for bands 2, 3, and 4 exceed the 1.0 g/cm^2 assumed in generating calculated T_B's for these runs. It is therefore expected that the observed biases for these 3 bands will include an environmental bias which is proportional to the difference between the model-assumed WVC and the actual water vapor content. An estimate of the environmental biases for each band may be obtained from Table 6 by subtracting the calculated T_B values corresponding to the assumed 1.0 g/cm^2 from those corresponding to the mean WVC for the band. The resulting predicted environmental biases for bands 1-4 are displayed in Table 4.2.

An instrument bias corresponding to each channel, for each band, can now be calculated by subtracting the predicted environmental bias from the observed bias. These results are shown in Table 4.3. The final column of this table contains a weighted average of the instrument biases calculated for each band. Note that the instrument biases for band 1 are identical to the observed biases since the predicted environmental biases are zero.

Several observations are made regarding the calculated instrument biases of Table 4.3:

(1) For each channel, the instrument biases agree fairly well from band to band, although there is some scatter due to the scarcity of data points (e.g., band 3 contains only 4 points). Considering this data scarcity and the lack of atmospheric water data, this agreement is fairly remarkable.

(2) Although the entries in Table 4.3 represent our best estimates of instrument biases, these numbers probably still contain some residual environmental contributions. This is due to the inadequacies inherent in using the observed 21 V values as the sole determinant of atmospheric water content.

(3) Since the 21 V channel has been used as an atmospheric water indicator, all of the instrument biases in Table 4.3 are somewhat relative to the 21 V biases. If the true 21 V instrument bias is found to be significantly different from zero, our estimated biases for all other channels will have to be adjusted according to their respective sensitivities to atmospheric water. However, even if our estimates are found to be inaccurate in an absolute sense, they still indicate a significant variation of instrument bias from channel to channel.

(4) For each frequency, the estimated instrument bias for the H channel is always positive and is always greater in value than that for the V channel. The V biases are either close to zero or significantly negative.

(5) The magnitudes of the differences between the H and V biases for each frequency increase in the order of increasing sensitivity to atmospheric water (i.e., 6.6, 10.69, 18, 37, 21 GHz). This probably indicates the presence of some environmental effect. This phenomenon is possibly related to the interim APC polarization rotation correction, though this possible relationship is not currently understood.

3.4.2 Discussion of Runs 1 Through 8. Runs 1 through 5 are executions of the measured versus calculated T_B software corresponding to the five 21 V T_B bands discussed previously. Runs 6 and 7 are executions of the same program for the entire data set of 38 "hits." The calculated T_B's for runs 1 through 6 were produced assuming a constant WVC of 1.0 g/cm^2, while those for run 7 were produced assuming 2.4 g/cm^2. Run 8 is an additional execution of the same software for the four available radiosonde points which coincide with SMMR overflights. The model-calculated T_B's for this run were produced using the 4 values of WVC obtained by integrating the radiosonde data.

Plots and statistics corresponding to these runs are displayed in tables and figures 7 through 14. The following observations are made regarding the individual runs:

(1) For the 18, 21, and 37 GHz channels, the observed biases generally increase in value from band 1 to band 5. This is attributable to the fact that (a) the model-assumed integrated WVC is fixed at 1.0 g/cm^2 for the runs involving the 5 bands, and (b) the true atmospheric water content increases from band 1 to band 5.

(2) For the 18, 21, and 37 GHz channels, the observed increase in the biases is largest between bands 4 and 5. This is due to the fact that the ranges of 21 V values for the first 4 bands each span 5°K, while that of band 5 spans almost 20°K. Therefore, band 5 contains a much larger range of atmospheric water contents than do the other bands.

(3) Again for the 18, 21, and 37 GHz channels, the RMS values about the biased line of unit slope are about the same for bands 1 through 4, and are slightly larger for band 5. This is also attributable to the larger range of water contents contained in band 5.

(4) The above three observations apply to a lesser degree for the 6.6 and 10.69 GHz channels. This is due to their lesser sensitivity to variations in atmospheric water content.

(5) For all five bands, the RMS values about the biased line of unit slope do not greatly exceed the RMS values about the best fitted curves for each channel. However, the actual curve fits for the individual channels rarely approach unit slope due to the scarcity of data points.

(6) The observed biases for run 6 (data from all bands, WVC = 1.0 g/cm^2) generally fall between those for bands 3 and 4. The run 6 RMS values are generally higher than those for the individual bands. This is especially true for the more water-sensitive 18, 21, and 37 GHz channels.

(7) As expected, the observed biases for run 7 (data from all bands, WVC = 2.4 g/cm^2) are generally much lower than those for all other runs. The RMS values for this run are close to those for run 6.

(8) The observed biases for run 8 (four radiosonde points) are generally higher than those for band 1, but somewhat lower than those for run 6. This seems to imply that the radiosonde-derived WVC values do not adequately account for all of the atmospheric water. This is also supported by the observation that the run 8 RMS values about the fitted curves for the 18, 21, and 37 GHz channels are larger than those for runs 1 through 4, but smaller than those for run 6.

3.4.3 Discussion of Runs 9 Through 12 - Cross-Track Gradients. Runs 9 through 12 are executions of the T_B cross-track gradient versus latitude program for portions of 4 different SEASAT orbits. The plots and statistics corresponding to these runs may be found in tables and figures 15 through 18. Note that statistics for all 10 channels are included only for the runs corresponding to orbit numbers 1255 and 1206 (runs 9 and 10). Statistics presented for the other 2 runs have been restricted to the 6.6 GHz channels to avoid voluminous repetition of similar results. The following observations are made regarding these runs:

(1) If observed cross-track gradients are due solely to variations in environmental factors across the scan, the gradients for each frequency should exhibit the following characteristics: (a) if the V gradient is zero, the H gradient should also be

zero, (b) if the V gradient is positive, the H gradient should be more positive, and (c) if the V gradient is negative, the H gradient should be more negative. This behavior is expected since the H channel for each frequency is more sensitive to variations in wind speed and atmospheric water content than the corresponding V channel.

(2) All of the plots show variations in the cross-track gradients which are undoubtedly due to real environmental effects. For example, the plots which span the region between 10° and 15° north latitude (runs 9, 11, and 12) show effects which are attributable to the Intertropical Convergence Zone.

(3) For the 6.6 GHz channels, the V gradients are often positive or zero, while the corresponding H gradients are negative. Examples of these opposing cross-track gradients are strongly evident in runs 10 and 11.

(4) For the 10.69 GHz channels, the H gradients are generally higher in value than the corresponding V gradients. Run 9 contains cases in which the V gradient is more negative than the corresponding H gradient.

(5) For the 18 GHz channels, the V gradients are generally higher in value than the H gradients. Runs 9, 10, and 12 all contain cases in which the V gradients are positive while the corresponding H gradients are negative. In this sense, the 18 GHz channels mimic the behavior of the 6.6 GHz channels.

(6) The behavior of the 21 GHz channels is similar to that of the 6.6 and 18 GHz channels in that the V gradients are generally higher in value than the H gradients. Runs 9 and 11 contain examples of V gradients which are close to zero while the corresponding H gradients are negative. In addition, runs 9, 10, and 11 contain examples in which the V gradients are more strongly positive than corresponding positive H gradients.

(7) The behavior of the 37 GHz channels is similar to that of the 10.69 GHz channels in that the H gradients are somewhat higher in value than the corresponding V gradients. Runs 9, 11, and 12 contain cases in which the V gradients are close to zero while the H gradients are positive. Note, however, that most of the time, the 37 GHz gradients exhibit the expected behavior outlined in (1) above.

(8) Mean values of the cross-track gradients for all channels have been calculated for two short time periods during which clear weather conditions prevailed. These gradient values are displayed in Table 19.1 in units of degrees Kelvin per cell and also as total variations across the SMMR swath. Note that the difference between V and H gradients for the 6.6, 18, and 21 GHz channels is larger than that for the 10.69 and 37 GHz channels.

(9) In an effort to determine if Faraday rotation effects are present in the data, mean values of the 6.6 GHz cross-track gradients have been calculated for segments of two ascending orbits (runs 9 and 12), and two descending orbits (runs 10 and 11). The descending orbits correspond to local night passes and the ascending orbits to local day passes. The results are displayed in Table 19.2. Note that the difference between the V and H gradients is smaller for the day passes. Since Faraday rotation is minimal during the night, the cross-track gradients observed during the night passes should contain little contribution from uncorrected Faraday rotation effects. If the smaller gradient differences observed for the day passes are indeed related to Faraday effects, this implies that Faraday rotation is acting to compensate for some of the instrument-induced cross-track gradients. As expected, this effect is observed only for the 6.6 GHz channels, i.e. the cross-track gradients for the higher frequency channels are independent of day/night conditions.

4.0 CONCLUSIONS

Several major conclusions may be drawn from the results discussed in the previous Section 3.4:

(1) There appears to exist a different instrument bias for each of the ten channels of SMMR brightness temperatures output by the interim APC algorithm. Our best estimates of these instrument biases appear as the final column of Table 4.3. For all frequencies, the estimated instrument biases for the H channels are always significantly positive while the V biases are either close to zero or significantly negative.

(2) If the observed biases are removed from the measured T_B data, the resulting values agree fairly well with model-predicted values. This is best illustrated by the RMS dispersions shown in Table 7 for band 1. The dispersions for the individual V channels generally lie between 1^o and 2^oK. Those for the H channels range between 2^o and 4^o K.

(3) For the 6.6, 18, and 21 GHz channels, there appear to exist opposing cross-track gradients in the V and H brightness temperature data output by the interim APC algorithm. These gradients are opposing in the sense that the vertical T_B values tend to increase across the SMMR swath from left to right, whereas the horizontal T_B values tend to decrease. An estimate of the total variation across the swath for each channel is given in Table 19.1. The 10.69 and 37 GHz channels do not exhibit significant cross-track gradients in comparison with the other channels.

(4) Faraday rotation effects appear to be present in the 6.6 GHz brightness temperatures output by the interim APC algorithm. These effects become evident when cross-track gradients observed during night passes are compared with those observed during day passes. The magnitudes of the 6.6 GHz gradients are smaller for day passes than for night passes as shown in Table 19.2.

5.0 RECOMMENDATIONS

As a result of this study, we feel that the following recommendations are appropriate:

(1) Upon completion of the final APC algorithm, several runs made for this study should be repeated using final APC brightness temperature data. This will allow a determination of whether instrument biases, cross-track gradients, and Faraday rotation effects are still apparent.

(2) If the T_B cross-track gradients are still evident in the final APC output, it is recommended that a detailed analysis of the T_A input data be performed to determine the cause of the gradients.

(3) In order to further refine estimates of the observed instrument biases, it is recommended that this analysis be extended to include better quality radiosonde data than that currently available. This would eliminate the uncertainties inherent in using the SMMR data itself to estimate atmospheric water content.

6.0 NEW TECHNOLOGY

No new technology has been developed in the course of this study.

7.0 REFERENCES

Acknowledgment should be given to four general sources of information used for this study.

(1) Kitzis, S. N. and Kitzis J. L., "Evaluation and Analysis of SEASAT-A SMMR APC Algorithm: 6.6 GHz T_B vs. $T_{surface\ truth}$ Comparison Results," March 16, 1979.

(2) "Seasat Gulf of Alaska Workshop Report," Volume 1, JPL Publication 622-101.

(3) Njoku, E. G., "Antenna Pattern Correction Procedures for the SMMR," JPL Publication.

(4) "Seasat Gulf of Alaska Experiment Surface Truth Data Inventory," NOAA Publication 622-99.

Table 1. SMMR APC Brightness Temperature Grids

Grid Number	Grid Size (cells)	Cell Dimension (km)	SMMR Channels Output on Grid	
1	4 x 4	149 x 149	6.6 V	6.6 H
			10.69 V	10.69 H
			18 V	18 H
			21 V	21 H
			37 V	37 H
2	7 x 7	85 x 85	10.69 V	10.69 H
			18 V	18 H
			21 V	21 H
			37 V	37 H
3	11 x 11	54 x 54	18 V	18 H
			21 V	21 H
			37 V	37 H
4	22 x 22	27 x 27	37 V	37 H

Table 2.1. Spacecraft T_B Data Inventory

Orbit Number	Start Time	Stop Time	Start Latitude	Stop Latitude	GOASEX Item No.	Surface Truth Hit ID
1120	256,7,50,12	256,8,14,13	77	4	—	1,2,41
1126	256,17,25,10	256,17,49,14	-15	66	—	3,4,42
1134	257,7,26,12	257,7,41,12	67	16	11	5,6
1135	257,9,4,10	257,9,19,10	74	26	12	—
1163	259,8,6,10	259,8,21,10	73	24	6	7,8,43
1164	259,9,46,11	259,10,1,11	74	26	7	—
1168	259,15,50,12	259,16,14,17	-38	44	—	—
1177	260,7,39,10	260,7,52,40	67	21	9	9,10
1178	260,9,16,10	260,9,32,41	75	23	10	—
1191	261,7,10,10	261,7,27,42	66	6	—	—
1198	261,18,20,10	261,18,44,13	-8	67	—	11,44,61
1205	262,6,40,13	262,7,4,15	67	-14	—	—
1206	262,8,19,13	262,8,34,13	72	23	14	12,13,14,45
1207	262,9,58,12	262,10,14,41	76	24	15	—
1212	262,17,59,10	262,18,15,42	14	69	13	15,16,17,46
1235	264,9,0,13	264,9,23,42	74	-2	—	18
1248	265,6,50,11	265,7,14,12	74	-4	—	—
1255	265,18,0,11	265,18,24,14	-26	56	—	19,20,21,47
1291	268,7,5,12	268,7,27,43	69	-7	—	—
1292	268,8,44,11	268,8,59,11	73	24	4	22,23,24,48
1293	268,10,24,12	268,10,39,11	75	27	5	25
1298	268,18,25,10	268,18,41,9	15	69	3	26,27,28,49
1313	269,19,25,11	269,19,49,14	-23	59	—	—
1327	270,18,55,10	270,19,18,43	-26	55	—	—

Times are in Days, Hours, Minutes, Seconds from beginning of year 1978.

Latitudes are in degrees, positive for north latitude, negative for south latitude.

Table 2.2. Surface Truth Hit Inventory

Surface Truth Hit ID	Site ID	Latitude	Longitude	Orbit No.	Time of Overflight	Radiosonde Available
1	46005	46.0	229.0	1120	256,8,1,26	—
2	46006	41.0	222.0	1120	256,8,3,18	—
3	46002	42.5	230.0	1126	256,17,41,43	—
4	46005	46.0	229.0	1126	256,17,42,49	—
5	46005	46.0	229.0	1134	257,7,32,33	—
6	46002	42.5	230.0	1134	257,7,33,42	—
7	46005	46.0	229.0	1163	259,8,14,2	—
8	46006	41.0	222.0	1163	259,8,15,54	—
9	46005	46.0	229.0	1177	260,7,45,32	—
10	46002	42.5	230.0	1177	260,7,46,16	—
11	46006	41.0	222.0	1198	261,18,36,19	—
12	46004	51.0	224.0	1206	262,8,25,56	—
13	46005	46.0	229.0	1206	262,8,27,4	—
14	46006	41.0	222.0	1206	262,8,28,35	—
15	46002	42.5	230.0	1212	262,18,7,25	—
16	46005	46.0	229.0	1212	262,18,8,11	—
17	46004	51.0	224.0	1212	262,18,10,3	—
18	46004	51.0	224.0	1235	264,9,7,19	—
19	46002	42.5	230.0	1255	265,18,20,6	—
20	46005	46.0	229.0	1255	265,18,21,14	—
21	46004	51.0	224.0	1255	265,18,22,44	—
22	46004	51.0	224.0	1292	268,8,51,41	—
23	46005	46.0	229.0	1292	268,8,52,25	—
24	46006	41.0	222.0	1292	268,8,54,17	—
25	46001	56.0	212.0	1293	268,10,30,11	—
26	46002	42.5	230.0	1298	268,18,32,51	—
27	46005	46.0	229.0	1298	268,18,33,59	—
28	46004	51.0	224.0	1298	268,18,35,29	—
41	Oc.	48.7	223.5	1120	256,8,1,4	—
42	Oc.	48.7	226.7	1126	256,17,43,35	—
43	Oc.	48.5	224.0	1163	259,8,14,2	Yes
44	Oc.	48.7	218.3	1198	261,18,38,35	—
45	Oc.	48.7	223.6	1206	262,8,26,42	—
46	Oc.	48.7	226.7	1212	262,18,9,17	Yes
47	Oc.	48.7	226.7	1255	265,18,21,58	—
48	Oc.	48.7	226.6	1292	268,8,52,3	Yes
49	Oc.	48.6	230.2	1298	268,18,34,21	Yes
61	PAPA	50.1	215.1	1198	261,18,38,57	—

Site ID's are either the NOAA data buoy ID (e.g., 46001), "Oc." for the Oceanographer, or "PAPA" for Ocean Station P.

Latitudes are in degrees north of the equator.

Longitudes are in degrees east of the prime meridian.

Times are in Days, Hours, Minutes, Seconds from beginning of year 1978.

Table 2.3. Surface Truth Accuracies

	Measurement Accuracies*			
Site ID	Air Temp (K)	Sea Surf. Temp (K)	Wind Speed (m/s)	Pressure (mb)
46001	0.2	0.2	0.4	0.6
46002	0.2	0.2	0.4	0.6
46003	0.2	0.2	0.4	0.6
46004	0.2	0.2	0.4	0.6
46005	0.2	0.2	0.4	0.6
46006	0.2	0.2	0.4	0.6
Oc.	0.1	0.2	1.0	0.2
PAPA	0.1	0.2	1.0	0.2

*Accuracies taken from references 2 and 4.

Table 3. Run Summary

Run No.	Run Type	Orbit No.	Start Latitude	Stop Latitude	Surface Truth Hit ID's	Figure and Table Numbers	Comments
1	A	—	—	—	1,17,18,20,21,25, 41,43	7	Band 1, Model WVC = 1.0
2	A	—	—	—	3,4,7,9,10,22,42, 47,49	8	Band 2, Model WVC = 1.0
3	A	—	—	—	11,23,26,27	9	Band 3, Model WVC = 1.0
4	A	—	—	—	2,8,14,15,28,48	10	Band 4, Model WVC = 1.0
5	A	—	—	—	5,6,12,13,16,19,24, 44,45,46,61	11	Band 5, Model WVC = 1.0
6	A	—	—	—	1-28,41-49,61	12	All points, Model WVC = 1.0
7	A	—	—	—	1-28,41-49,61	13	All points, Model WVC = 2.4
8	A	—	—	—	43,46,48,49	14	Radiosonde-derived model WVC values
9	B	1255	-25	15	—	15	Ascending Orbit
10	B	1206	49	23	—	16	Descending Orbit
11	B	1205	25	-14	—	17	Descending Orbit
12	B	1198	-15	20	—	18	Ascending Orbit

Run Type Definitions: A — Measured vs. Calculated T_B Plots and Statistics
B — Cross-Track Gradients vs. Latitude

Latitudes are in degrees, positive for north latitude, negative for south latitude.

Table 4.1. Observed Biases for Runs 1 through 7

		Run 1 Band 1 Model WVC = 1.0	Run 2 Band 2 Model WVC = 1.0	Run 3 Band 3 Model WVC = 1.0	Run 4 Band 4 Model WVC = 1.0	Run 5 Band 5 Model WVC = 1.0	Run 6 All points Model WVC = 1.0	Run 7 All points Model WVC = 2.4
6.6	V	-0.05	0.85	1.26	-0.62	1.53	0.67	0.12
6.6	H	3.06	2.36	5.89	2.51	4.35	3.48	2.66
10.69	V	0.45	0.87	1.00	2.06	3.76	1.82	0.30
10.69	H	6.92	6.21	6.15	7.63	11.82	8.20	5.87
18	V	-5.59	-3.24	-2.07	0.76	7.21	0.05	-7.65
18	H	4.91	6.22	10.36	12.38	23.25	12.28	0.04
21	V	-0.68	4.62	10.79	15.15	25.40	11.83	-5.87
21	H	13.73	18.97	30.39	36.33	53.27	31.74	2.91
37	V	-4.58	-3.91	2.48	1.29	12.47	2.18	-5.76
37	H	6.85	8.98	15.27	16.21	36.34	18.26	4.24

Table 4.2. Predicted Environmental Biases for Bands 1 through 4

		Band 1	Band 2	Band 3	Band 4
6.6	V	0	0.15	0.31	0.47
6.6	H	0	0.24	0.48	0.72
10.69	V	0	0.44	0.88	1.32
10.69	H	0	0.67	1.34	2.02
18	V	0	2.26	4.49	6.71
18	H	0	3.61	7.17	10.71
21	V	0	5.54	10.73	15.58
21	H	0	9.05	17.53	25.48
37	V	0	2.35	4.65	6.91
37	H	0	4.17	8.28	12.31

Table 4.3. Estimated Instrument Biases

	Band 1 8 Points	Band 2 9 Points	Band 3 4 Points	Band 4 6 Points	Weighted Average
6.6 V	-0.05	0.70	0.95	-1.09	0.12
6.6 H	3.06	2.12	5.41	1.79	2.81
10.69 V	0.45	0.43	0.12	0.74	0.46
10.69 H	6.92	5.54	4.81	5.61	5.86
18 V	-5.59	-5.50	-6.56	-5.95	-5.78
18 H	4.91	2.61	3.19	1.67	3.17
21 V	-0.68	-0.92	0.06	-0.43	-0.59
21 H	13.73	9.92	12.86	10.85	11.69
37 V	-4.58	-6.26	-2.17	-5.62	-5.01
37 H	6.85	4.81	6.99	3.90	5.54

Table 5. Radiosonde — Derived WVC Values

Site ID	Orbit No.	Time	Derived WVC Value (g/cm^2)	Surface Truth Hit ID
PAPA	1135	257,9,11	1.36	—
PAPA	1164	259,9,53	0.93	—
PAPA	1169	259,17,56	1.13	—
PAPA	1178	260,9,23	1.25	—
PAPA	1207	262,10,5	1.27	—
PAPA	1212	262,18,9	1.75	—
PAPA	1293	268,10,30	1.28	—
PAPA	1298	268,18,34	1.07	—
Oc.	1135	257,9,4	1.40	—
Oc.	1140	257,17,56	1.31	—
Oc.	1163	259,8,19	1.09	43
Oc.	1169	259,17,56	1.20	—
Oc.	1183	260,17,27	1.57	—
Oc.	1212	262,18,25	2.20	46
Oc.	1292	268,9,14	1.98	48
Oc.	1298	268,18,45	1.84	49

Site ID's are either "Oc." for the Oceanographer or "PAPA" for Ocean Station P.

Times are in Days, Hours, Minutes for beginning of year 1978.

Table 6. Variation of Brightness Temperature with WVC

WVC (g/cm^2)	Model-Calculated Brightness Temperatures									
	6.6 V	6.6 H	10.69 V	10.69 H	18 V	18 H	21 V	21 H	37 V	37 H
0.5	150.06	82.55	154.56	86.03	165.68	96.50	174.79	108.27	193.45	125.14
0.6	150.10	82.61	154.67	86.20	166.27	97.43	176.34	110.73	194.06	126.21
0.7	150.14	82.67	154.77	86.36	166.85	98.36	177.86	113.28	194.66	127.28
0.8	150.18	82.73	154.88	86.53	167.42	99.27	179.36	115.72	195.25	128.35
0.9	150.22	82.79	154.99	86.70	167.99	100.19	180.83	118.12	195.85	129.41
1.0	150.26	82.84	155.10	86.87	168.57	101.11	182.25	120.45	196.44	130.47
1.1	150.30	82.90	155.21	87.03	169.13	102.01	183.68	122.78	197.03	131.52
1.2	150.34	82.96	155.32	87.19	169.70	102.91	185.08	125.07	197.62	132.56
1.3	150.37	83.02	155.43	87.37	170.28	103.83	186.46	127.32	198.21	133.61
1.4	150.41	83.08	155.54	87.54	170.83	104.72	187.79	129.50	198.79	134.64
1.5	150.45	83.14	155.65	87.70	171.39	105.61	189.13	131.68	199.37	135.68
1.6	150.49	83.20	155.75	87.87	171.96	106.52	190.44	133.83	199.94	136.71
1.7	150.53	83.25	155.87	88.04	172.51	107.40	191.74	135.94	200.52	137.73
1.8	150.57	83.32	155.98	88.21	173.06	108.28	192.98	137.98	201.09	138.75
1.9	150.61	83.38	156.09	88.38	173.63	109.19	194.23	140.03	201.66	139.76
2.0	150.65	83.44	156.20	88.55	174.18	110.06	195.46	142.04	202.22	140.77
2.1	150.69	83.50	156.31	88.72	174.72	110.93	196.67	144.03	202.79	141.78
2.2	150.73	83.56	156.42	88.89	175.28	111.82	197.83	145.93	203.35	142.78
2.3	150.77	83.62	156.53	89.06	175.82	112.68	199.01	147.86	203.91	143.78
2.4	150.81	83.68	156.64	89.23	176.36	113.55	200.16	149.75	204.46	144.77

Model Brightness Temperatures are calculated with the assumptions of sea surface temperature equal to 15°C, wind speeds less than 7 meters/second, cloud-free conditions, a standard atmosphere, and WVC values as shown above.

Table 7

Run 1 Statistical Summary

CURVE FITS FOR SMMR TB VS. CALCULATED TB

CHANNEL	CONSTANT TERM	LINEAR TERM	RMS
6.6 V	43.00	.71	1.988
6.6 H	23.65	.76	2.507
10.69 V	66.73	.58	.875
10.69 H	11.51	.95	2.160
18.0 V	87.44	.45	1.477
18.0 H	29.37	.76	1.589
21.0 V	182.62	.00	1.511
21.0 H	136.71	.00	2.456
37.0 V	192.98	.00	1.131
37.0 H	23.65	.87	3.796
ALL V	12.79	.91	2.654
ALL H	-3.94	1.10	4.107
ALL V+H	16.93	.90	4.620

DISPERSION ABOUT LINE OF UNIT SLOPE

CHANNEL	BIAS	RMS ABOUT BIASED CURVE
6.6 V	-.05	2.042
6.6 H	3.06	2.585
10.69 V	.45	1.134
10.69 H	6.92	2.165
18.0 V	-5.59	1.660
18.0 H	4.91	1.721
21.0 V	-.68	2.173
21.0 H	13.73	3.112
37.0 V	-4.58	1.557
37.0 H	6.85	3.816
ALL V	-2.09	3.046
ALL H	7.10	4.556
ALL V+H	2.50	6.009

Figure 7.1

Run 1

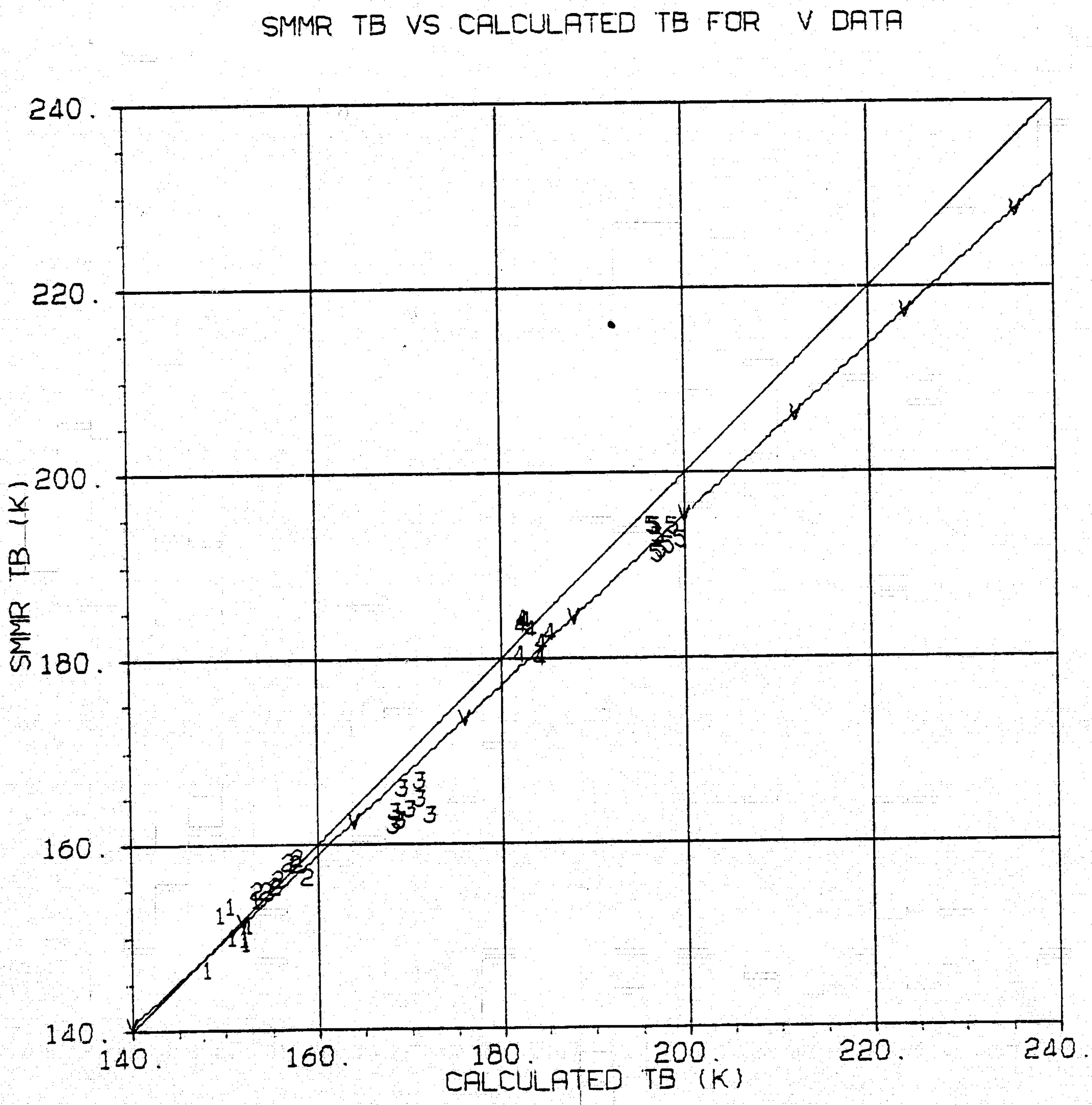

Figure 7.2

Run 1

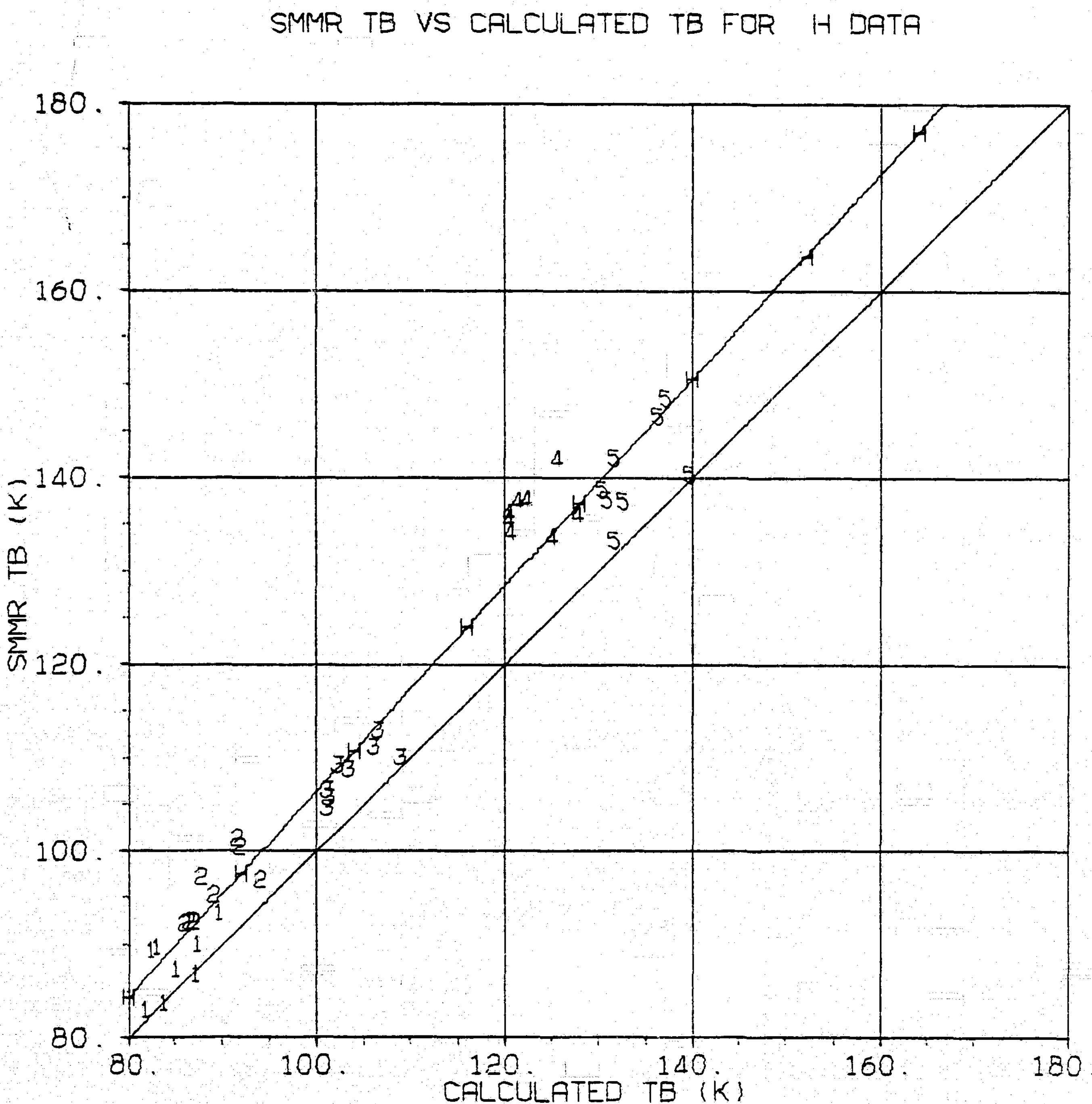

Figure 7.3

Run 1

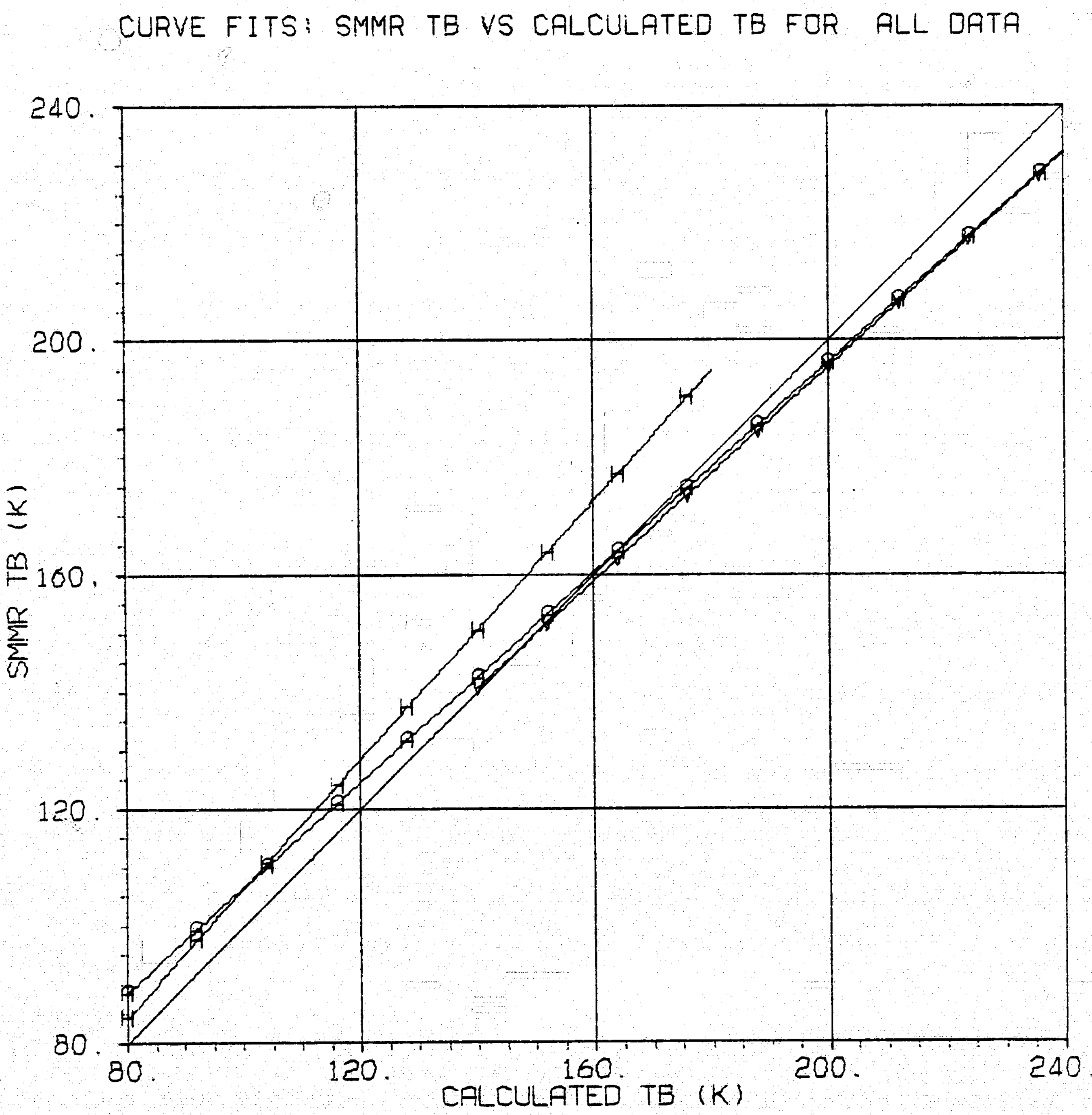

Figure 7.4

Run 1

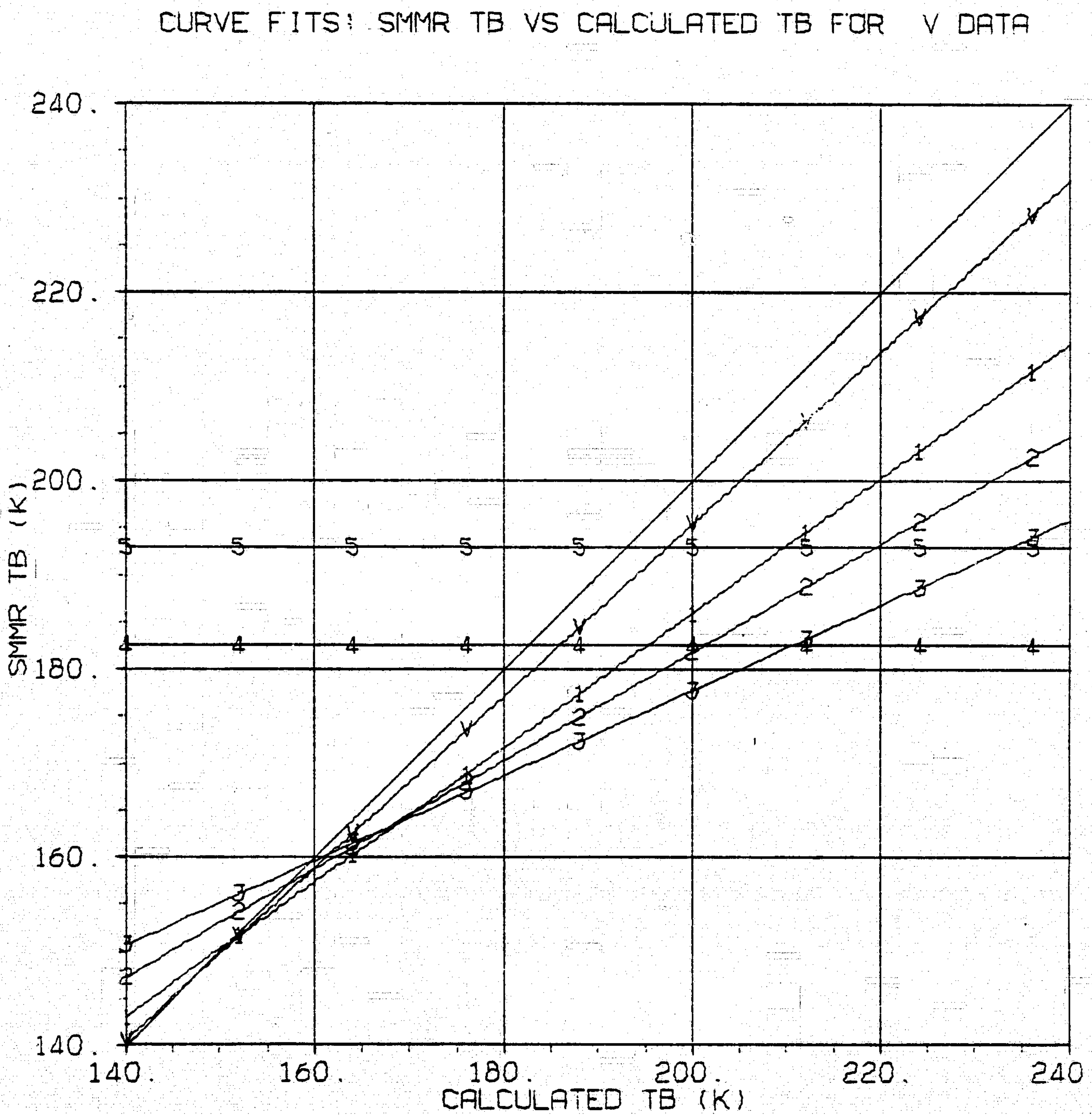

Figure 7.5

Run 1

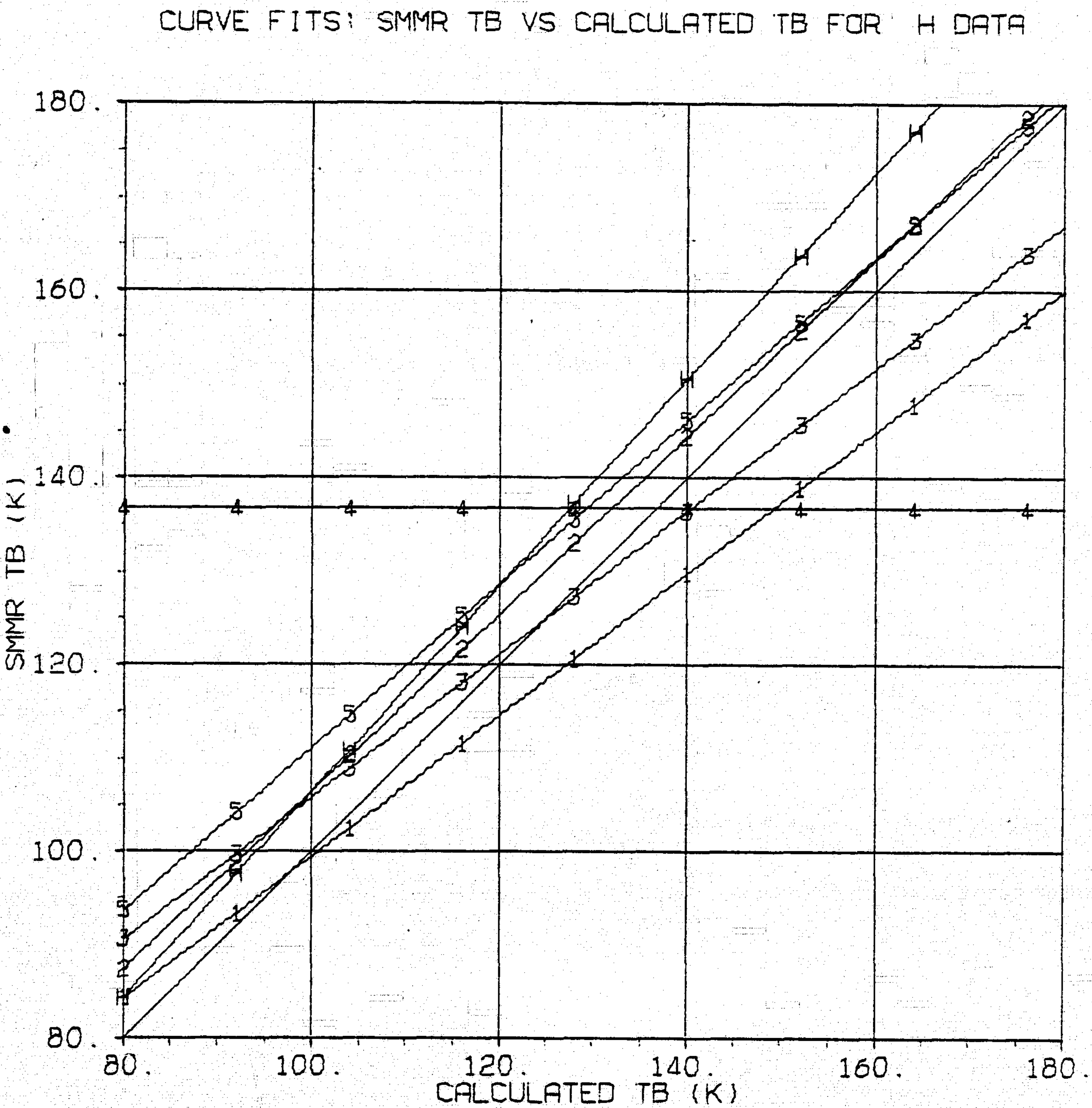

Figure 7.6

Run 1

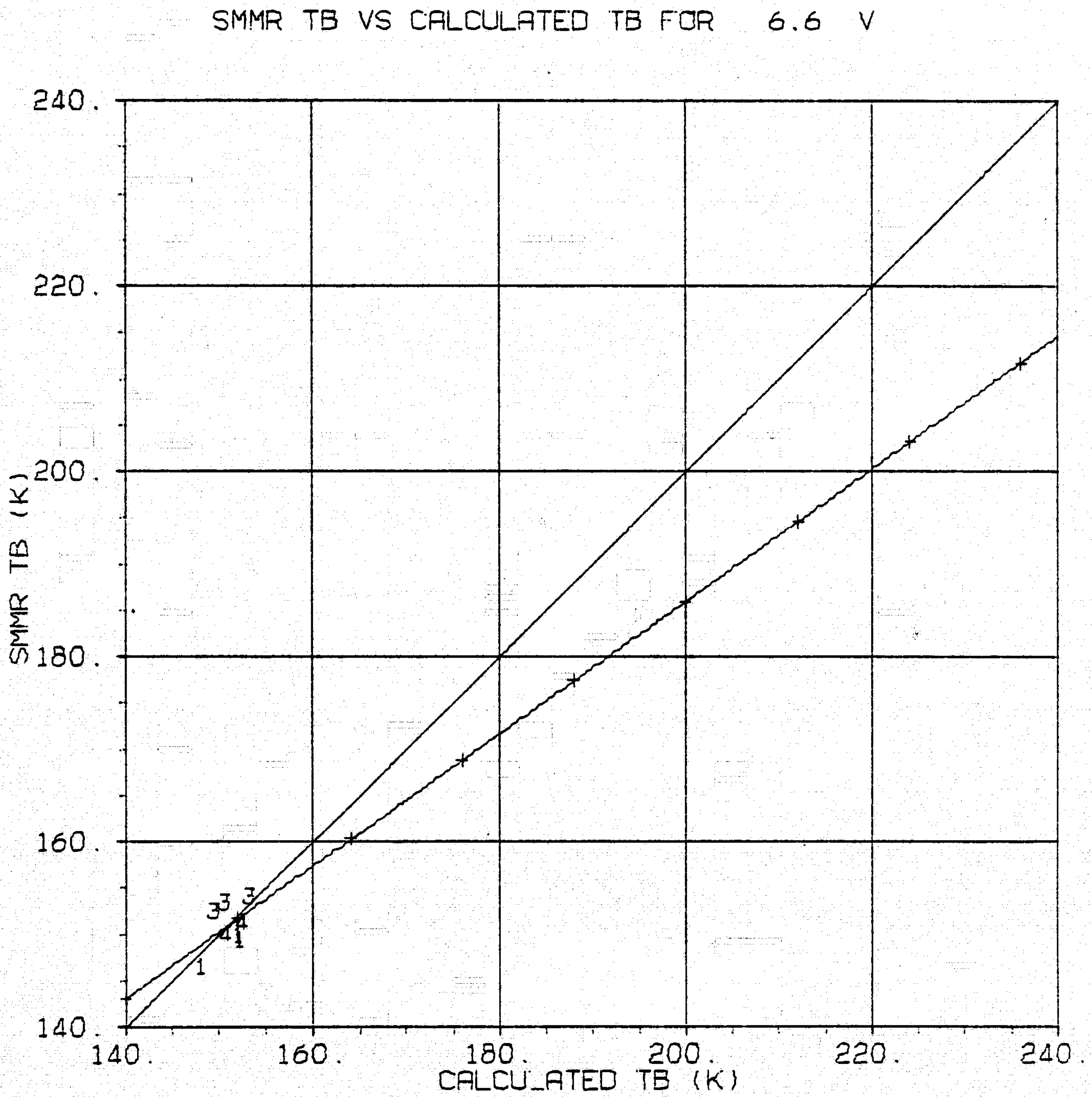

Figure 7.7

Run 1

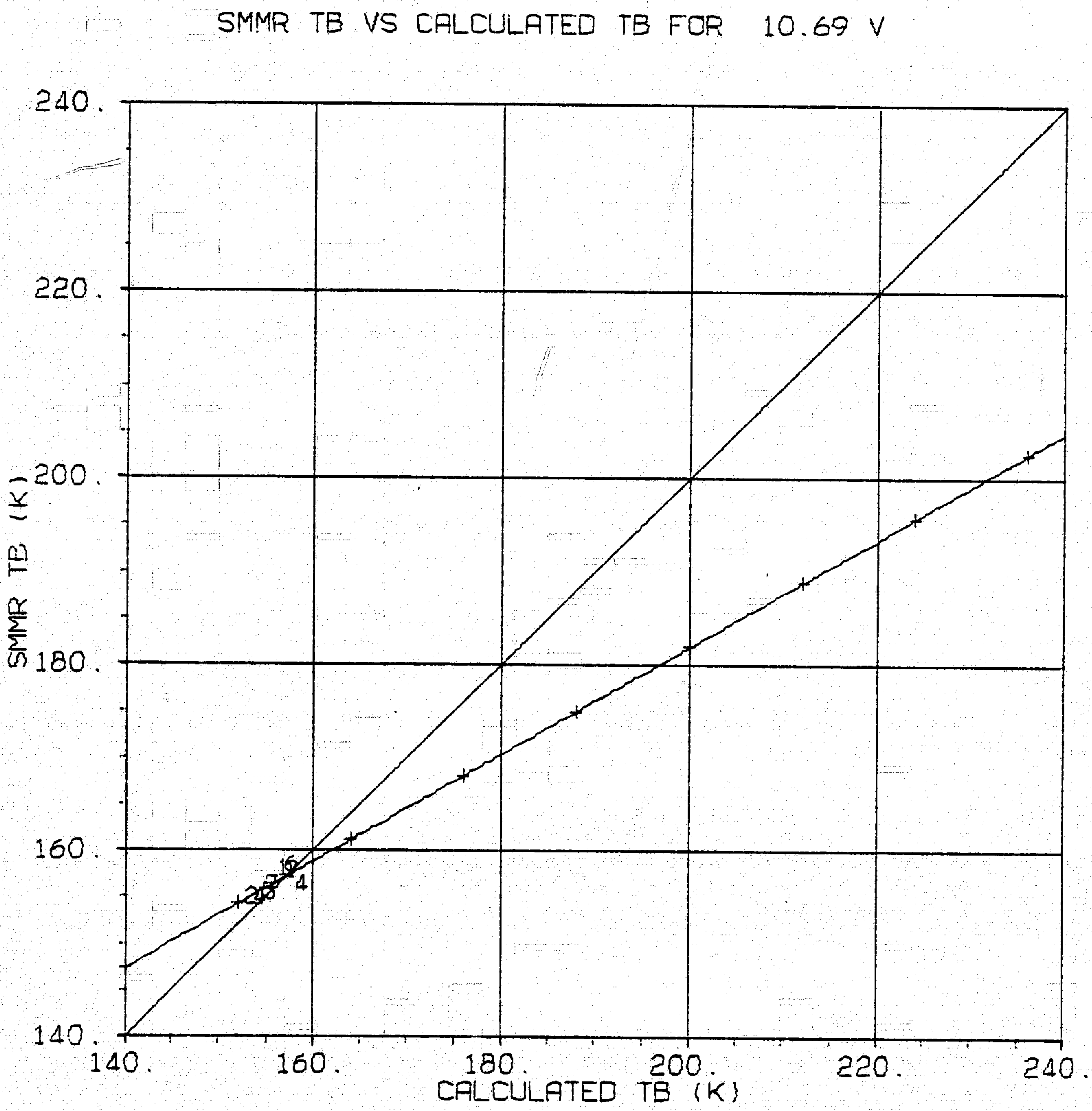

Figure 7.8

Run 1

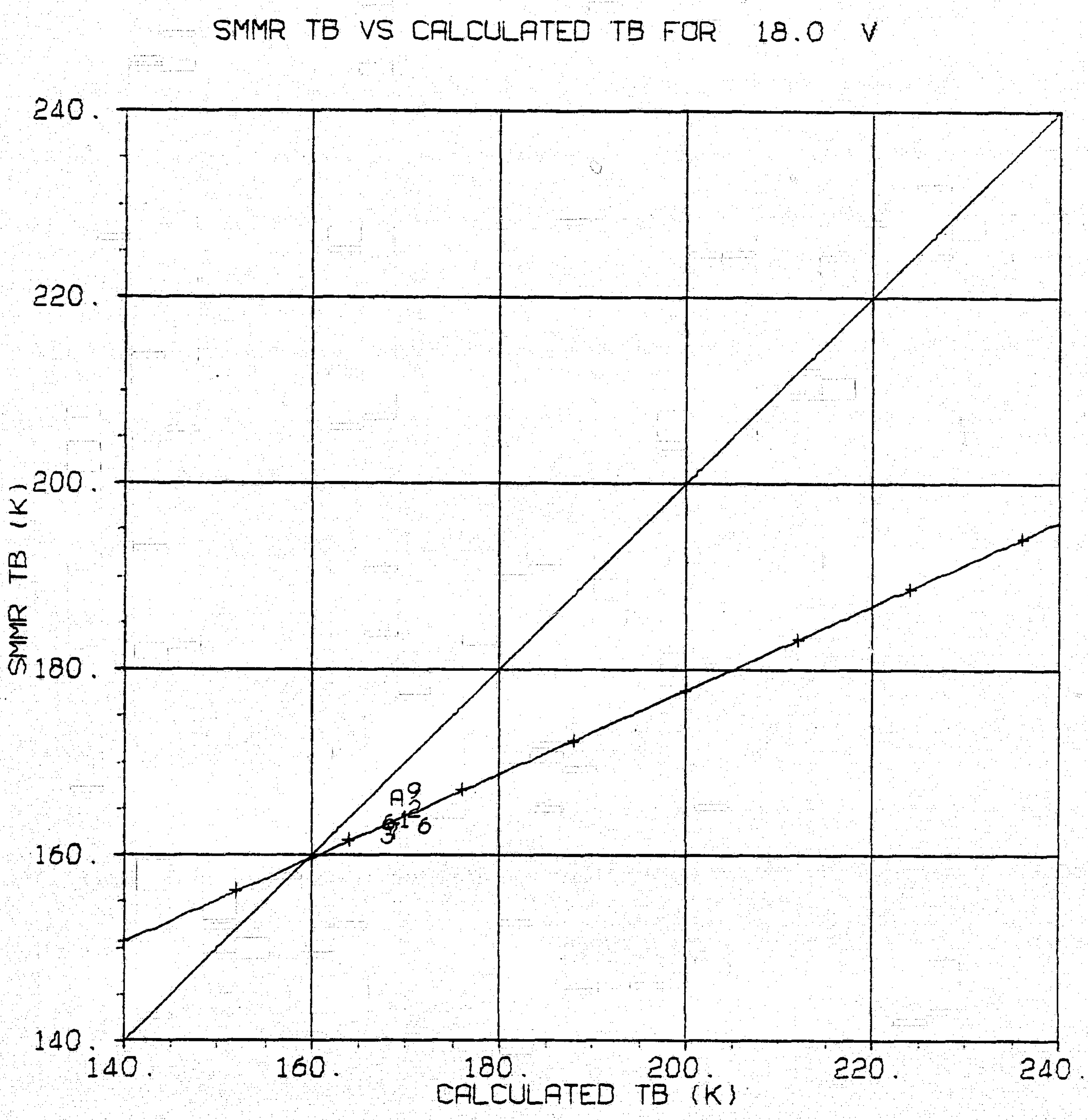

Figure 7.9

Run 1

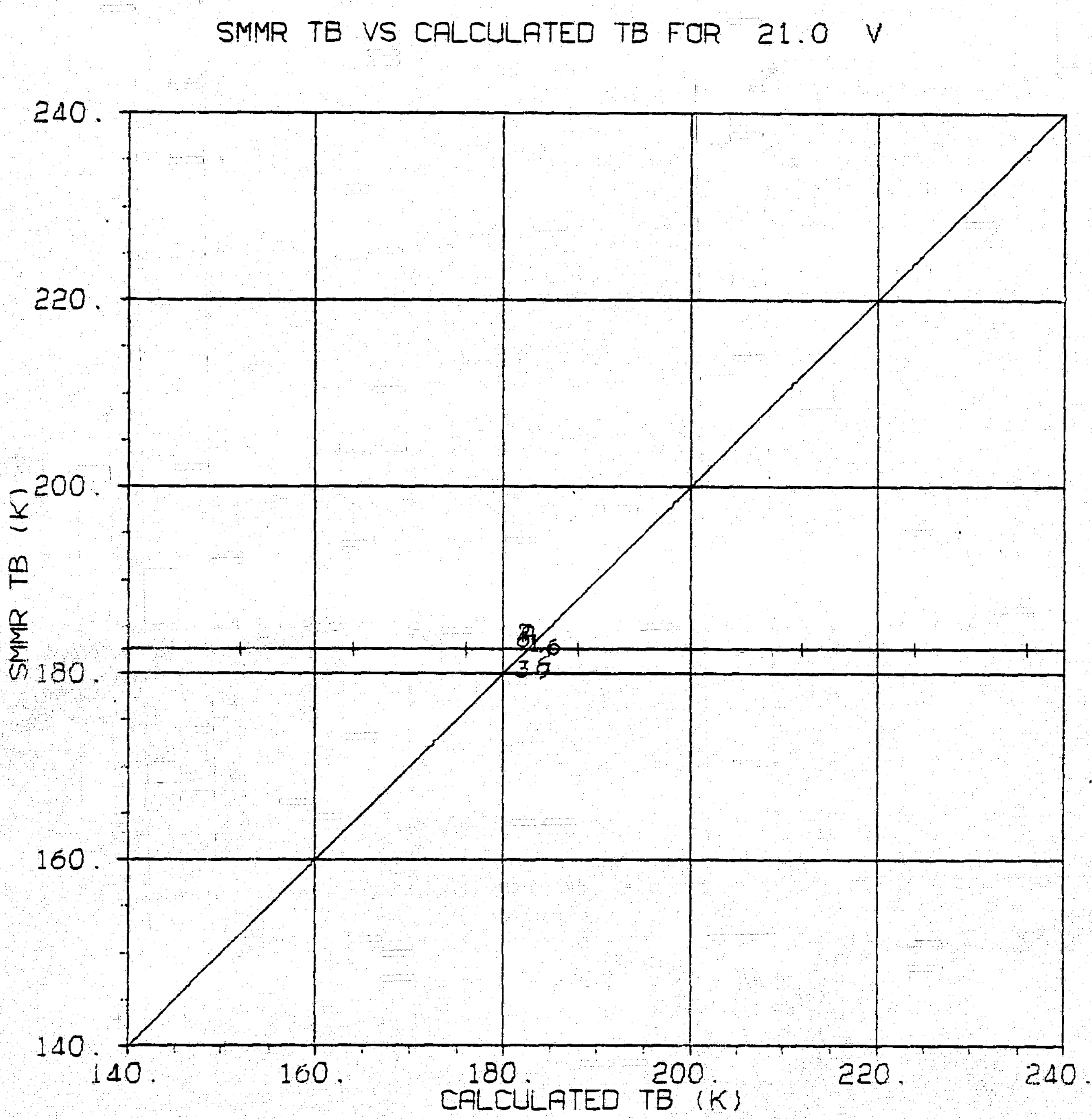

Figure 7.10

Run 1

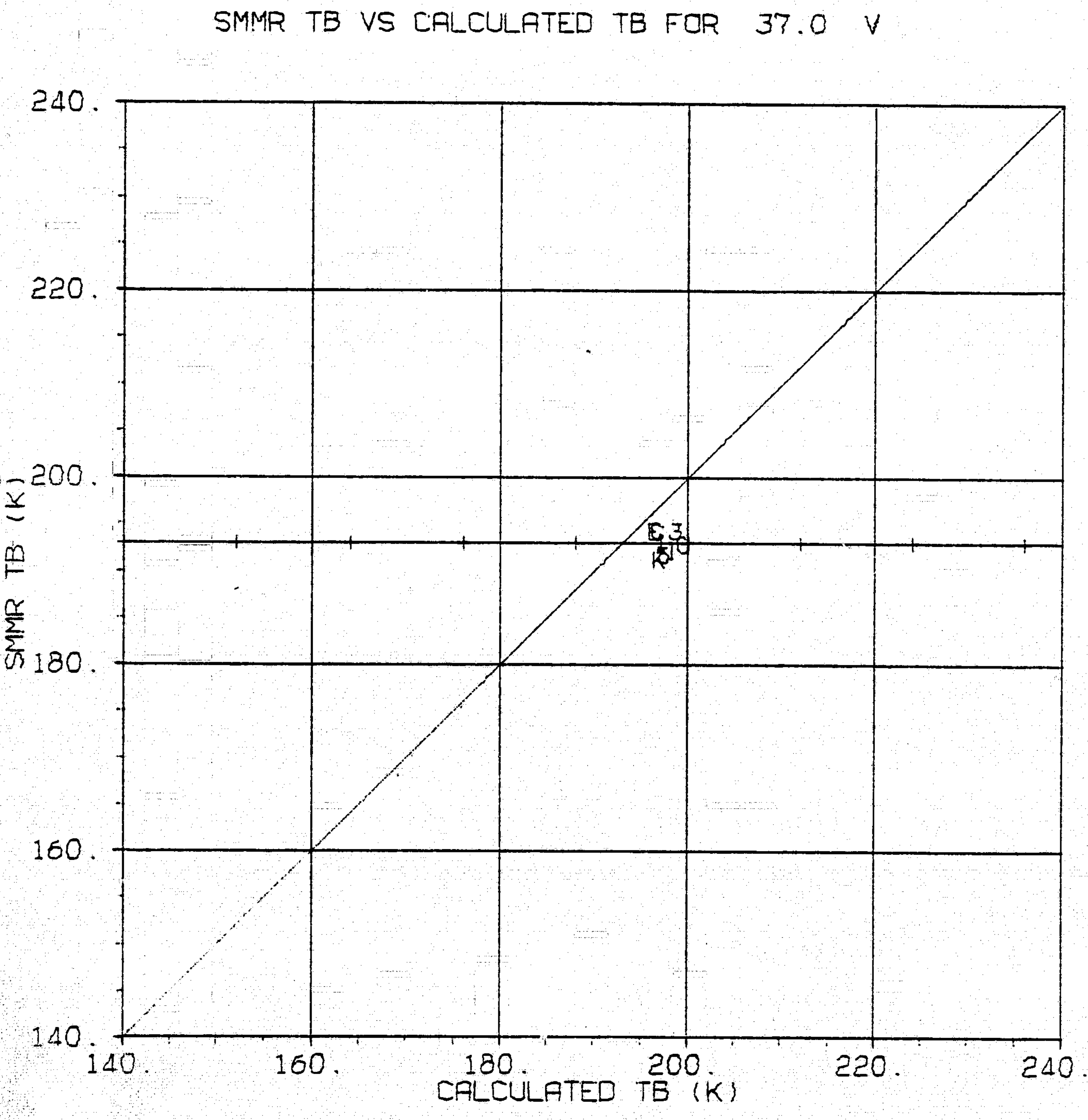

Figure 7.11

Run 1

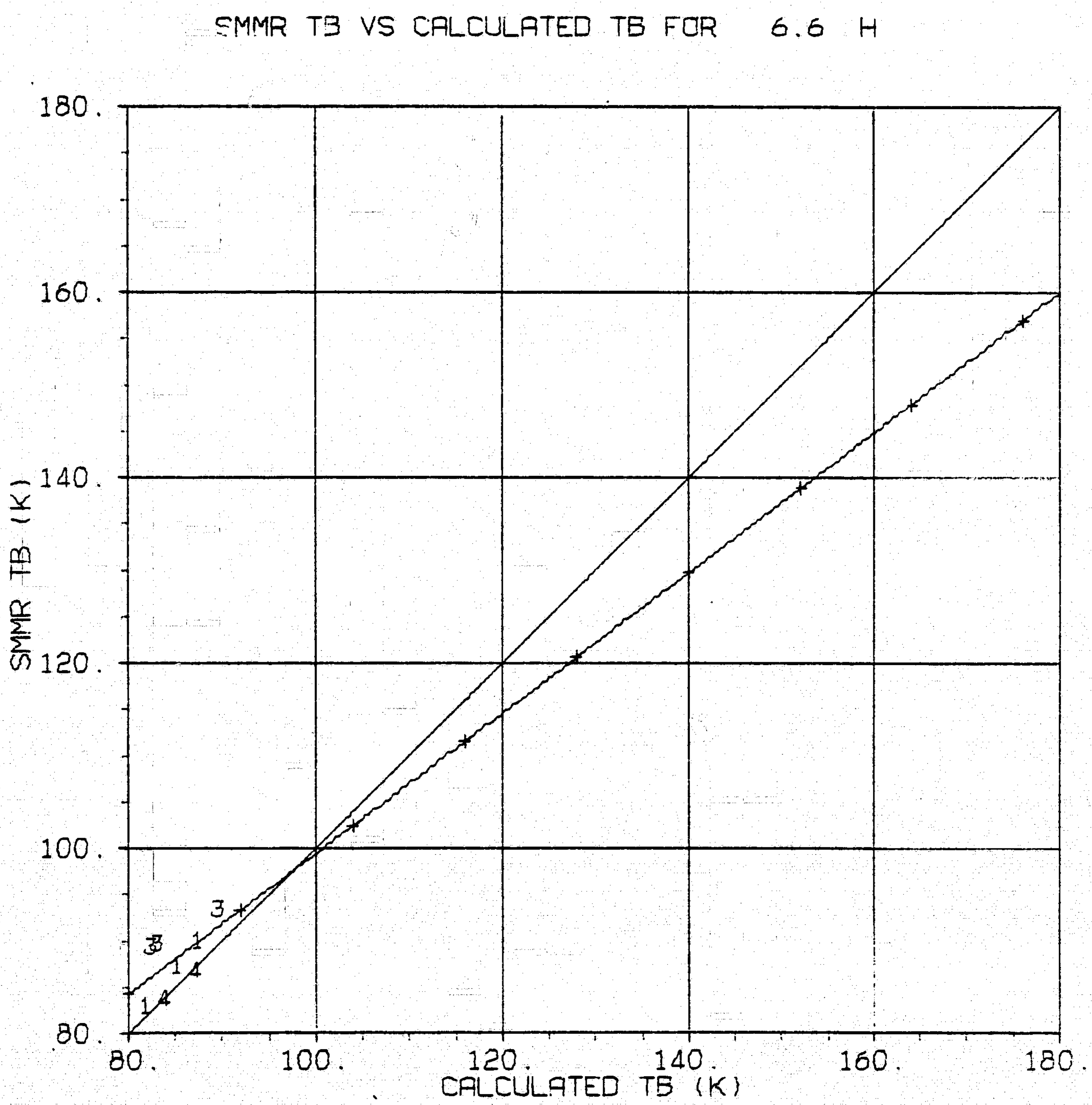

Figure 7.12

Run 1

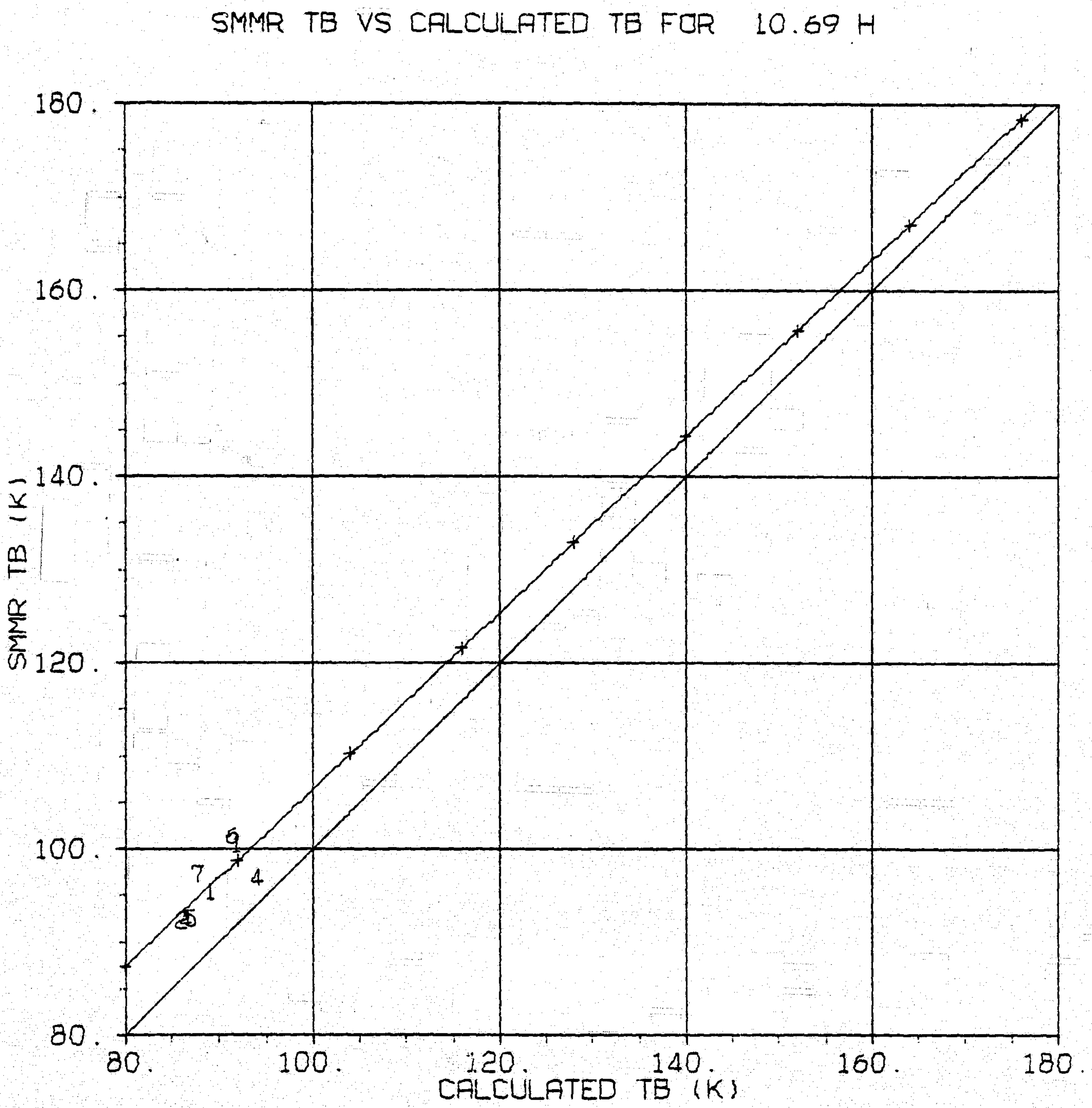

Figure 7.13

Run 1

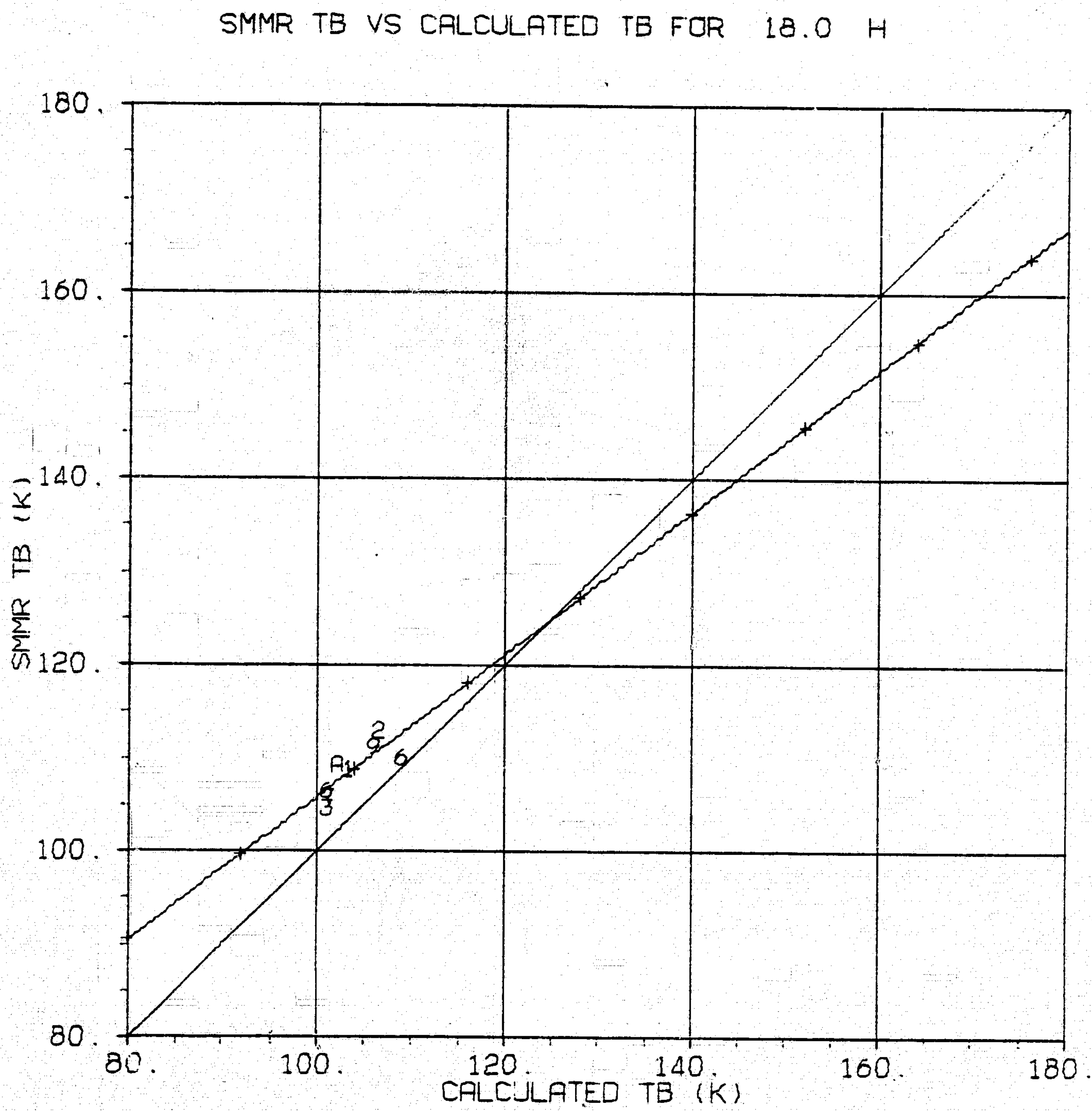

Figure 7.14

Run 1

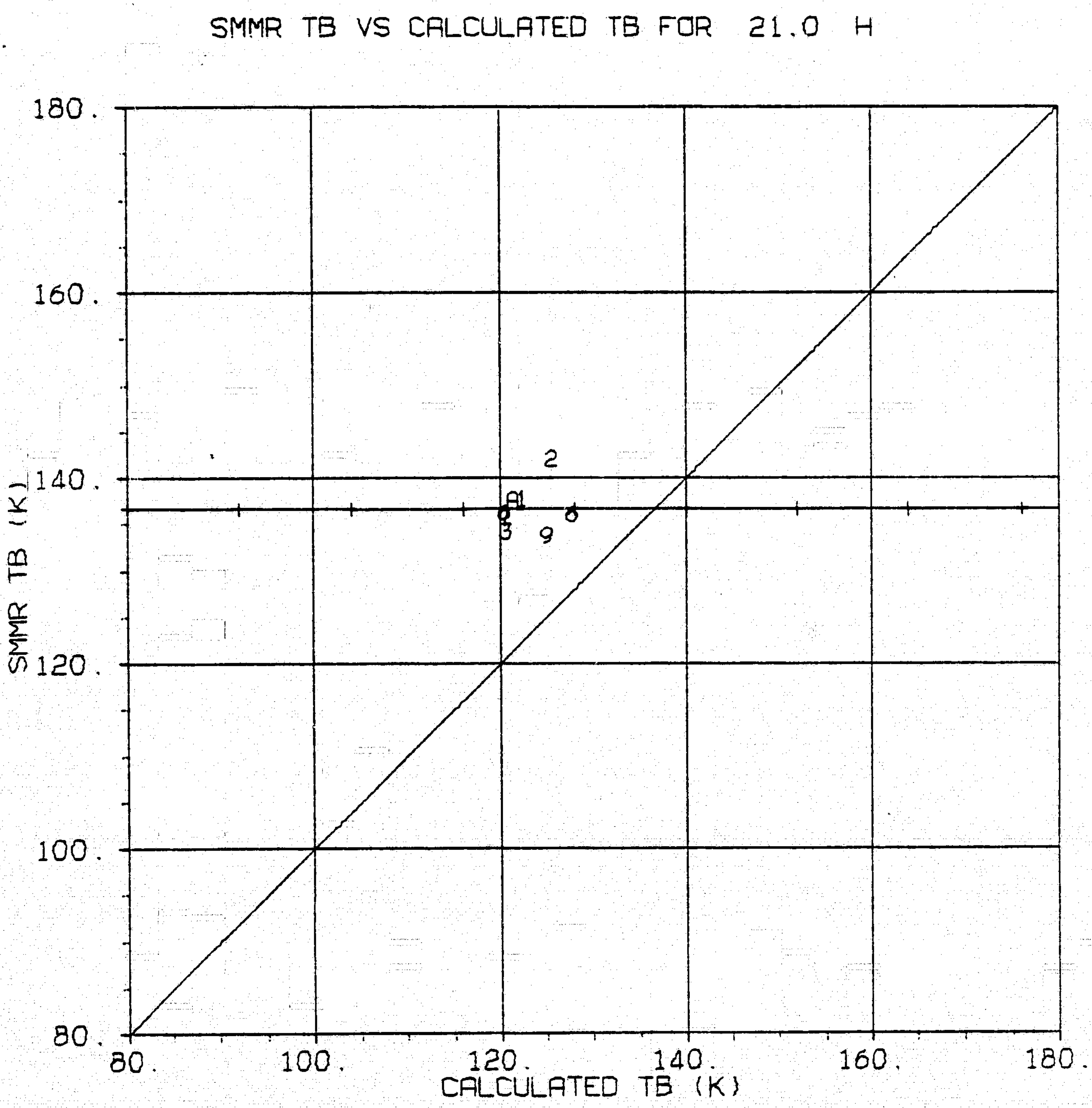

Figure 7.15

Run 1

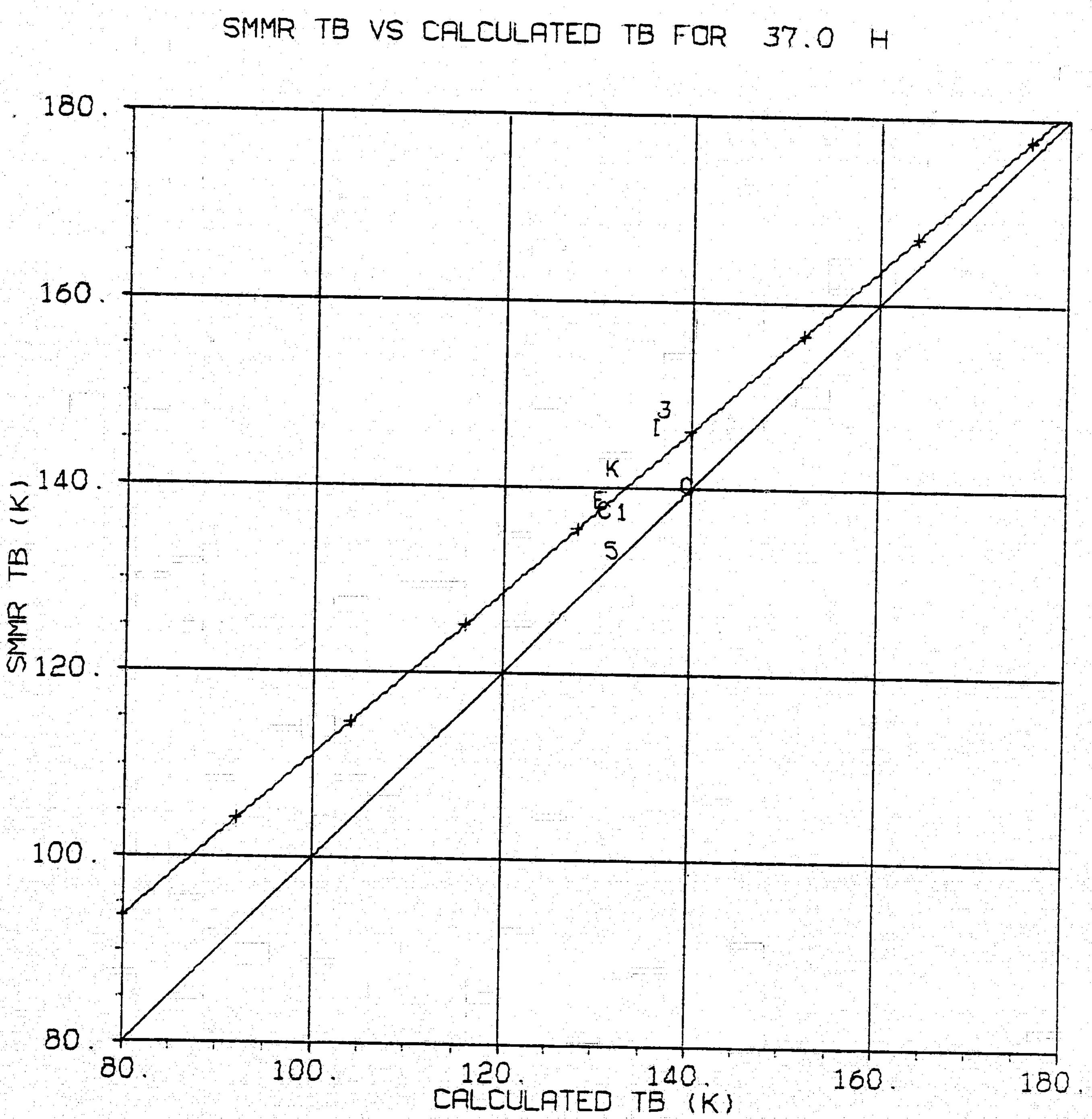

Table 8

Run 2 Statistical Summary

CURVE FITS FOR SMMR TB VS. CALCULATED TB

CHANNEL	CONSTANT TERM	LINEAR TERM	RMS
6.6 V	57.03	.63	1.425
6.6 H	87.57	.00	1.974
10.69 V	-31.54	1.21	1.085
10.69 H	-18.89	1.28	2.600
18.0 V	-141.69	1.81	1.653
18.0 H	-10.51	1.16	2.714
21.0 V	187.99	.00	1.444
21.0 H	141.60	.00	3.086
37.0 V	193.22	.00	1.643
37.0 H	31.31	.83	2.448
ALL V	8.41	.95	3.435
ALL H	-12.84	1.20	5.146
ALL V+H	15.72	.92	6.003

DISPERSION ABOUT LINE OF UNIT SLOPE

CHANNEL	BIAS	RMS ABOUT BIASED CURVE
6.6 V	.85	1.541
6.6 H	2.36	2.696
10.69 V	.87	1.135
10.69 H	6.21	2.685
18.0 V	-3.24	1.952
18.0 H	6.22	2.742
21.0 V	4.62	1.840
21.0 H	18.97	4.047
37.0 V	-3.91	1.792
37.0 H	8.98	2.488
ALL V	-.16	3.535
ALL H	8.55	6.364
ALL V+H	4.19	6.743

Figure 8.1

Run 2

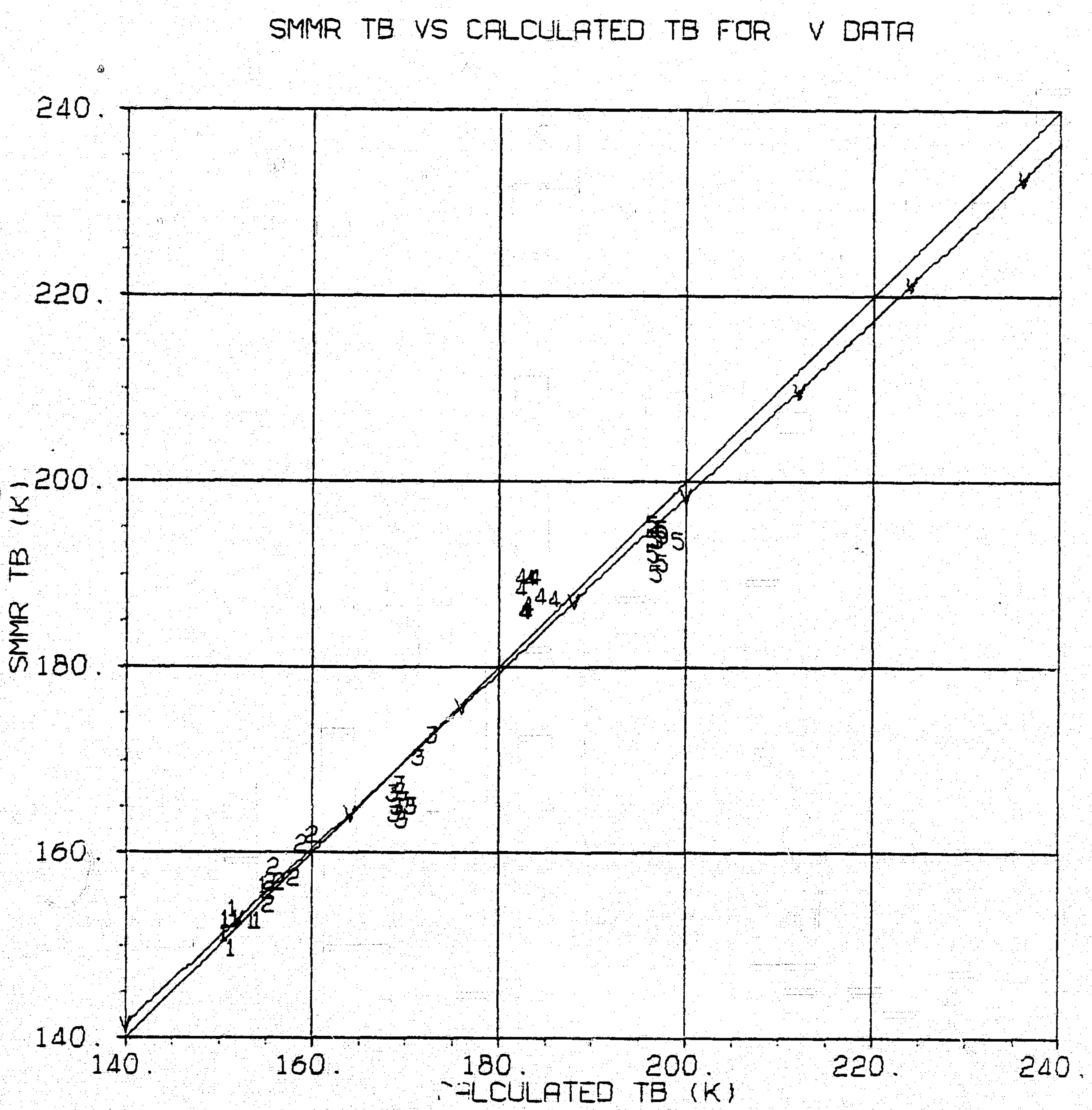

Figure 8.2

Run 2

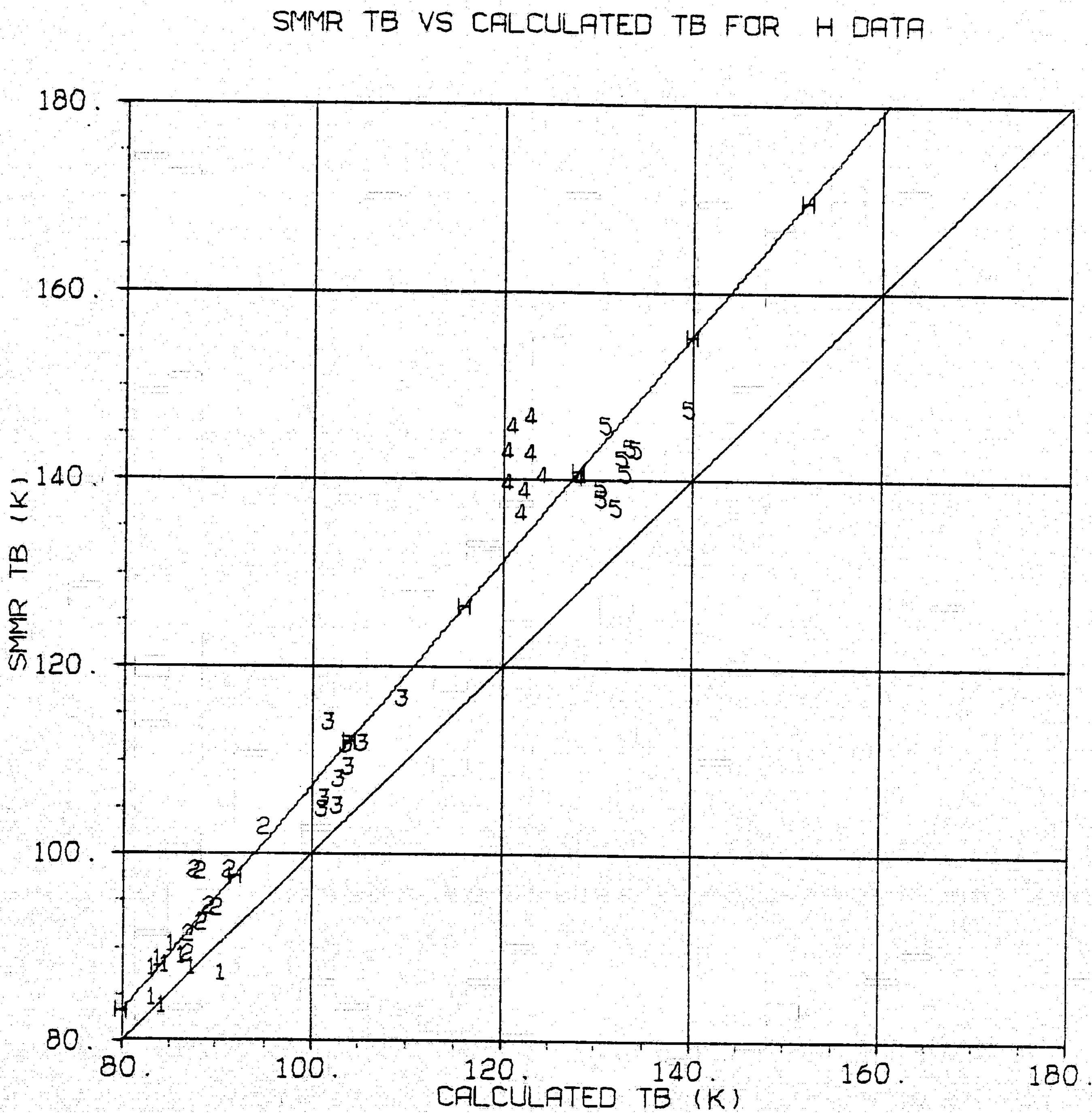

Figure 8.3

Run 2

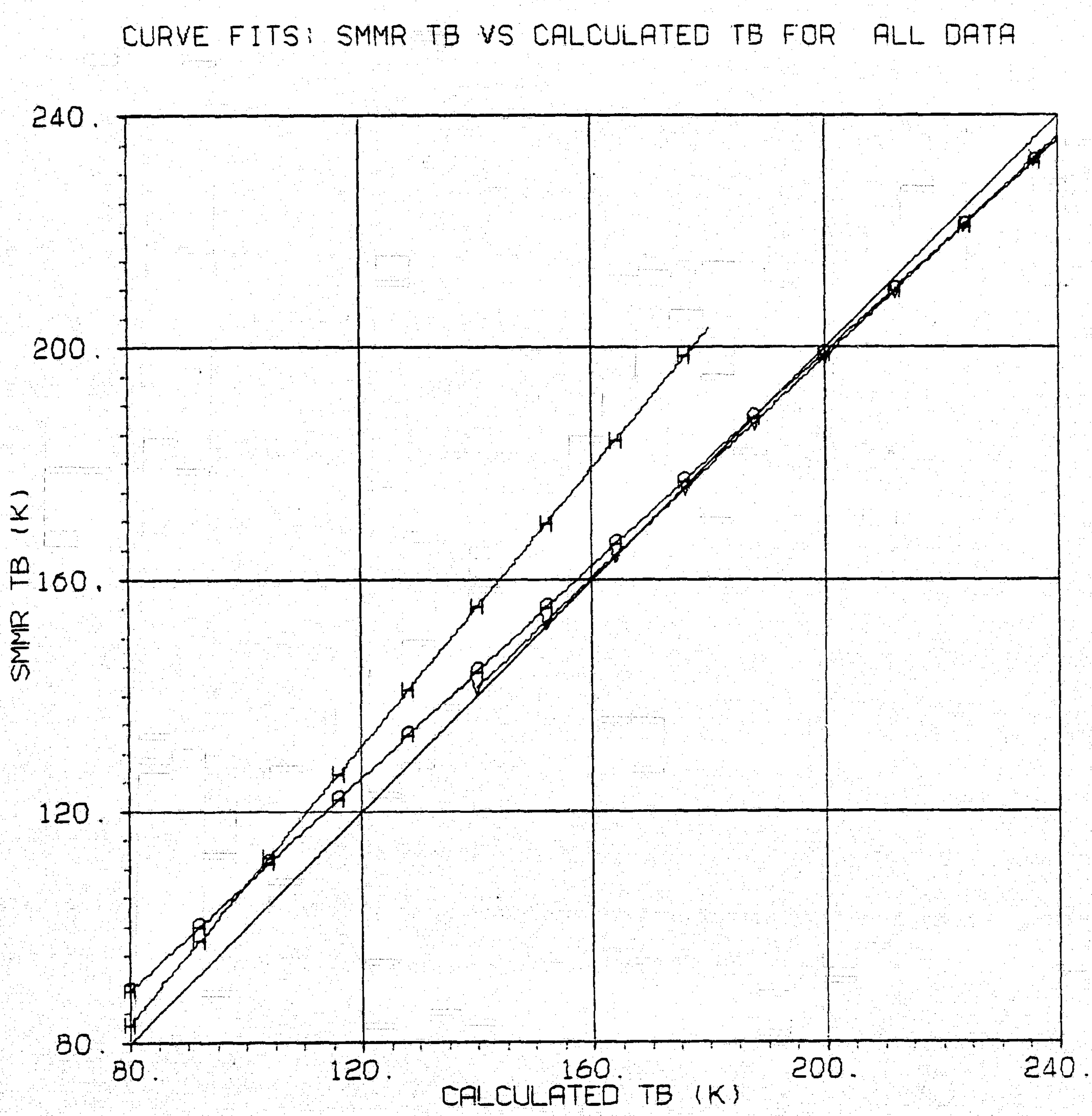

Table 9

Run 3 Statistical Summary

CURVE FITS FOR SMMR TB VS. CALCULATED TB

CHANNEL	CONSTANT TERM	LINEAR TERM	RMS
6.6 V	-145.11	1.96	1.097
6.6 H	-192.24	2.17	.494
10.69 V	157.43	.00	1.357
10.69 H	94.31	.00	3.749
18.0 V	167.34	.00	1.244
18.0 H	112.50	.00	4.336
21.0 V	583.57	-2.13	.706
21.0 H	151.73	.00	5.076
37.0 V	199.02	.00	2.141
37.0 H	146.40	.00	4.804
ALL V	-15.90	1.11	4.256
ALL H	-24.46	1.36	7.582
ALL V+H	18.53	.92	9.126

DISPERSION ABOUT LINE OF UNIT SLOPE

CHANNEL	BIAS	RMS ABOUT BIASED CURVE
6.6 V	1.26	1.419
6.6 H	5.89	1.307
10.69 V	1.00	1.530
10.69 H	6.15	4.058
18.0 V	-2.07	1.494
18.0 H	10.36	4.694
21.0 V	10.79	1.707
21.0 H	30.39	5.592
37.0 V	2.48	2.046
37.0 H	15.27	4.966
ALL V	2.69	4.622
ALL H	13.61	10.063
ALL V+H	8.15	9.547

Figure 9.1

Run 3

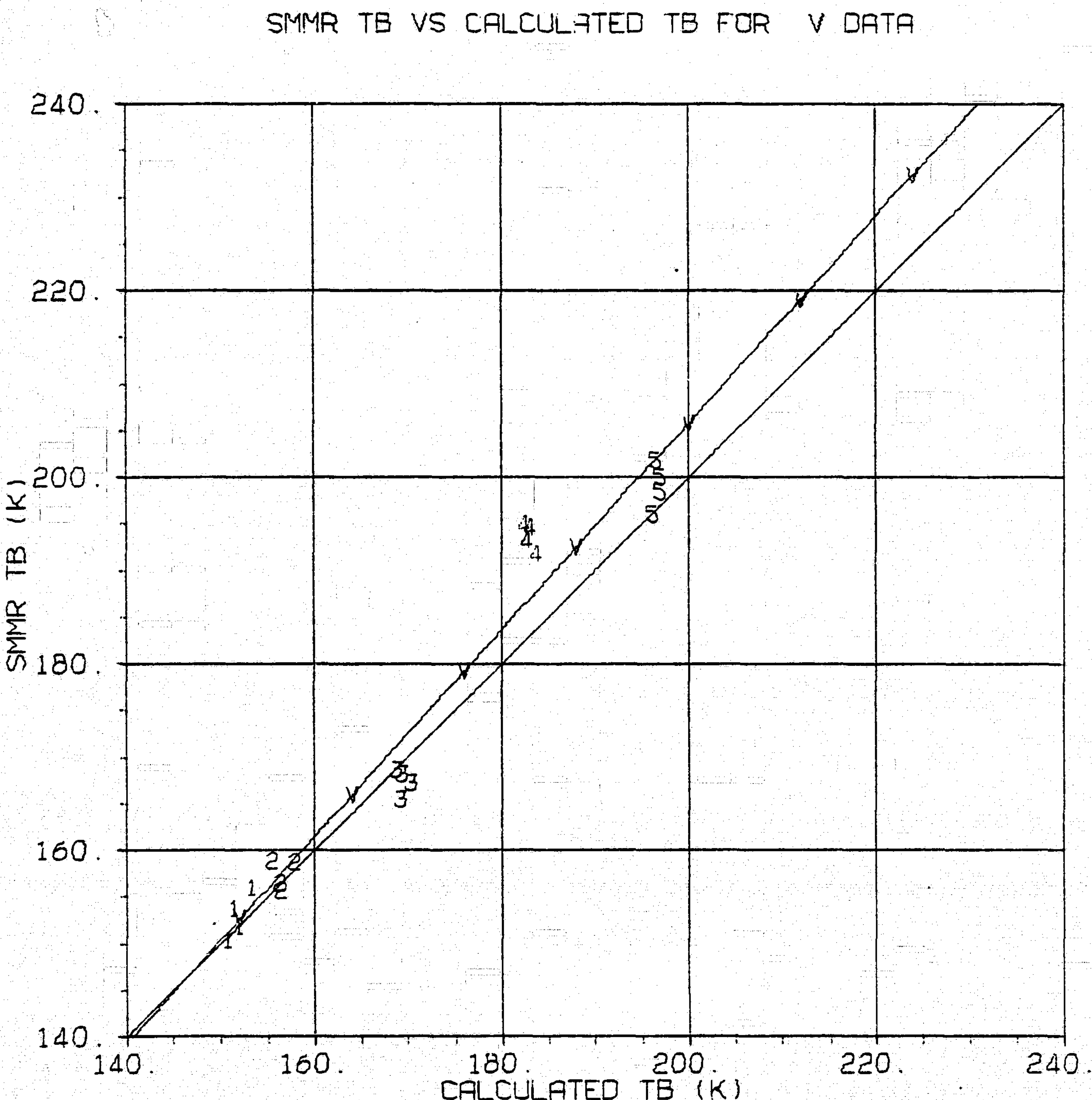

Figure 9.2

Run 3

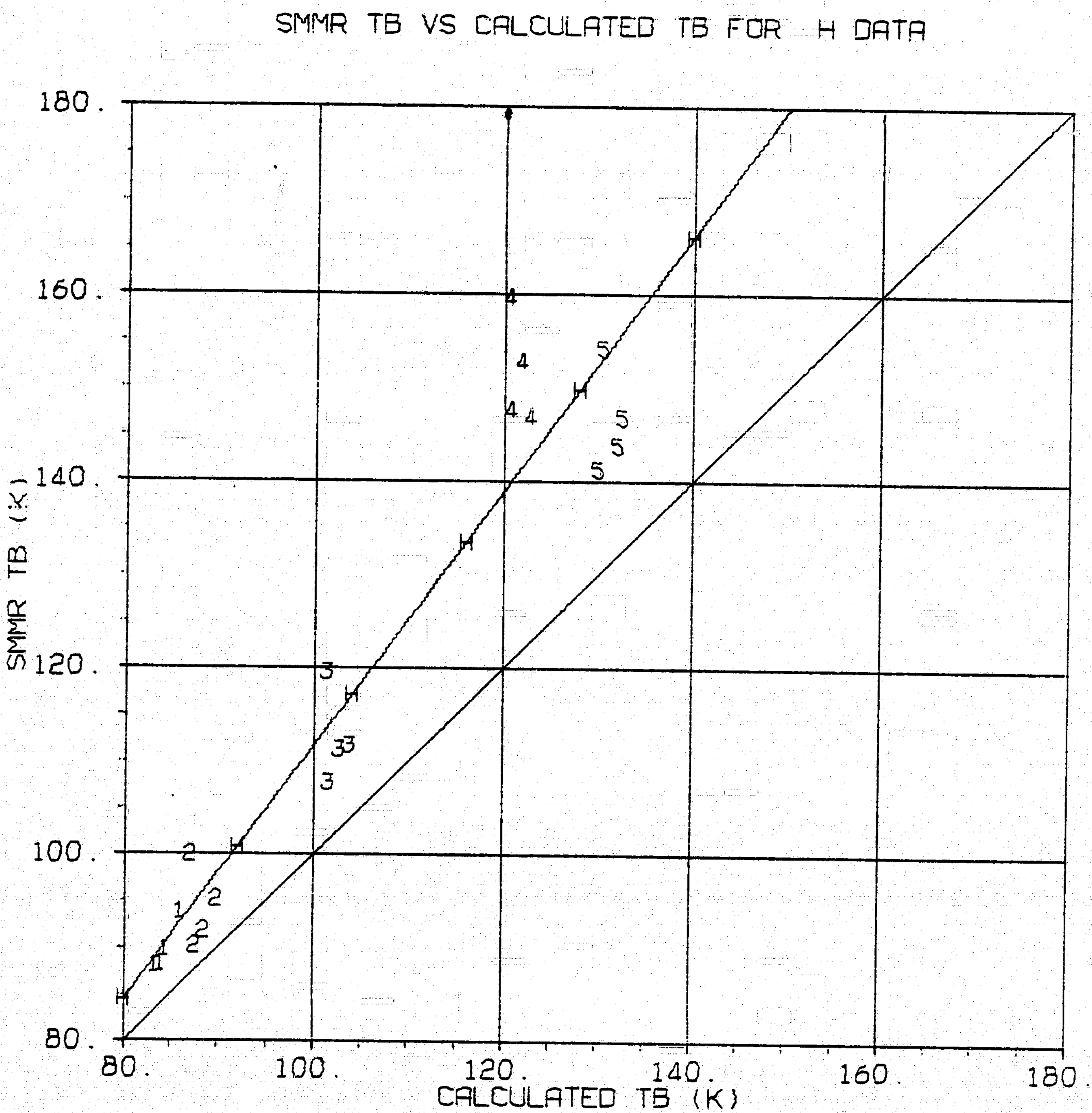

Figure 9.3

Run 3

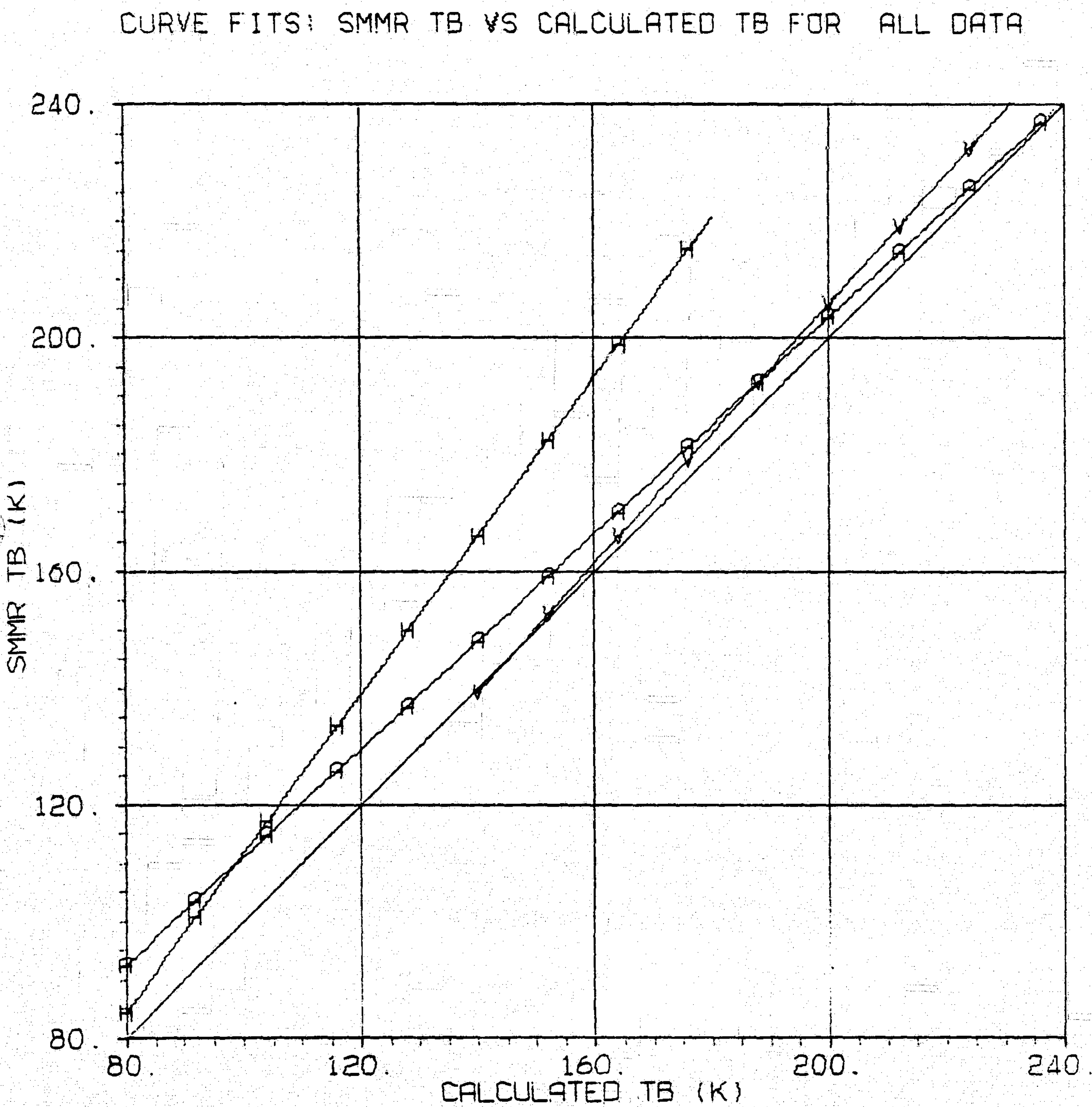

Table 10

Run 4 Statistical Summary

CURVE FITS FOR SMMR TB VS. CALCULATED TB

CHANNEL	CONSTANT TERM	LINEAR TERM	RMS
6.6 V	151.37	.00	1.709
6.6 H	32.28	.65	2.529
10.69 V	269.75	-.71	1.045
10.69 H	96.48	.00	2.343
18.0 V	170.51	.00	2.658
18.0 H	115.30	.00	3.378
21.0 V	198.37	.00	1.268
21.0 H	158.41	.00	3.427
37.0 V	198.14	.00	2.441
37.0 H	148.27	.00	6.633
ALL V	-18.61	1.13	5.817
ALL H	-31.55	1.44	9.212
ALL V+H	18.54	.93	10.984

DISPERSION ABOUT LINE OF UNIT SLOPE

CHANNEL	BIAS	RMS ABOUT BIASED CURVE
6.6 V	-.62	1.715
6.6 H	2.51	2.633
10.69 V	2.06	2.181
10.69 H	7.63	3.298
18.0 V	.76	3.038
18.0 H	12.38	3.354
21.0 V	15.15	1.754
21.0 H	36.33	3.568
37.0 V	1.29	2.408
37.0 H	16.21	6.355
ALL V	3.73	6.207
ALL H	15.01	12.294
ALL V+H	9.37	11.255

Figure 10.1

Run 4

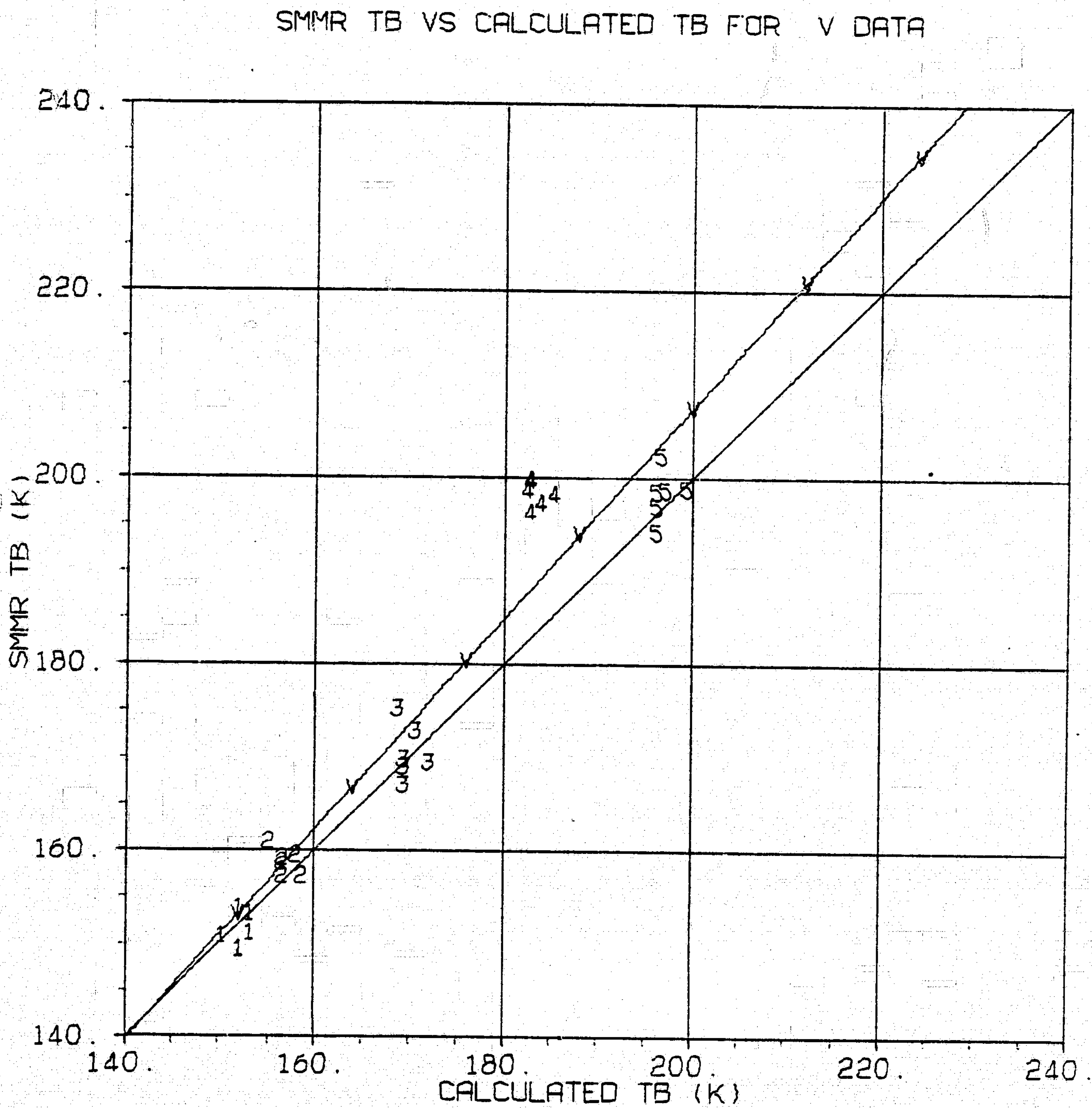

Figure 10.2

Run 4

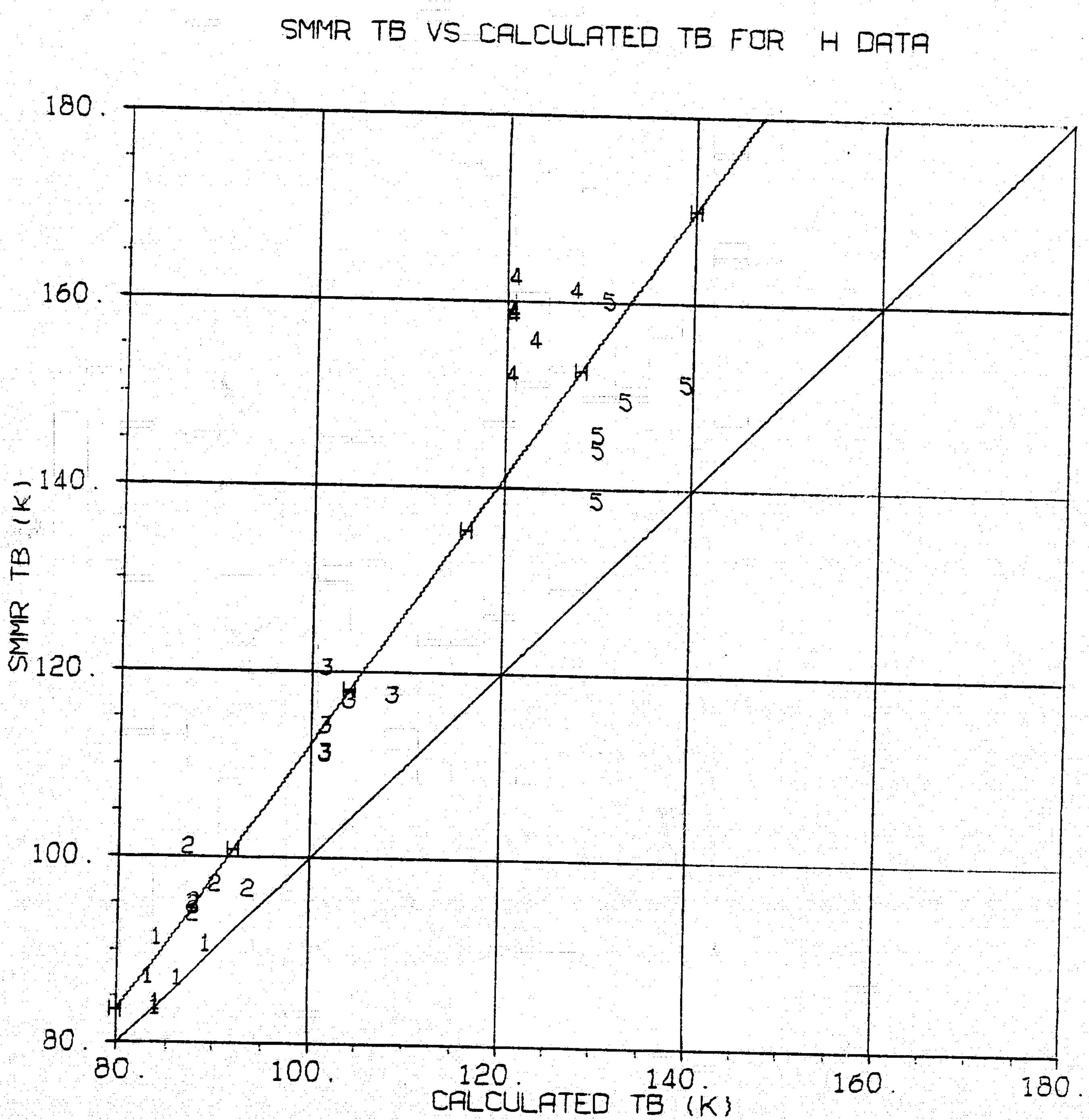

Figure 10.3

Run 4

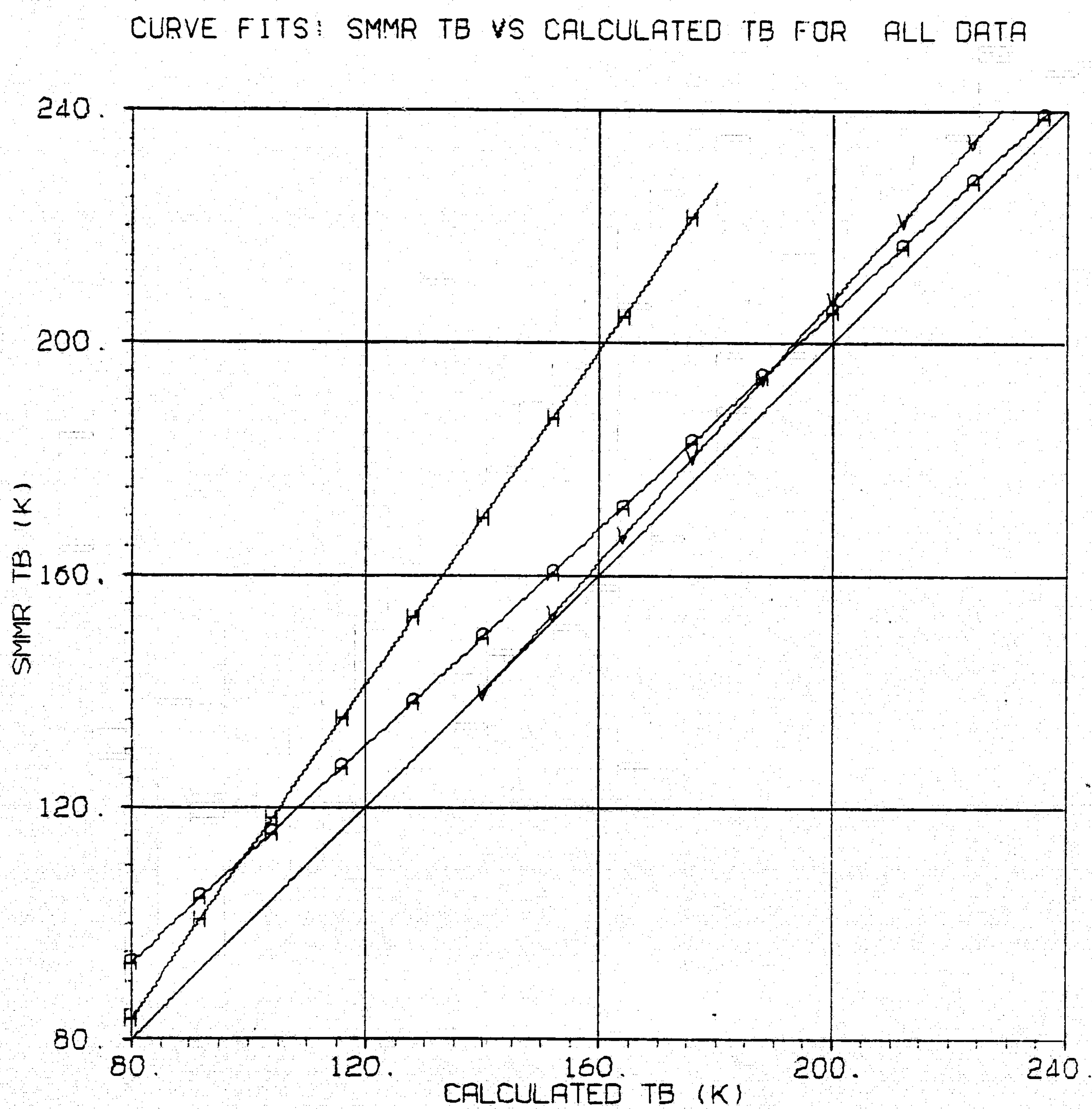

Table 11

Run 5 Statistical Summary

CURVE FITS FOR SMMR TB VS. CALCULATED TB

CHANNEL	CONSTANT TERM	LINEAR TERM	RMS
6.6 V	154.30	.00	1.825
6.6 H	56.35	.40	2.716
10.69 V	47.03	.73	1.987
10.69 H	16.90	.94	4.303
18.0 V	-89.12	1.56	4.676
18.0 H	-2.66	1.24	6.488
21.0 V	-69.57	1.52	4.459
21.0 H	-3.85	1.46	7.039
37.0 V	-245.69	2.30	7.559
37.0 H	-50.52	1.64	11.762
ALL V	-52.69	1.36	7.580
ALL H	-61.45	1.80	11.259
ALL V+H	23.71	.96	16.927

DISPERSION ABOUT LINE OF UNIT SLOPE

CHANNEL	BIAS	RMS ABOUT BIASED CURVE
6.6 V	1.53	1.883
6.6 H	4.35	3.186
10.69 V	3.76	2.029
10.69 H	11.82	4.306
18.0 V	7.21	4.749
18.0 H	23.25	6.542
21.0 V	25.40	4.511
21.0 H	53.27	7.195
37.0 V	12.47	7.779
37.0 H	36.34	12.069
ALL V	10.07	9.723
ALL H	25.81	18.954
ALL V+H	17.94	16.993

Figure 11.1

Run 5

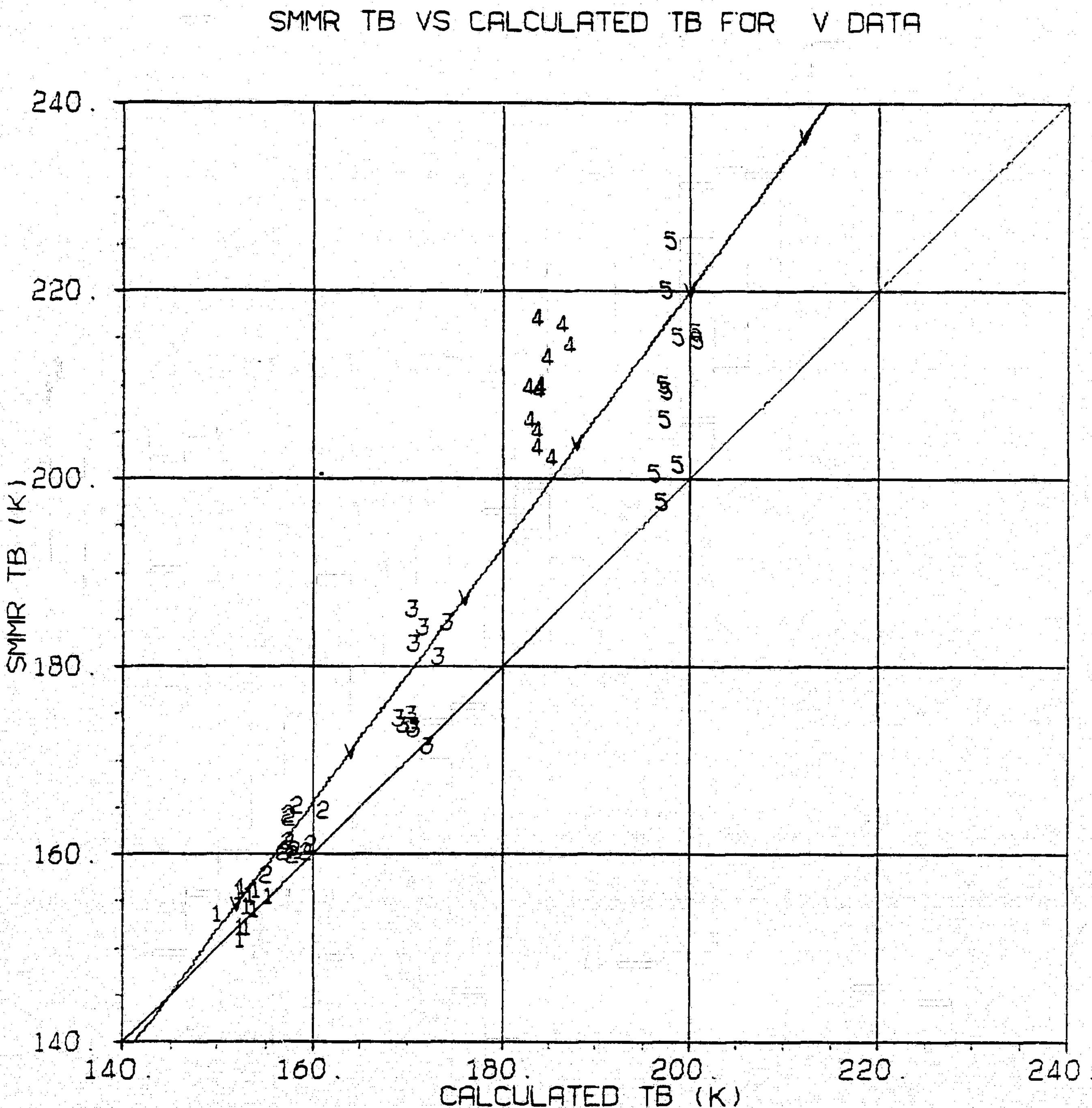

Figure 11.2

Run 5

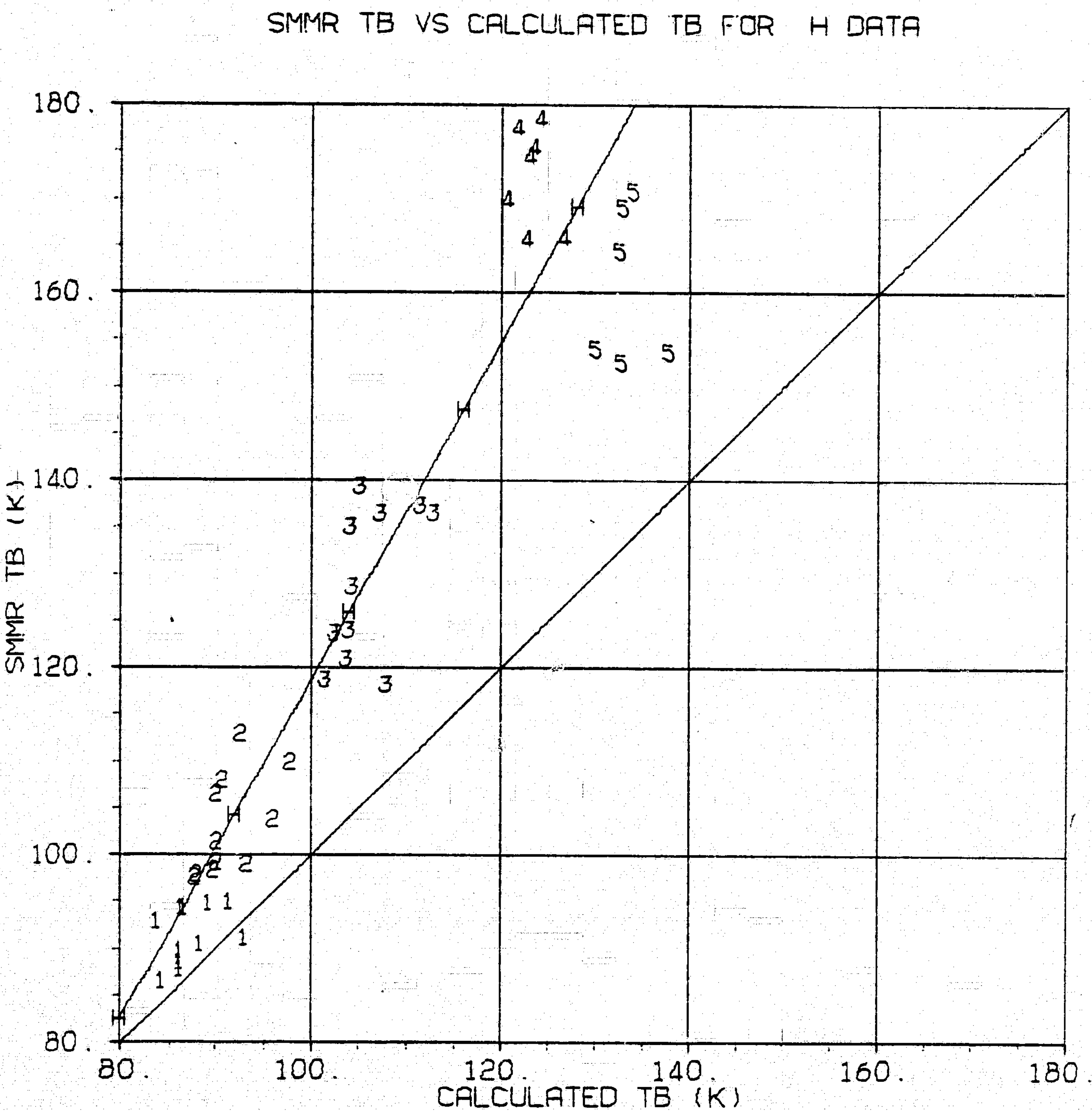

Figure 11.3

Run 5

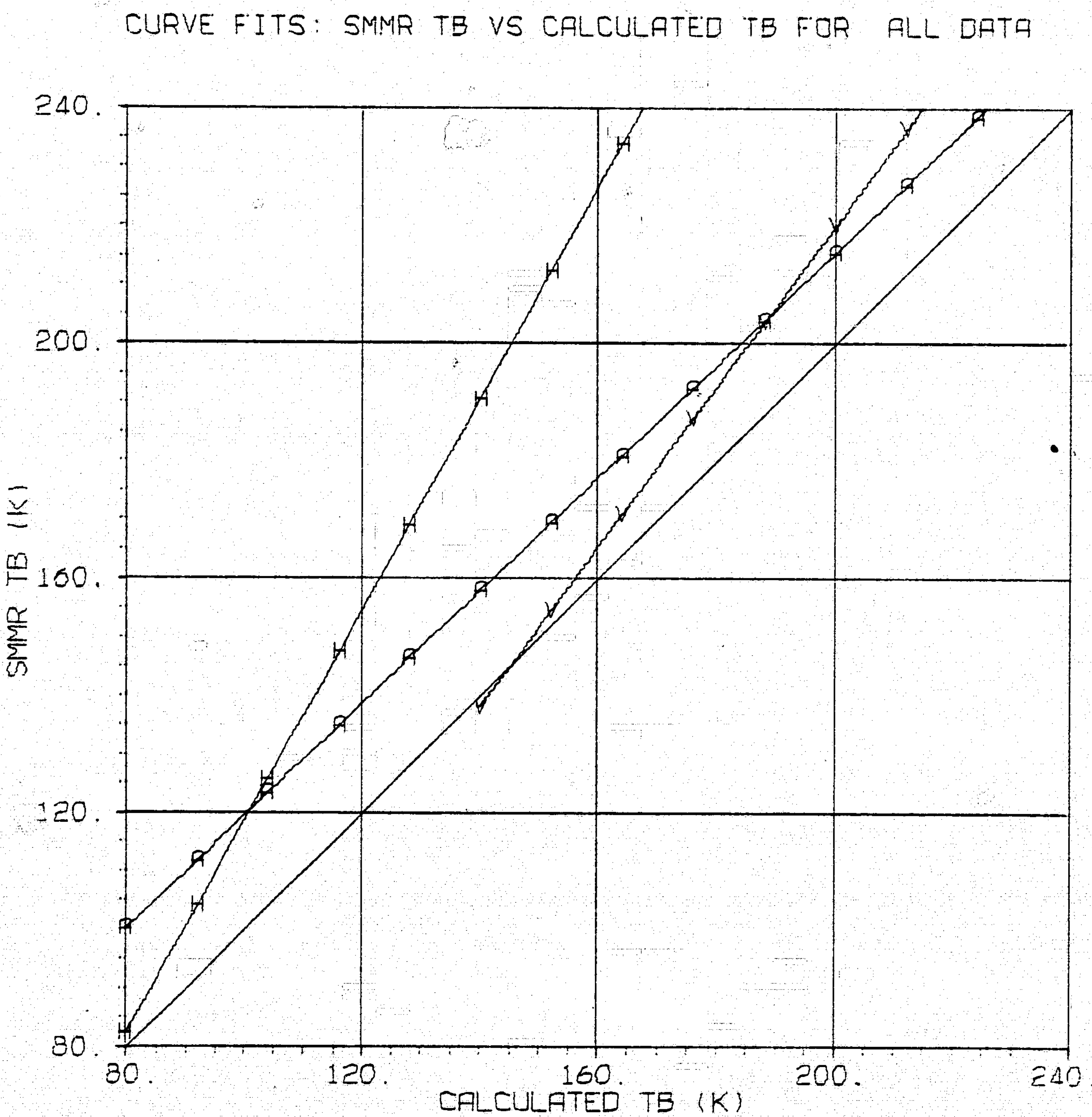

Table 12

Run 6 Statistical Summary

CURVE FITS FOR SHMR TB VS. CALCULATED TB

CHANNEL	CONSTANT TERM	LINEAR TERM	RMS
6.6 V	21.42	.86	1.931
6.6 H	34.92	.63	2.780
10.69 V	-4.69	1.04	2.130
10.69 H	-10.37	1.21	4.092
18.0 V	-224.36	2.32	5.560
18.0 H	-67.30	1.77	8.299
21.0 V	-361.11	3.03	10.132
21.0 H	-117.16	2.21	16.087
37.0 V	-327.99	2.67	8.086
37.0 H	-134.48	2.14	13.513
ALL V	-15.99	1.11	7.704
ALL H	-31.05	1.43	12.018
ALL V+H	18.64	.93	12.755

DISPERSION ABOUT LINE OF UNIT SLOPE

CHANNEL	BIAS	RMS ABOUT BIASED CURVE
6.6 V	.67	1.942
6.6 H	3.48	2.941
10.69 V	1.82	2.131
10.69 H	8.20	4.133
18.0 V	.05	5.860
18.0 H	12.28	8.615
21.0 V	11.83	10.439
21.0 H	31.74	16.455
37.0 V	2.18	8.325
37.0 H	18.26	14.130
ALL V	3.31	7.932
ALL H	14.79	14.472
ALL V+H	9.05	13.006

Figure 12.1

Run 6

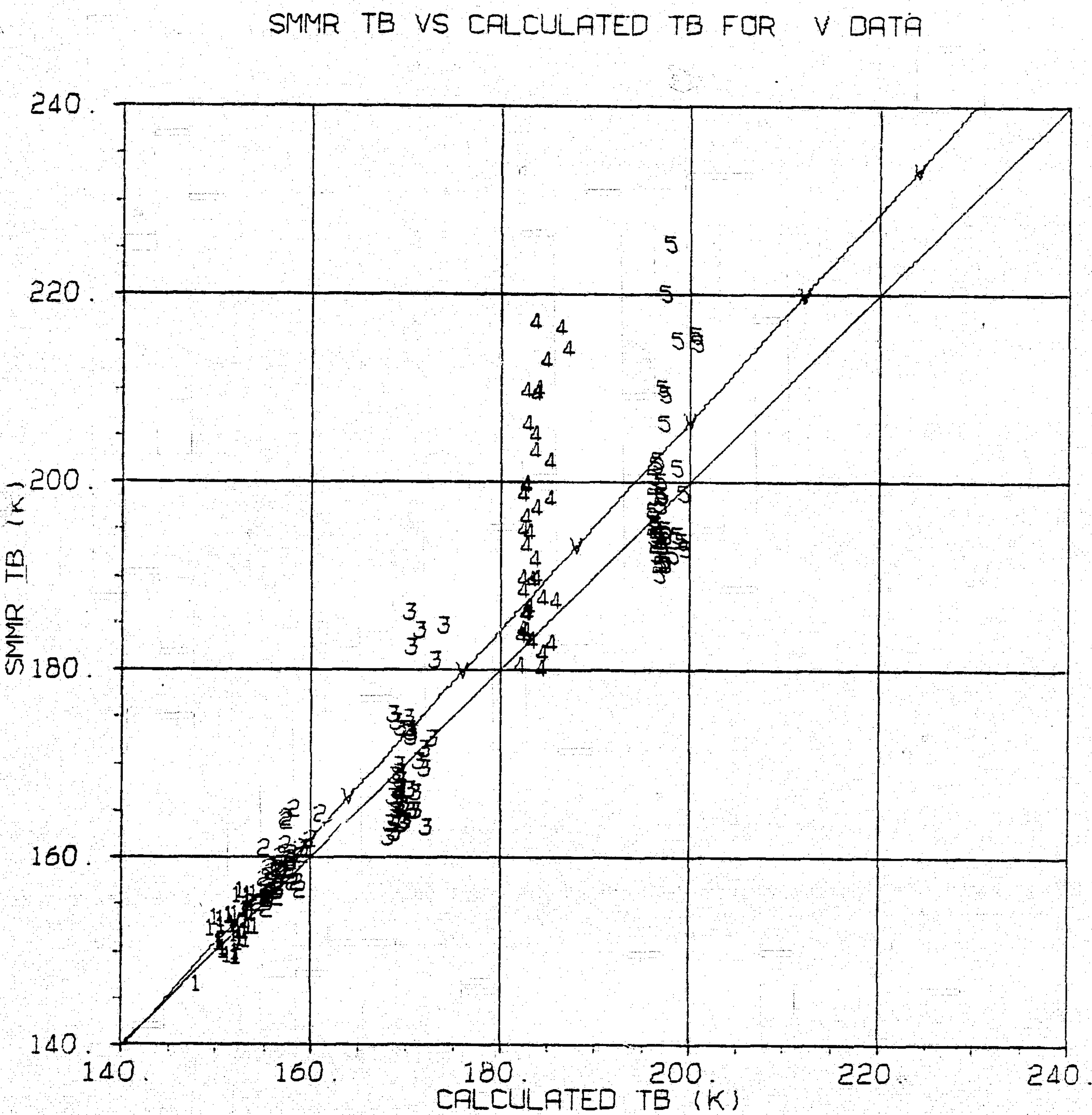

Figure 12.2

Run 6

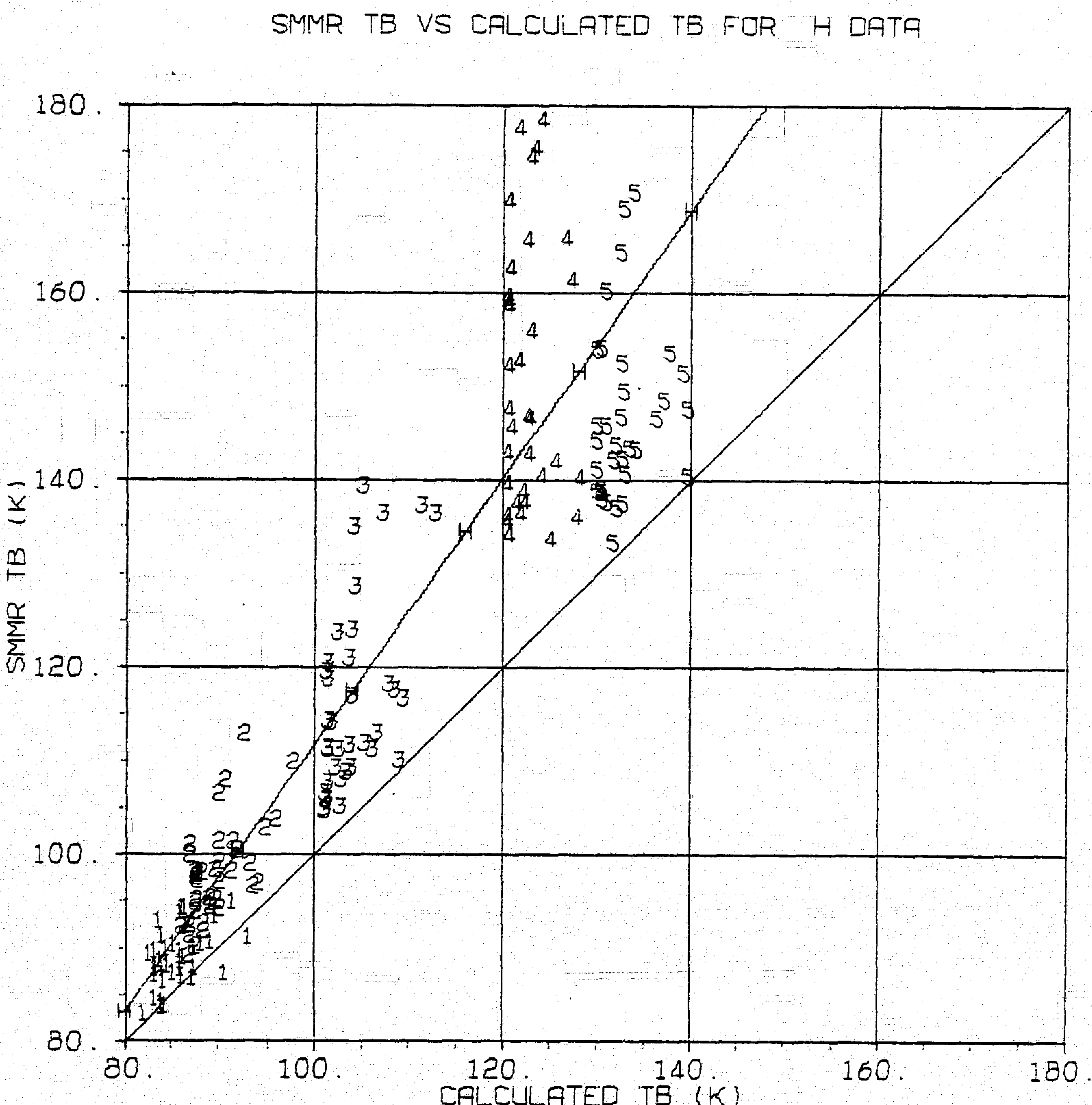

Figure 12.3

Run 6

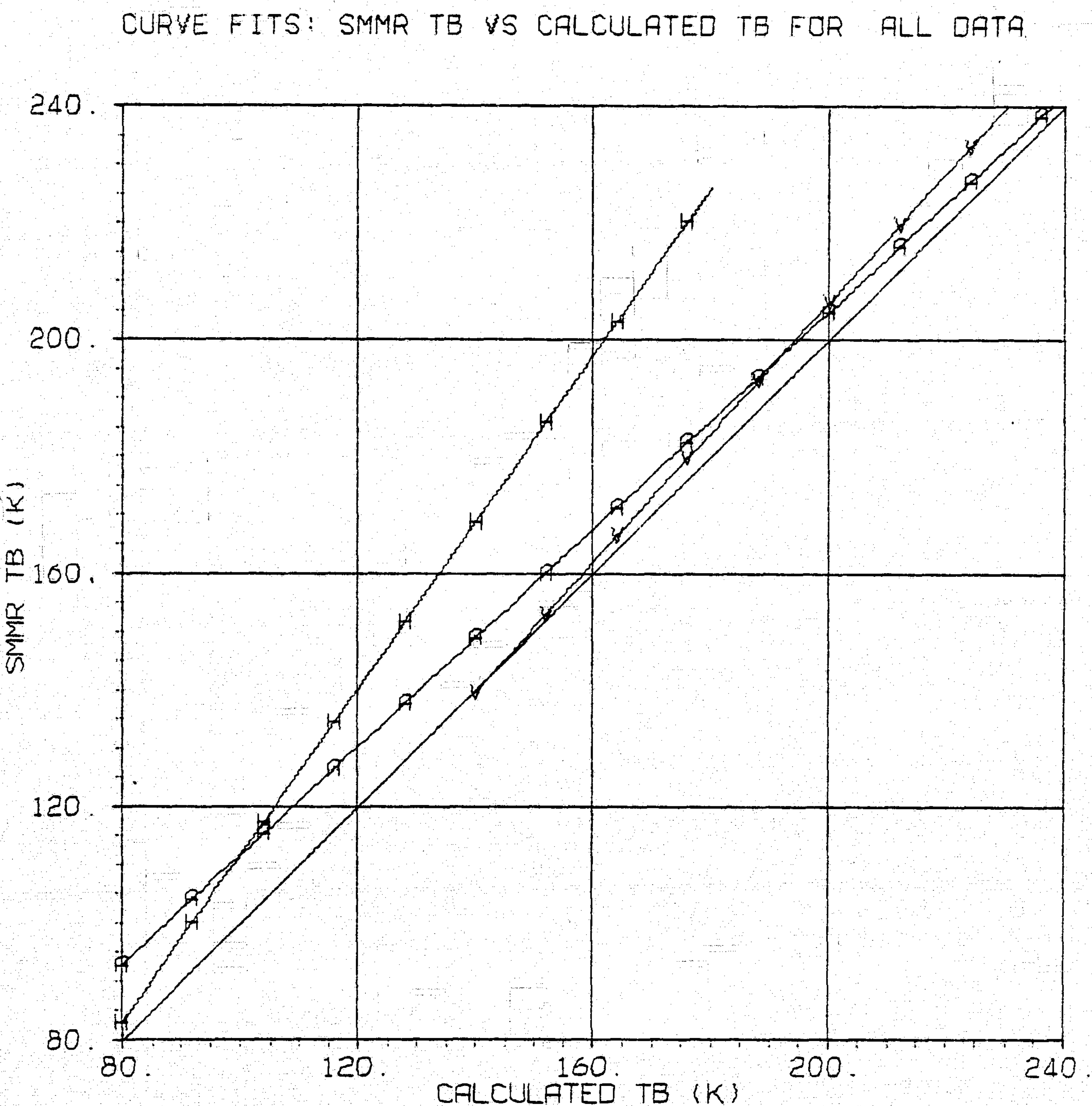

Table 13

Run 7 Statistical Summary

CURVE FITS FOR SMMR TB VS. CALCULATED TB

CHANNEL	CONSTANT TERM	LINEAR TERM	RMS
6.6 V	20.52	.87	1.932
6.6 H	34.18	.64	2.780
10.69 V	-8.22	1.05	2.130
10.69 H	-14.59	1.22	4.092
18.0 V	-274.42	2.50	5.557
18.0 H	-104.69	1.70	8.297
21.0 V	-589.13	3.70	10.080
21.0 H	-262.19	2.74	16.071
37.0 V	-429.79	3.07	8.072
37.0 H	-199.59	2.38	13.508
ALL V	17.34	.88	7.009
ALL H	2.99	1.00	10.926
ALL V+H	12.58	.91	9.385

DISPERSION ABOUT LINE OF UNIT SLOPE

CHANNEL	BIAS	RMS ABOUT BIASED CURVE
6.6 V	.12	1.942
6.6 H	2.66	2.933
10.69 V	.30	2.132
10.69 H	5.87	4.138
18.0 V	-7.65	5.890
18.0 H	.04	8.674
21.0 V	-5.87	10.485
21.0 H	2.91	16.572
37.0 V	-5.76	8.355
37.0 H	4.24	14.237
ALL V	-3.77	7.455
ALL H	3.14	10.926
ALL V+H	-.31	9.972

Figure 13.1

Run 7

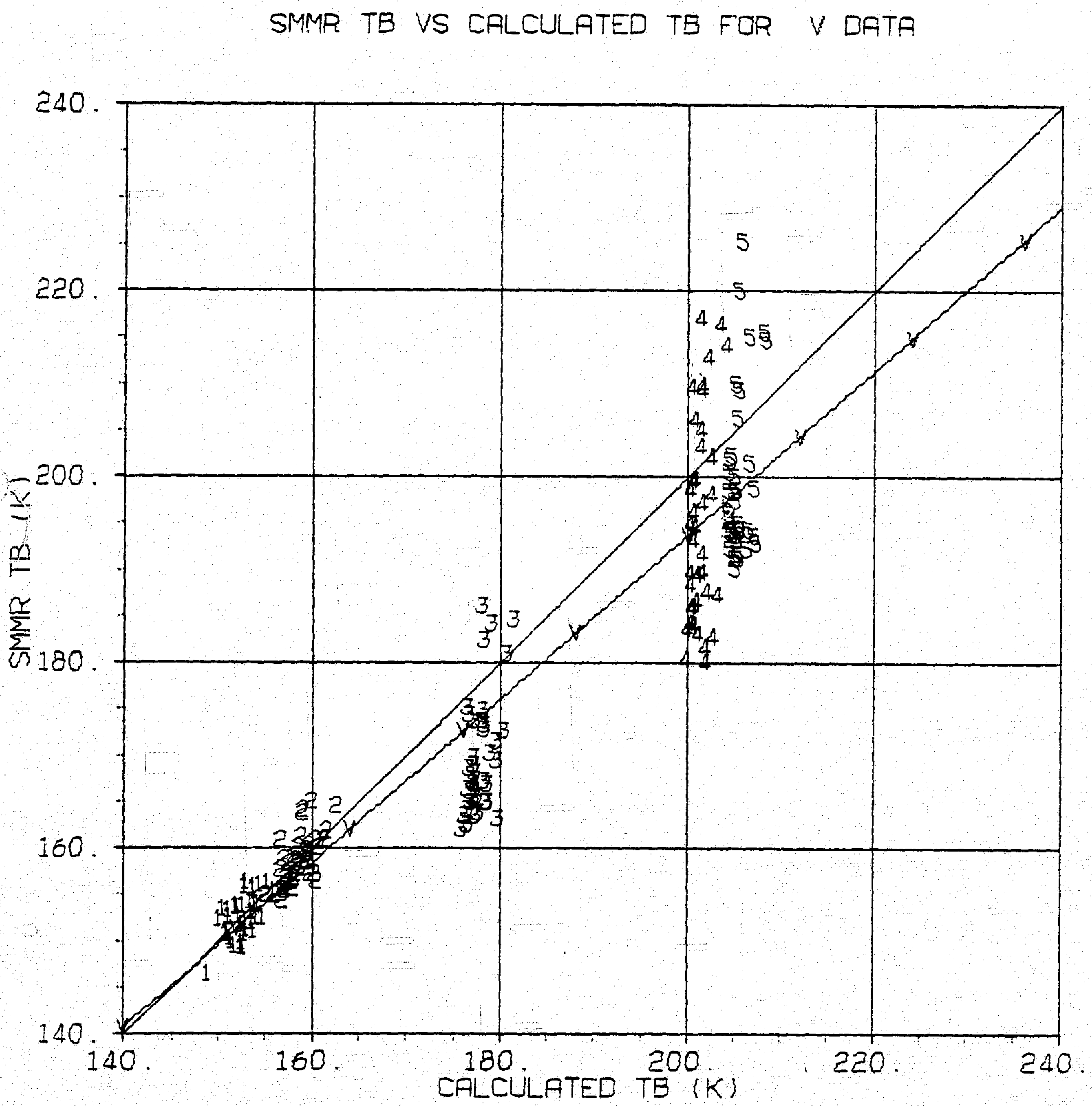

Figure 13.2

Run 7

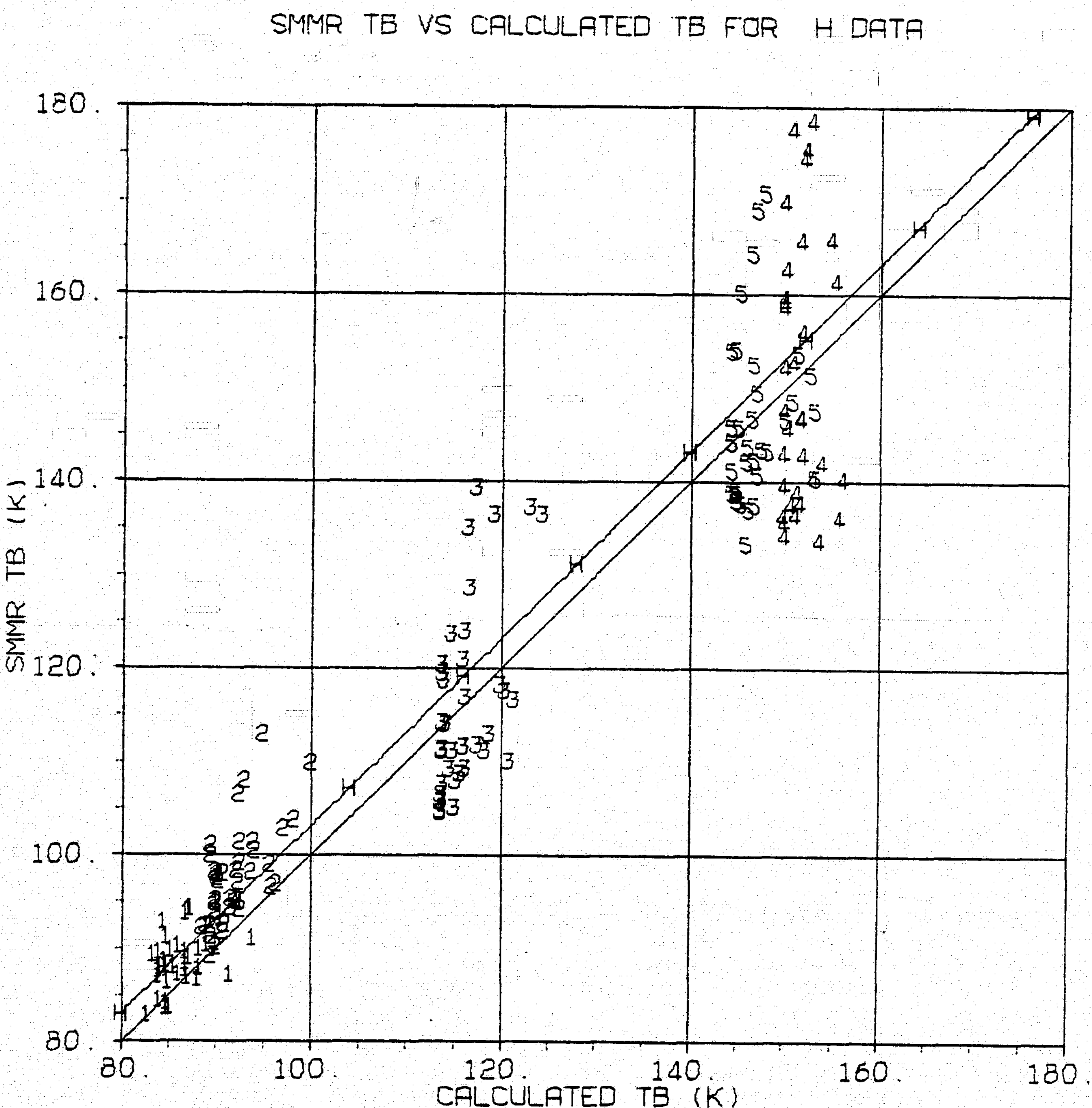

Figure 13.3

Run 7

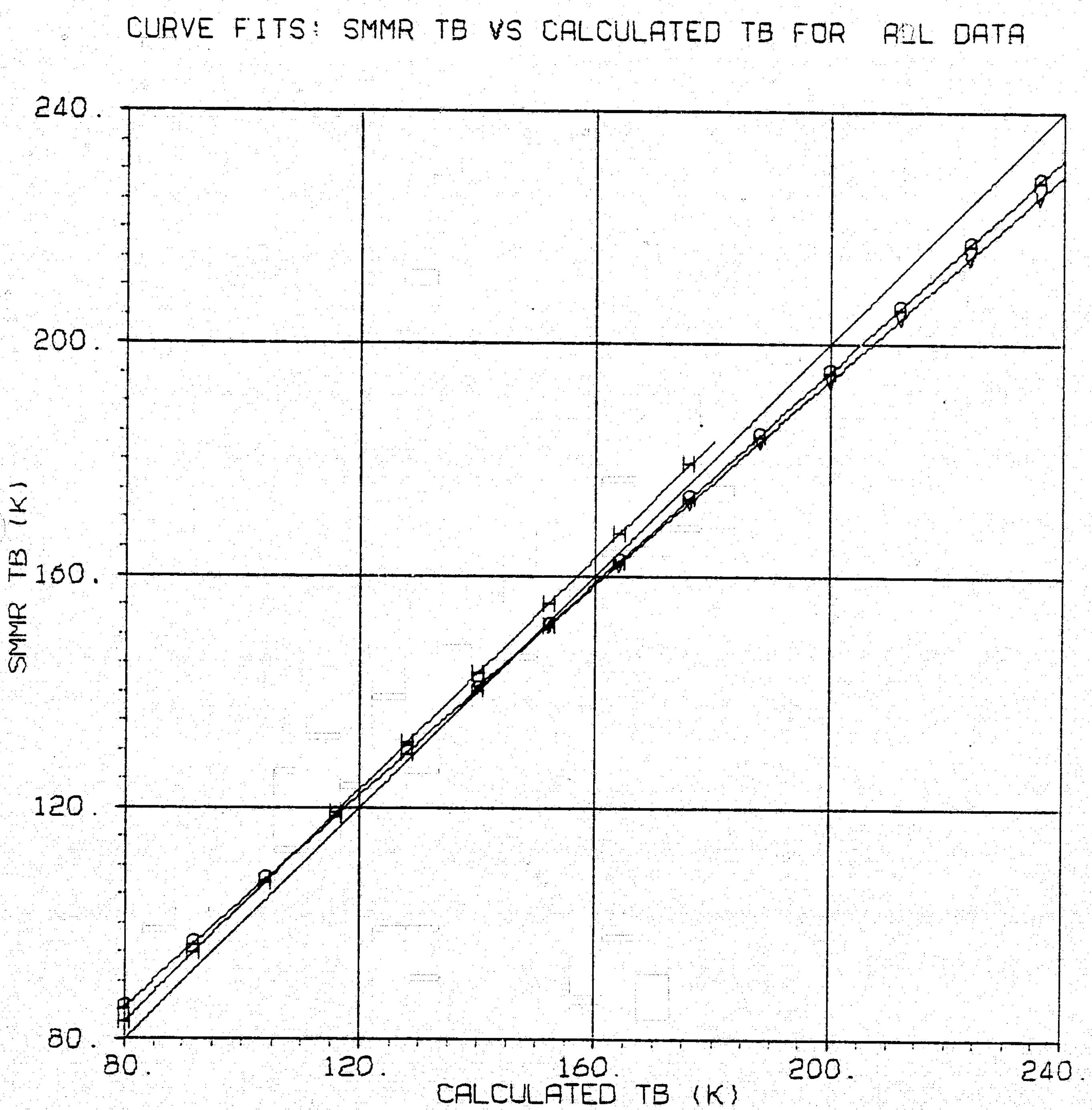

Table 14

Run 8 Statistical Summary

CURVE FITS FOR SMMR TB VS. CALCULATED TB

CHANNEL	CONSTANT TERM	LINEAR TERM	RMS
6.6 V	152.80	.00	2.008
6.6 H	-20.58	1.28	2.865
10.69 V	-178.13	2.15	2.741
10.69 H	-163.40	2.92	4.165
18.0 V	-342.51	2.96	2.655
18.0 H	-294.14	3.75	4.911
21.0 V	-214.94	2.12	3.157
21.0 H	-132.26	2.06	6.170
37.0 V	-937.68	5.66	5.220
37.0 H	-460.75	4.38	6.147
ALL V	-4.43	1.03	6.387
ALL H	-15.96	1.23	8.930
ALL V+H	13.31	.95	9.739

DISPERSION ABOUT LINE OF UNIT SLOPE

CHANNEL	BIAS	RMS ABOUT BIASED CURVE
6.6 V	1.24	1.684
6.6 H	2.98	2.910
10.69 V	2.39	2.994
10.69 H	9.70	5.443
18.0 V	-1.28	4.793
18.0 H	8.69	10.121
21.0 V	1.27	6.385
21.0 H	15.30	10.384
37.0 V	2.04	11.050
37.0 H	16.43	13.742
ALL V	1.13	6.417
ALL H	10.62	10.544
ALL V+H	5.88	9.934

Figure 14.1

Run 8

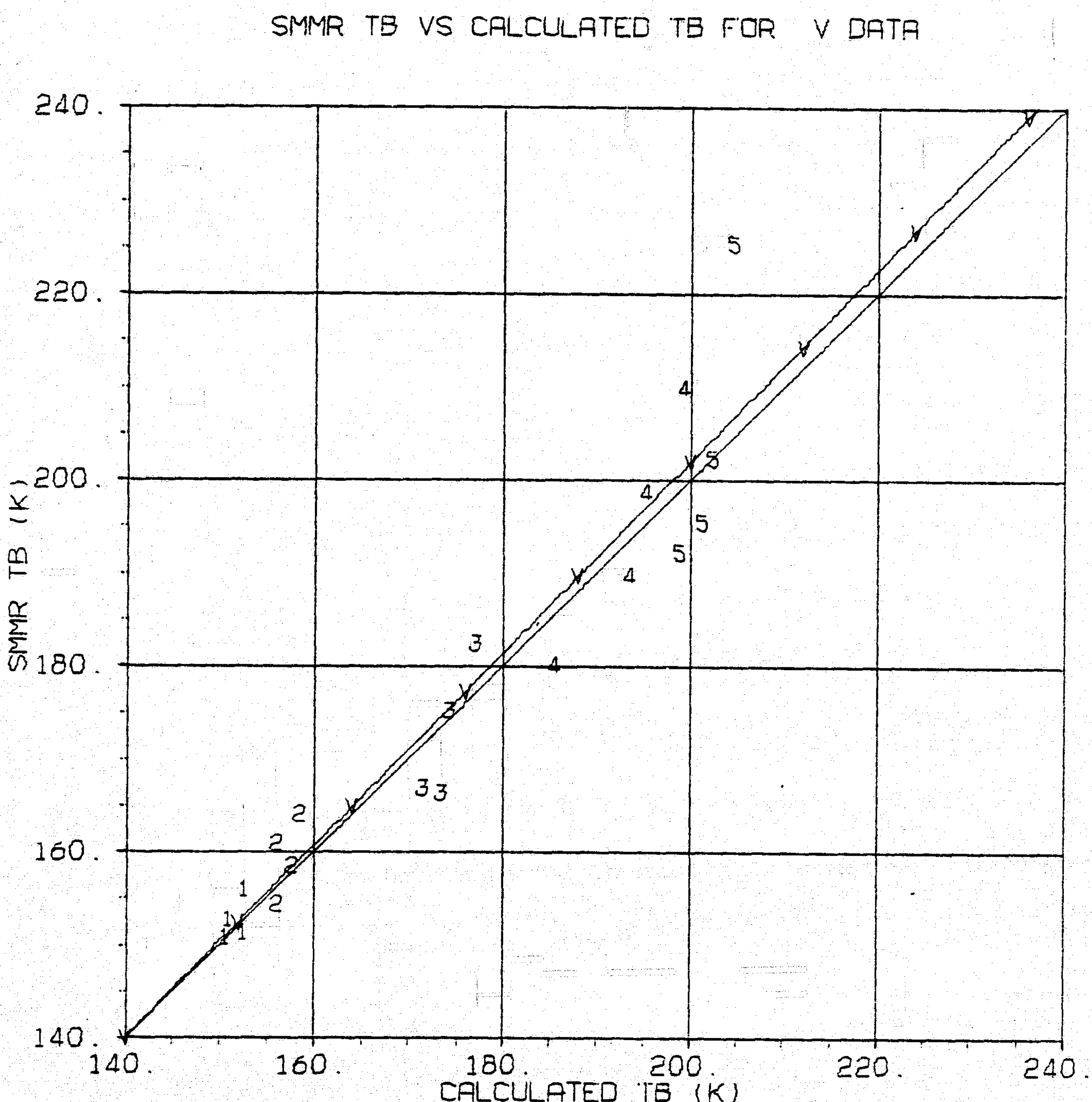

Figure 14.2

Run 8

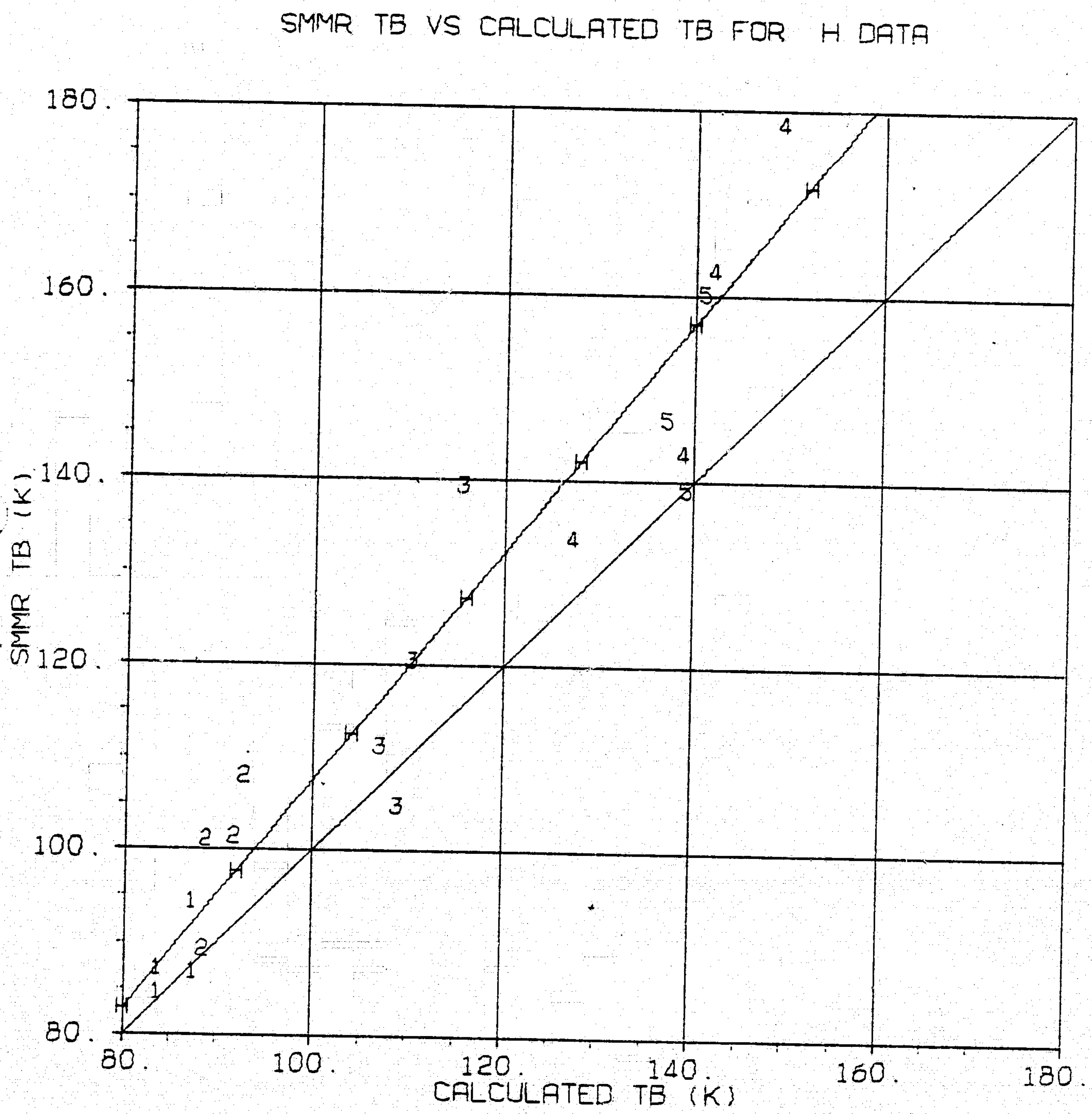

Figure 14.3

Run 8

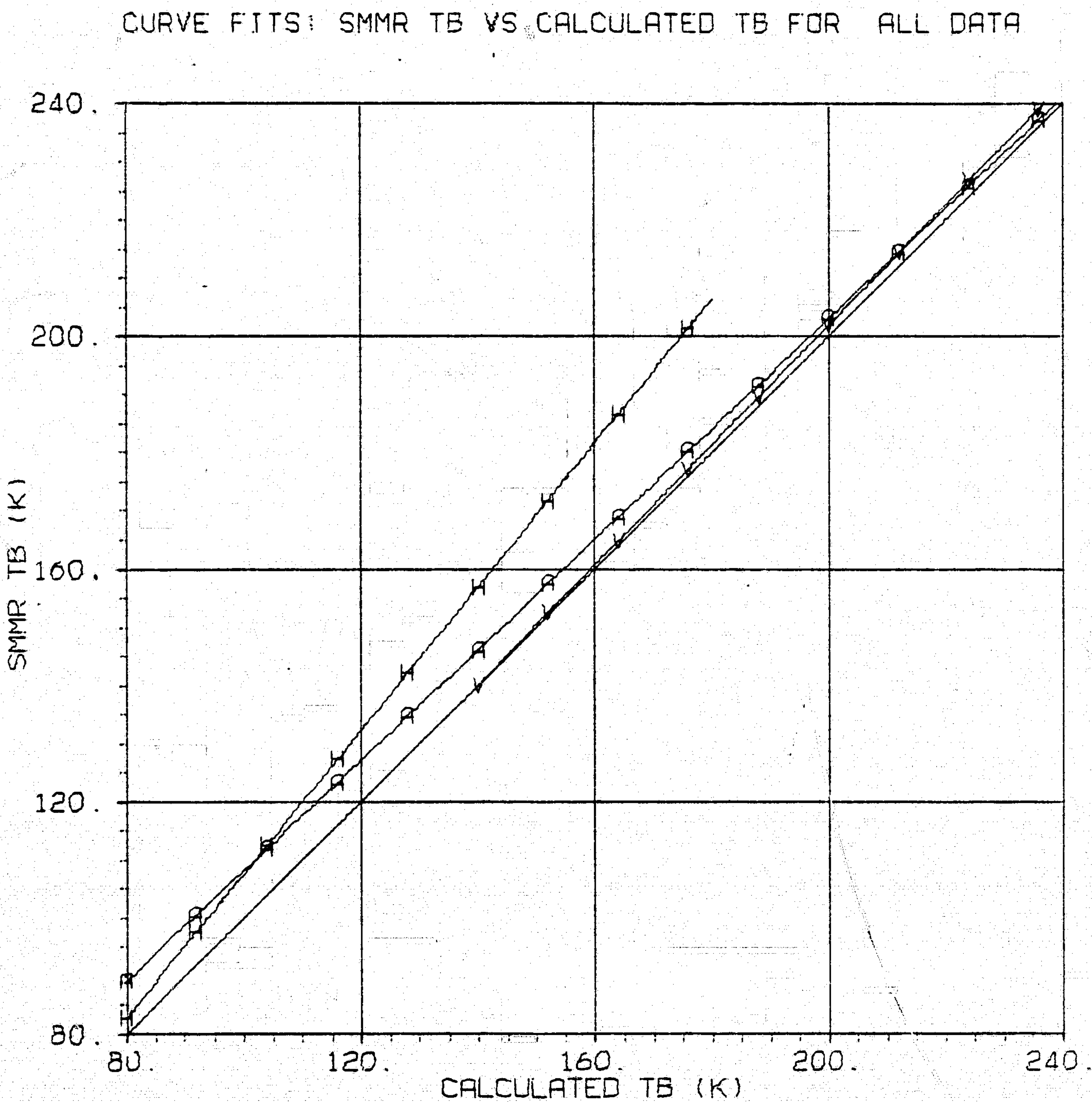

Table 15.1

Run 9

CURVE FITS FOR SMMR 6.6 GHZ TB VERSUS CELL NUMBER

BLOCK	ROW	AVERAGE LATITUDE	V POL. LINEAR TERM	V POL. CONSTANT TERM	V POL. RMS	H POL. LINEAR TERM	H POL. CONSTANT TERM	H POL. RMS
1	1	-24.68	.000	154.272	.158	-1.064	90.025	.245
	2	-23.43	-.050	154.770	.058	-1.112	90.585	.344
	3	-22.17	-.306	155.775	.301	-1.270	91.255	.378
	4	-20.92	.000	154.670	.212	-1.080	90.705	.569
2	1	-19.66	-.184	155.210	.222	-1.124	90.690	.548
	2	-18.40	-.193	155.280	.141	-1.078	90.995	.447
	3	-17.13	.000	154.610	.110	-1.239	91.350	.364
	4	-15.87	-.154	155.030	.111	-1.253	91.210	.347
3	1	-14.60	.000	154.630	.343	-1.018	91.000	.555
	2	-13.34	-.105	155.400	.114	-1.202	91.110	.225
	3	-12.07	.000	155.062	.256	-1.269	91.320	.457
	4	-10.80	.000	154.902	.307	-1.328	91.380	.576
4	1	-9.53	.000	154.725	.084	-1.086	90.340	.360
	2	-8.25	.000	154.267	.093	-1.235	90.250	.283
	3	-6.98	.000	154.120	.191	-1.217	90.120	.325
	4	-5.71	-.169	154.345	.233	-1.686	91.380	.360
5	1	-4.44	-.336	154.430	.143	-1.520	90.295	.352
	2	-3.16	.000	153.707	.304	-1.567	90.500	.542
	3	-1.89	.000	153.327	.189	-1.604	90.220	.506
	4	-.61	.000	153.002	.231	-1.482	89.585	.507
6	1	.65	.413	152.085	.162	-.979	88.765	.380
	2	1.93	.548	153.380	.262	-.858	89.450	.509
	3	3.21	.649	154.390	.185	-.824	90.495	.376
	4	4.48	.690	154.585	.240	-.578	89.735	.205
7	1	5.76	1.000	153.930	.119	-.256	89.325	.295
	2	7.04	.952	154.155	.189	-.304	89.865	.413
	3	8.32	.897	154.975	.077	-.592	91.440	.353
	4	9.59	.516	156.305	.301	-.813	92.350	.651
8	1	10.87	.459	157.015	.713	-1.373	94.335	1.036
	2	12.15	.283	157.740	.397	-1.818	95.495	.807
	3	13.42	.000	158.770	.372	-2.268	97.015	.345
	4	14.70	-.630	160.960	.168	-2.737	98.410	.272

Table 15.2

Run 9

CURVE FITS FOR SMMR 10.69 GHZ TB VERSUS CELL NUMBER

			V POL.			H POL.		
BLOCK	ROW	AVERAGE LATITUDE	LINEAR TERM	CONSTANT TERM	RMS	LINEAR TERM	CONSTANT TERM	RMS
1	1	-24.95	-.080	158.779	.279	.000	93.031	.537
	2	-24.23	-.250	159.464	.289	-.161	93.727	.403
	3	-23.52	-.253	159.756	.391	-.095	93.870	.372
	4	-22.80	-.313	160.444	.409	.000	94.076	.505
	5	-22.08	-.440	160.979	.296	-.322	95.236	.409
	6	-21.36	-.259	159.821	.499	.000	93.437	.366
	7	-20.64	-.206	159.689	.419	.174	92.851	.592
2	1	-19.93	-.515	161.089	.711	.000	93.604	.406
	2	-19.20	-.321	160.401	.288	-.203	95.179	.416
	3	-18.49	-.307	160.381	.290	.000	94.413	.326
	4	-17.76	-.243	159.816	.644	.000	93.814	.383
	5	-17.04	-.175	159.571	.536	.000	93.697	.362
	6	-16.32	-.386	160.160	.371	-.200	94.546	.389
	7	-15.59	-.319	159.687	.157	.000	93.447	.342
3	1	-14.87	-.268	159.467	.506	.000	93.344	.295
	2	-14.15	-.226	159.769	.653	-.110	94.229	.188
	3	-13.42	-.429	160.804	.231	-.164	94.384	.324
	4	-12.70	-.394	160.271	.252	-.163	94.257	.356
	5	-11.98	-.334	159.987	.176	-.156	94.184	.193
	6	-11.25	-.329	159.989	.515	-.123	94.013	.202
	7	-10.52	-.184	159.344	.522	.000	93.087	.392
4	1	-9.80	-.279	159.666	.422	.000	92.864	.318
	2	-9.07	-.314	159.637	.161	-.120	93.066	.145
	3	-8.34	-.314	159.174	.308	-.151	93.081	.348
	4	-7.62	-.166	158.500	.131	.000	92.269	.512
	5	-6.89	-.196	158.623	.583	-.133	93.024	.212
	6	-6.17	-.431	159.607	.451	-.283	94.044	.303
	7	-5.44	-.547	159.866	.387	-.436	93.937	.443
5	1	-4.71	-.422	159.200	.193	-.325	93.054	.446
	2	-3.98	-.241	158.530	.498	-.099	92.300	.249
	3	-3.25	-.321	159.007	.557	-.202	92.897	.439
	4	-2.52	-.305	158.760	.489	.000	92.089	.290
	5	-1.79	-.245	158.400	.661	.000	91.563	.136
	6	-1.07	-.201	157.639	.571	-.106	91.330	.315
	7	-.34	-.138	157.183	.324	.000	90.887	.386

Table 15.2 Continued

Run 9

CURVE FITS FOR SMMR 10.69 GHZ TB VERSUS CELL NUMBER

BLOCK	ROW	AVERAGE LATITUDE	V POL. LINEAR TERM	V POL. CONSTANT TERM	V POL. RMS	H POL. LINEAR TERM	H POL. CONSTANT TERM	H POL. RMS
6	1	.39	.000	156.876	.333	.269	90.277	.272
	2	1.11	.000	157.753	.569	.317	90.210	.269
	3	1.84	.000	158.557	.628	.369	90.909	.170
	4	2.57	.000	159.737	.569	.337	92.111	.102
	5	3.30	.182	159.477	.359	.431	92.471	.170
	6	4.03	.117	159.644	.209	.369	92.704	.222
	7	4.76	.192	159.549	.344	.596	91.679	.401
7	1	5.49	.341	159.257	.311	.741	91.537	.393
	2	6.22	.326	159.337	.466	.829	91.344	.088
	3	6.95	.383	159.560	.498	.808	92.060	.512
	4	7.68	.281	160.787	.409	.745	93.646	.283
	5	8.41	.256	161.274	.294	.720	94.379	.355
	6	9.14	.294	161.236	.261	.699	94.910	.332
	7	9.87	.000	162.507	.628	.290	96.576	.865
8	1	10.60	.000	163.759	2.134	.000	99.384	3.052
	2	11.33	.000	163.770	1.736	.000	99.560	2.197
	3	12.06	-.242	164.480	.872	-.261	100.079	.930
	4	12.79	.000	164.046	1.333	-.510	101.257	.656
	5	13.52	-.637	166.846	.776	-1.261	104.887	1.046
	6	14.25	-1.281	170.323	.510	-2.725	112.474	1.717
	7	14.98	-1.544	171.316	1.067	-2.935	113.151	3.076

Table [illegible].3

Run 9

CURVE FITS FOR SMMR 18.0 GHZ TB VERSUS CELL NUMBER

			V POL.			H POL.		
BLOCK	ROW	AVERAGE LATITUDE	LINEAR TERM	CONSTANT TERM	RMS	LINEAR TERM	CONSTANT TERM	RMS
1	1	-25.08	.371	164.714	.966	-.455	111.494	1.413
	2	-24.63	.455	164.193	.722	-.210	110.443	.860
	3	-24.17	.204	165.398	.767	-.650	112.651	.891
	4	-23.71	.158	166.418	.807	-.778	113.851	.817
	5	-23.26	.329	166.182	.678	-.351	113.229	.799
	6	-22.80	.445	166.219	.969	.000	111.352	.909
	7	-22.34	.150	167.694	1.025	-.768	116.119	1.002
	8	-21.89	.000	168.231	.643	-1.161	117.787	1.572
	9	-21.43	.133	167.225	1.088	-.462	113.029	1.826
	10	-20.97	.647	164.108	.502	.162	109.713	1.110
	11	-20.51	.484	165.980	1.497	.000	112.332	2.181
2	1	-20.06	.000	169.472	2.370	-.349	114.766	2.487
	2	-19.60	.317	167.865	1.370	-.319	115.292	1.853
	3	-19.14	.000	170.466	.764	-.546	117.758	1.416
	4	-18.68	.235	169.122	.674	-.382	117.392	.491
	5	-18.22	.266	168.227	.748	-.499	117.111	1.063
	6	-17.76	.211	167.883	1.241	-.597	116.850	1.125
	7	-17.30	.300	167.008	1.099	-.364	114.709	.943
	8	-16.84	.454	165.989	.609	-.159	113.023	.849
	9	-16.38	.405	166.306	.891	-.309	113.759	.536
	10	-15.92	.186	167.954	.687	-.539	115.651	.657
	11	-15.46	.378	166.056	.559	-.385	113.833	1.226
3	1	-15.00	.495	164.940	.570	-.325	113.083	.865
	2	-14.54	.486	165.287	.965	-.187	112.225	.852
	3	-14.08	.344	166.661	1.305	-.199	113.271	1.480
	4	-13.62	.152	168.488	1.187	-.524	115.695	1.393
	5	-13.16	.000	169.255	.983	-.644	116.633	1.427
	6	-12.70	.229	167.379	.806	-.395	113.851	.768
	7	-12.24	.320	166.942	.786	-.358	114.090	.787
	8	-11.78	.175	167.740	.373	-.645	116.512	.563
	9	-11.32	.194	167.950	.499	-.590	116.279	.733
	10	-10.85	.486	165.785	.730	-.300	113.819	.863
	11	-10.39	.511	165.196	.988	-.216	112.265	1.539

Table 15.3 Continued

Run 9

CURVE FITS FOR SMMR 18.0 GHZ TB VERSUS CELL NUMBER

			V POL.			H POL.		
BLOCK	ROW	AVERAGE LATITUDE	LINEAR TERM	CONSTANT TERM	RMS	LINEAR TERM	CONSTANT TERM	RMS
4	1	-9.93	.302	166.160	1.076	-.386	113.308	1.253
	2	-9.47	.346	165.801	.752	-.349	112.249	.904
	3	-9.01	.213	166.053	.419	-.368	111.609	1.304
	4	-8.54	.207	166.163	.911	-.311	111.481	1.169
	5	-8.08	.318	165.827	.618	-.413	112.545	1.175
	6	-7.62	.387	165.196	.473	-.319	111.589	1.065
	7	-7.16	.298	165.857	.381	-.336	112.187	1.121
	8	-6.69	.215	166.741	.766	-.635	114.846	1.094
	9	-6.23	.000	168.535	.948	-.599	115.131	1.607
	10	-5.77	.097	167.769	.896	-.654	114.971	1.149
	11	-5.30	.000	167.416	.970	-.687	114.007	2.116
5	1	-4.84	.152	166.339	.773	-.425	111.868	1.965
	2	-4.38	.308	165.322	.644	-.181	110.402	1.396
	3	-3.91	.413	165.087	.445	-.132	111.116	.777
	4	-3.45	.441	165.797	.865	.000	111.033	1.281
	5	-2.99	.572	165.347	.438	.193	111.037	.970
	6	-2.52	.735	164.006	.726	.256	110.200	1.287
	7	-2.06	.680	164.177	.774	.000	111.267	1.372
	8	-1.60	.667	164.023	.564	.111	110.450	.849
	9	-1.13	.650	163.525	.669	.000	110.111	.670
	10	-.67	.550	163.575	.521	.000	110.018	.592
	11	-.21	.653	163.609	.635	.091	109.602	.747
6	1	.25	.842	162.830	.585	.463	108.079	.942
	2	.72	.879	162.964	.566	.415	108.950	.688
	3	1.18	.841	163.817	1.060	.240	110.596	1.253
	4	1.64	.774	164.496	.798	.182	110.687	.949
	5	2.11	.735	165.117	.691	.183	111.134	.683
	6	2.57	.698	166.277	.831	.047	112.855	.434
	7	3.04	.748	166.623	.387	.216	112.952	.516
	8	3.50	.582	168.445	.726	.290	113.781	.519
	9	3.96	.687	168.490	.676	.186	115.328	.606
	10	4.43	.653	168.429	.711	.187	115.759	1.050
	11	4.89	.806	168.001	.730	.550	114.060	1.002

Table 15.3 Continued

Run 9

CURVE FITS FOR SMMR 18.0 GHZ TB VERSUS CELL NUMBER

			V POL.			H POL.		
BLOCK	ROW	AVERAGE LATITUDE	LINEAR TERM	CONSTANT TERM	RMS	LINEAR TERM	CONSTANT TERM	RMS
7	1	5.36	.983	168.530	.382	.575	115.740	1.038
	2	5.82	.970	169.229	.532	.703	116.248	.529
	3	6.29	.998	169.078	.879	.788	116.061	.491
	4	6.75	1.038	170.007	.955	.900	116.917	.946
	5	7.22	1.193	170.494	.926	1.001	119.131	.518
	6	7.68	1.245	171.711	.408	1.231	119.916	.839
	7	8.14	1.050	173.619	.644	.809	123.598	1.479
	8	8.61	1.239	173.527	1.056	1.151	123.599	1.718
	9	9.07	1.054	174.632	.465	.946	124.244	.629
	10	9.54	.986	175.913	.843	.594	127.687	1.451
	11	10.00	.485	178.025	1.889	-.195	130.767	1.773
8	1	10.47	.621	179.516	5.383	.000	133.037	6.711
	2	10.93	.700	180.821	6.042	.000	136.032	9.152
	3	11.39	.000	183.716	3.675	-.655	138.247	5.838
	4	11.86	.000	183.212	2.362	-1.012	139.413	3.239
	5	12.32	.000	183.525	2.534	-.752	137.977	3.395
	6	12.79	.000	183.892	3.303	-1.018	139.685	4.193
	7	13.25	.000	183.705	2.394	-1.500	142.004	3.300
	8	13.72	-.895	190.261	2.722	-2.782	152.634	3.738
	9	14.18	-1.669	196.404	2.451	-4.075	162.656	1.527
	10	14.64	-2.535	201.759	3.233	-6.145	176.853	8.903
	11	15.11	-2.459	199.418	3.646	-5.001	164.626	8.501

Table .4

Run 9

CURVE FITS FOR SMMR 21.0 GHZ TB VERSUS CELL NUMBER

			V POL.			H POL.		
BLOCK	ROW	AVERAGE LATITUDE	LINEAR TERM	CONSTANT TERM	RMS	LINEAR TERM	CONSTANT TERM	RMS
1	1	-25.08	.000	190.670	1.138	-.786	148.922	2.036
	2	-24.63	.281	189.117	.891	-.328	146.097	1.887
	3	-24.17	-.222	191.210	1.385	-.903	148.717	1.294
	4	-23.71	-.300	192.201	.911	-1.144	149.896	1.437
	5	-23.26	.137	191.699	1.074	-.574	150.339	1.399
	6	-22.80	.289	191.696	1.346	.000	147.420	1.297
	7	-22.34	.000	193.828	1.193	-.964	154.415	1.656
	8	-21.89	-.637	197.499	.982	-1.623	157.909	2.053
	9	-21.43	.000	193.622	1.818	-.903	153.008	3.062
	10	-20.97	.620	190.691	1.735	.323	147.183	1.545
	11	-20.51	.576	193.215	2.195	.000	152.889	3.275
2	1	-20.06	.000	197.298	2.761	-.570	157.346	4.258
	2	-19.60	.000	197.217	1.573	-.459	157.435	2.547
	3	-19.14	-.259	200.031	.680	-.960	162.489	1.688
	4	-18.68	.000	199.116	.850	-.718	160.615	.886
	5	-18.22	-.137	198.533	1.024	-.769	159.572	1.119
	6	-17.76	.000	197.371	1.833	-.929	159.474	1.937
	7	-17.30	.000	196.155	.899	-.609	155.584	1.581
	8	-16.84	.337	193.283	1.342	.000	151.095	1.192
	9	-16.38	.187	194.630	1.709	-.233	153.115	1.484
	10	-15.92	.000	195.886	.797	-.666	156.484	1.325
	11	-15.46	.276	193.937	.966	-.497	154.728	1.977
3	1	-15.00	.254	193.802	1.120	-.373	153.273	1.518
	2	-14.54	.243	194.030	1.463	-.187	152.327	1.632
	3	-14.08	.176	195.010	1.634	-.375	154.584	2.171
	4	-13.62	.000	196.882	1.916	-.743	157.849	2.473
	5	-13.16	-.325	199.017	1.580	-1.047	159.984	1.824
	6	-12.70	-.083	197.109	.619	-.634	155.771	1.464
	7	-12.24	.000	196.335	.563	-.550	155.803	.662
	8	-11.78	-.170	197.894	.864	-1.045	160.186	.914
	9	-11.32	-.280	199.229	.932	-.890	159.949	1.364
	10	-10.85	.000	196.742	1.449	-.415	155.330	1.540
	11	-10.39	.000	196.142	1.867	-.405	154.184	2.514

Table 15.4 Continued

Run 9

CURVE FITS FOR SMMR 21.0 GHZ TB VERSUS CELL NUMBER

BLOCK	ROW	AVERAGE LATITUDE	V POL. LINEAR TERM	V POL. CONSTANT TERM	V POL. RMS	H POL. LINEAR TERM	H POL. CONSTANT TERM	H POL. RMS
4	1	-9.93	.000	195.754	1.542	-.616	155.078	2.625
	2	-9.47	.000	195.341	1.102	-.411	153.075	1.074
	3	-9.01	.000	194.795	.681	-.699	154.356	1.874
	4	-8.54	.000	195.336	1.352	-.607	154.333	2.208
	5	-8.08	-.167	197.265	1.330	-.946	157.208	2.628
	6	-7.62	.000	195.972	1.090	-.883	156.384	1.684
	7	-7.16	.000	195.915	1.195	-.748	157.072	1.926
	8	-6.69	-.369	199.366	1.209	-1.175	160.869	1.868
	9	-6.23	-.351	199.997	1.631	-1.061	160.933	1.997
	10	-5.77	-.401	199.714	1.079	-1.201	161.352	1.876
	11	-5.30	-.361	198.299	1.565	-1.158	158.758	3.374
5	1	-4.84	.000	195.805	1.690	-.697	155.124	3.604
	2	-4.38	.192	194.531	1.489	.000	151.414	3.757
	3	-3.91	.339	194.686	.652	.000	152.623	2.373
	4	-3.45	.568	194.600	1.160	.404	153.226	1.910
	5	-2.99	.964	193.898	1.192	.715	153.210	2.087
	6	-2.52	1.086	193.368	1.034	.922	152.585	2.117
	7	-2.06	.938	194.184	.852	.787	153.388	1.963
	8	-1.60	.977	193.745	.971	.852	152.869	1.509
	9	-1.13	.907	193.647	.927	.638	152.942	1.206
	10	-.67	.845	194.343	.524	.593	152.985	.917
	11	-.21	.917	194.053	.837	.714	153.115	1.195
6	1	.25	1.060	194.192	1.201	.947	152.810	.933
	2	.72	1.103	194.243	1.168	.902	154.155	.756
	3	1.18	.961	195.730	1.591	.864	155.139	1.641
	4	1.64	.959	196.084	1.194	.805	155.524	1.293
	5	2.11	.997	195.706	1.219	.689	156.100	1.053
	6	2.57	.845	197.770	1.249	.418	159.790	1.195
	7	3.04	.859	199.576	1.286	.529	161.109	1.217
	8	3.50	.837	201.062	1.188	.569	163.594	.829
	9	3.96	.778	202.585	.809	.508	165.945	1.076
	10	4.43	.652	204.328	.747	.293	167.916	1.897
	11	4.89	.886	203.782	.993	.650	167.809	1.933

Table 15.4 Continued

Run 9

CURVE FITS FOR SMMR 21.0 GHZ TB VERSUS CELL NUMBER

BLOCK	ROW	AVERAGE LATITUDE	V POL. LINEAR TERM	V POL. CONSTANT TERM	V POL. RMS	H POL. LINEAR TERM	H POL. CONSTANT TERM	H POL. RMS
7	1	5.36	1.027	205.314	.815	.969	169.449	1.506
	2	5.82	1.030	207.428	.711	1.209	171.275	.465
	3	6.29	1.049	208.356	.995	1.314	171.965	.900
	4	6.75	1.320	208.503	1.087	1.538	173.446	.842
	5	7.22	1.369	210.881	.815	1.733	177.298	.674
	6	7.68	1.434	213.187	1.102	1.690	181.534	1.338
	7	8.14	1.038	217.407	.803	1.186	187.623	1.240
	8	8.61	1.064	218.977	.899	1.464	188.959	1.205
	9	9.07	.934	219.897	1.194	1.051	191.910	.952
	10	9.54	.723	222.066	1.568	.461	196.784	1.543
	11	10.00	.000	225.172	2.355	-.532	200.601	3.182
8	1	10.47	.000	226.802	4.896	.000	200.678	8.222
	2	10.93	.000	228.887	5.738	.000	204.536	9.037
	3	11.39	-.470	230.776	4.081	-1.265	210.119	5.841
	4	11.86	-.551	231.152	3.599	-1.580	212.217	4.495
	5	12.32	-.757	232.603	3.429	-1.416	211.035	4.738
	6	12.79	-.802	233.072	3.534	-1.613	211.964	6.023
	7	13.25	-1.004	233.541	3.011	-2.338	214.600	3.677
	8	13.72	-1.723	238.656	2.642	-3.475	223.400	3.835
	9	14.18	-2.390	243.115	2.301	-4.647	231.194	1.653
	10	14.64	-2.980	244.928	2.322	-6.030	238.987	5.225
	11	15.11	-2.956	241.747	3.083	-5.577	230.056	5.247

Table 15.5

Run 9

CURVE FITS FOR SMMR 37.0 GHZ TB VERSUS CELL NUMBER

			V POL.			H POL.		
BLOCK	ROW	AVERAGE LATITUDE	LINEAR TERM	CONSTANT TERM	RMS	LINEAR TERM	CONSTANT TERM	RMS
1	1	-25.19	-.302	202.568	2.297	-.321	149.481	4.031
	2	-24.96	-.206	202.683	3.062	.000	148.713	5.913
	3	-24.74	-.097	201.158	2.619	.000	148.462	4.888
	4	-24.51	.000	199.637	1.858	.187	145.350	3.503
	5	-24.28	-.115	201.548	2.661	.000	148.345	4.391
	6	-24.05	-.499	205.649	2.163	-.706	155.463	3.545
	7	-23.83	-.359	203.719	2.141	-.519	152.316	3.813
	8	-23.60	-.374	204.371	1.238	-.519	153.180	2.413
	9	-23.37	-.190	204.131	1.761	-.188	152.810	2.816
	10	-23.14	.000	202.419	2.081	.000	152.365	4.767
	11	-22.92	.000	201.403	1.790	.115	148.642	3.155
	12	-22.69	.130	201.581	2.272	.340	147.867	3.421
	13	-22.46	-.148	204.618	2.180	.000	152.522	4.598
	14	-22.23	-.503	206.874	2.065	-.729	157.669	3.127
	15	-22.00	-.677	209.502	2.035	-1.076	161.956	3.201
	16	-21.77	-.600	207.527	2.475	-.859	158.104	3.951
	17	-21.54	-.561	206.796	3.975	-.695	155.752	6.346
	18	-21.31	-.165	201.675	2.843	.000	146.345	5.555
	19	-21.09	.000	200.105	2.572	.402	142.790	4.336
	20	-20.86	.269	198.097	1.812	.677	140.549	2.991
	21	-20.63	.252	199.540	2.902	.789	141.742	5.198
	22	-20.40	.000	202.542	3.768	.000	151.477	7.520

Table 15.5 Continued

Run 9

CURVE FITS FOR SMMR 37.0 GHZ TB VERSUS CELL NUMBER

			V POL.			H POL.		
BLOCK	ROW	AVERAGE LATITUDE	LINEAR TERM	CONSTANT TERM	RMS	LINEAR TERM	CONSTANT TERM	RMS
2	1	-20.17	-.262	205.687	4.389	.000	151.890	7.770
	2	-19.94	-.227	205.008	4.171	.000	151.608	7.681
	3	-19.71	-.171	204.594	2.963	.000	151.553	5.081
	4	-19.48	-.120	204.870	2.466	.000	153.157	4.233
	5	-19.25	-.385	208.502	2.772	-.422	159.421	4.254
	6	-19.03	-.477	210.881	3.012	-.660	164.510	5.041
	7	-18.80	-.212	207.901	2.553	-.189	159.103	4.006
	8	-18.57	-.118	206.271	1.713	.111	154.240	2.289
	9	-18.34	-.183	206.345	2.101	.000	154.492	3.923
	10	-18.11	-.145	205.396	1.613	.000	152.853	3.152
	11	-17.88	-.266	206.588	2.774	.000	153.382	5.192
	12	-17.65	-.233	206.409	2.452	-.281	156.735	3.453
	13	-17.42	-.157	204.037	1.635	.000	152.104	3.001
	14	-17.19	-.137	203.757	1.794	.000	151.111	3.229
	15	-16.96	.000	202.287	2.117	.228	148.251	3.073
	16	-16.73	.000	201.066	2.098	.218	147.390	3.071
	17	-16.50	-.073	202.147	1.756	.000	149.793	3.178
	18	-16.27	-.209	204.038	1.667	-.200	153.084	3.424
	19	-16.04	-.350	206.556	1.381	-.443	156.937	2.588
	20	-15.81	-.336	205.619	1.244	-.386	155.315	2.216
	21	-15.58	-.144	203.017	2.676	-.232	152.403	3.288
	22	-15.35	-.170	202.320	2.031	.000	147.820	3.167

Table 15.5 Continued

Run 9

CURVE FITS FOR SMMR 37.0 GHZ TB VERSUS CELL NUMBER

			V POL.			H POL.		
BLOCK	ROW	AVERAGE LATITUDE	LINEAR TERM	CONSTANT TERM	RMS	LINEAR TERM	CONSTANT TERM	RMS
3	1	-15.12	-.219	202.780	1.908	-.139	149.314	2.769
	2	-14.89	.000	200.325	1.708	.000	147.750	2.346
	3	-14.66	.000	200.205	1.604	.000	147.402	2.457
	4	-14.43	-.060	200.874	1.396	.000	147.441	2.355
	5	-14.20	.000	200.942	1.790	.114	146.990	3.165
	6	-13.97	-.097	203.001	2.400	.000	150.447	4.616
	7	-13.74	-.192	204.416	2.494	-.196	152.855	4.607
	8	-13.51	-.268	205.413	2.357	-.237	153.880	4.571
	9	-13.28	-.347	206.762	2.145	-.442	156.806	4.159
	10	-13.05	-.382	206.521	2.821	-.421	155.050	4.587
	11	-12.82	-.163	202.766	2.055	-.113	149.595	2.649
	12	-12.58	-.045	201.148	1.128	.080	147.079	1.429
	13	-12.36	-.054	201.506	1.315	.097	147.490	2.133
	14	-12.12	-.131	202.674	1.218	-.087	149.391	1.587
	15	-11.89	-.220	204.239	1.371	-.166	151.476	2.238
	16	-11.66	-.259	204.538	1.496	-.296	153.585	2.646
	17	-11.43	-.440	208.060	2.009	-.493	157.181	2.888
	18	-11.20	-.115	203.445	1.687	-.132	152.447	2.278
	19	-10.97	.000	201.644	1.939	.000	150.581	3.120
	20	-10.74	.126	199.238	1.306	.250	145.068	2.525
	21	-10.51	.000	200.500	1.385	.162	146.181	2.567
	22	-10.28	.000	200.920	2.735	.000	148.018	4.581

Table 15.5 Continued

Run 9

CURVE FITS FOR SMMR 37.0 GHZ TB VERSUS CELL NUMBER

BLOCK	ROW	AVERAGE LATITUDE	V POL. LINEAR TERM	V POL. CONSTANT TERM	V POL. RMS	H POL. LINEAR TERM	H POL. CONSTANT TERM	H POL. RMS
4	1	-10.05	-.165	202.117	2.248	.000	146.984	4.093
	2	-9.81	-.197	202.327	1.905	-.274	149.646	3.520
	3	-9.58	.000	199.740	1.580	.000	145.710	2.747
	4	-9.35	-.105	200.401	1.883	.000	145.509	2.538
	5	-9.12	-.132	200.422	1.105	.000	144.830	1.711
	6	-8.89	-.201	201.081	1.459	-.187	146.974	2.394
	7	-8.66	-.055	199.916	1.378	.115	143.736	2.371
	8	-8.43	-.158	200.998	1.880	.000	145.368	3.063
	9	-8.20	-.179	201.466	1.575	-.157	147.655	2.418
	10	-7.97	-.094	201.465	2.368	.000	147.157	4.197
	11	-7.73	.000	199.122	2.067	.000	145.514	3.256
	12	-7.50	-.132	200.242	1.068	.000	144.556	1.652
	13	-7.27	.000	199.015	1.619	.000	145.661	2.361
	14	-7.04	.000	200.140	1.811	.000	146.776	2.744
	15	-6.81	-.199	202.329	1.333	-.206	149.223	1.967
	16	-6.58	-.214	203.276	1.972	-.249	150.532	3.222
	17	-6.35	-.177	203.514	2.303	-.160	151.221	4.133
	18	-6.11	-.264	204.842	2.529	-.219	151.877	4.145
	19	-5.88	-.256	204.251	2.162	-.208	151.069	3.907
	20	-5.65	-.213	202.971	1.870	-.185	150.032	2.725
	21	-5.42	-.267	202.451	1.662	-.276	148.684	2.683
	22	-5.19	-.147	201.175	2.534	-.214	147.469	4.760

Table 15.5 Continued

Run 9

CURVE FITS FOR SMMR 37.0 GHZ TB VERSUS CELL NUMBER

BLOCK	ROW	AVERAGE LATITUDE	V POL. LINEAR TERM	V POL. CONSTANT TERM	V POL. RMS	H POL. LINEAR TERM	H POL. CONSTANT TERM	H POL. RMS
5	1	-4.96	-.089	200.011	2.288	.000	144.844	4.135
	2	-4.72	.000	199.009	2.082	.000	144.272	2.856
	3	-4.49	.000	198.723	1.766	.000	143.920	2.625
	4	-4.26	.000	199.001	1.530	.183	142.658	2.622
	5	-4.03	.000	199.277	1.466	.171	143.185	2.300
	6	-3.80	.000	199.809	1.703	.181	143.255	2.162
	7	-3.57	.109	199.490	2.425	.232	144.166	3.718
	8	-3.33	.159	199.128	2.454	.365	143.560	4.006
	9	-3.10	.165	199.515	2.003	.384	143.789	3.132
	10	-2.87	.175	199.509	1.836	.327	144.791	3.345
	11	-2.64	.296	197.430	1.887	.536	141.782	2.914
	12	-2.41	.244	197.980	2.036	.537	141.421	3.495
	13	-2.18	.122	198.977	1.855	.310	143.341	3.448
	14	-1.94	.084	199.140	1.479	.272	143.268	2.220
	15	-1.71	.121	198.834	1.446	.382	142.144	2.552
	16	-1.48	.115	198.708	1.725	.424	141.542	2.734
	17	-1.25	.106	198.488	1.859	.299	142.541	2.931
	18	-1.02	.075	198.020	1.001	.230	141.730	1.330
	19	-.78	.000	199.007	1.039	.186	141.439	.947
	20	-.55	.094	197.898	.781	.296	140.924	1.284
	21	-.32	.080	198.093	1.152	.303	141.016	1.547
	22	-.09	.124	197.858	.930	.291	141.451	1.207

Table 15.5 Continued

Run 9

CURVE FITS FOR SMMR 37.0 GHZ TB VERSUS CELL NUMBER

BLOCK	ROW	AVERAGE LATITUDE	V POL. LINEAR TERM	V POL. CONSTANT TERM	V POL. RMS	H POL. LINEAR TERM	H POL. CONSTANT TERM	H POL. RMS
6	1	.14	.223	197.328	.846	.515	139.948	1.572
	2	.37	.341	197.002	1.593	.765	138.656	2.427
	3	.60	.366	197.176	1.399	.732	139.525	3.147
	4	.83	.262	197.837	1.144	.589	140.791	1.719
	5	1.06	.189	199.067	2.339	.543	141.711	3.408
	6	1.29	.000	201.932	2.877	.234	146.221	4.684
	7	1.53	.122	199.728	1.727	.243	144.675	2.658
	8	1.76	.000	200.266	.682	.366	142.070	1.789
	9	1.99	.000	200.419	1.031	.204	144.564	1.429
	10	2.22	.000	200.301	.813	.229	143.944	1.306
	11	2.45	-.035	201.505	.951	.183	144.983	1.298
	12	2.69	.000	201.653	1.115	.144	147.057	1.456
	13	2.92	.000	201.761	.887	.244	146.122	1.093
	14	3.15	.095	201.188	.766	.354	145.552	.865
	15	3.38	.076	201.985	.707	.316	146.658	1.630
	16	3.61	.111	202.222	1.023	.436	146.404	1.407
	17	3.85	.107	202.573	1.151	.350	147.852	1.290
	18	4.08	.076	203.412	1.427	.244	149.994	1.567
	19	4.31	-.067	204.954	1.498	.176	151.168	1.751
	20	4.54	.077	202.951	1.057	.367	147.573	1.855
	21	4.78	.233	201.347	1.280	.617	145.242	2.285
	22	5.01	.350	200.956	1.404	.791	144.821	2.056

Table 15.5 Continued

Run 9

CURVE FITS FOR SMMR 37.0 GHZ TB VERSUS CELL NUMBER

			V POL.			H POL.		
BLOCK	ROW	AVERAGE LATITUDE	LINEAR TERM	CONSTANT TERM	RMS	LINEAR TERM	CONSTANT TERM	RMS
7	1	5.24	.294	202.536	.798	.722	146.772	1.028
	2	5.47	.246	203.427	.910	.640	149.408	1.612
	3	5.70	.369	203.431	1.335	.810	149.263	2.251
	4	5.94	.369	203.337	1.160	.825	148.520	1.966
	5	6.17	.305	202.776	1.029	.678	148.591	1.306
	6	6.40	.229	204.309	.983	.575	150.268	1.284
	7	6.63	.289	204.731	1.467	.744	150.173	2.604
	8	6.87	.284	204.856	1.345	.773	150.630	2.878
	9	7.10	.305	205.721	1.752	.741	153.044	2.756
	10	7.33	.421	205.964	1.260	.931	153.579	1.537
	11	7.56	.771	204.328	2.005	1.566	150.936	2.981
	12	7.80	.512	206.126	1.348	1.131	153.688	2.048
	13	8.03	.473	206.043	1.991	.837	156.159	2.640
	14	8.26	.279	208.098	1.625	.794	157.309	2.781
	15	8.49	.639	206.019	2.796	1.275	154.300	4.314
	16	8.72	.581	206.572	3.345	1.284	154.717	5.695
	17	8.96	.495	206.644	1.441	1.010	155.930	2.370
	18	9.19	.408	208.602	1.675	.959	157.032	2.414
	19	9.42	.423	209.191	2.389	.992	159.066	4.195
	20	9.65	.275	210.395	1.736	.734	161.251	2.844
	21	9.89	-.057	212.925	1.303	.104	166.049	2.607
	22	10.12	-.147	213.579	1.618	.000	166.563	3.351

Table 15.5 Continued

Run 9

CURVE FITS FOR SMMR 37.0 GHZ TB VERSUS CELL NUMBER

BLOCK	ROW	AVERAGE LATITUDE	V POL. LINEAR TERM	V POL. CONSTANT TERM	V POL. RMS	H POL. LINEAR TERM	H POL. CONSTANT TERM	H POL. RMS
8	1	10.35	.000	213.394	2.989	.000	168.165	5.309
	2	10.58	.000	217.889	9.722	.000	176.136	17.221
	3	10.81	.000	218.549	10.925	.000	177.750	18.665
	4	11.05	.000	217.612	8.669	.000	176.283	13.898
	5	11.28	.000	215.695	5.676	.000	174.068	11.347
	6	11.51	-.258	218.223	4.722	-.422	177.549	9.337
	7	11.74	-.181	216.979	3.375	-.360	175.945	5.908
	8	11.97	.000	215.693	3.440	.000	173.122	6.260
	9	12.21	.000	216.124	3.784	.000	173.652	6.130
	10	12.44	.000	215.181	3.712	.000	172.421	6.377
	11	12.67	.000	215.578	4.643	.000	172.784	7.549
	12	12.90	.000	216.390	4.839	.000	174.637	8.404
	13	13.13	-.204	217.866	4.132	-.492	178.018	6.055
	14	13.37	-.397	219.813	3.330	-.778	180.547	5.470
	15	13.60	-.761	226.316	4.424	-1.368	191.005	7.322
	16	13.83	-1.297	235.640	5.254	-2.336	207.767	9.361
	17	14.06	-1.230	234.825	4.344	-2.119	205.542	7.572
	18	14.29	-1.877	244.192	3.834	-3.184	221.055	6.982
	19	14.53	-2.238	248.490	6.698	-3.826	228.662	12.644
	20	14.76	-2.431	251.015	7.734	-4.108	231.999	13.781
	21	14.99	-2.167	245.876	6.550	-3.798	225.752	11.695
	22	15.22	-1.852	238.002	6.895	-3.233	212.345	12.707

Figure 15.1

Run 9

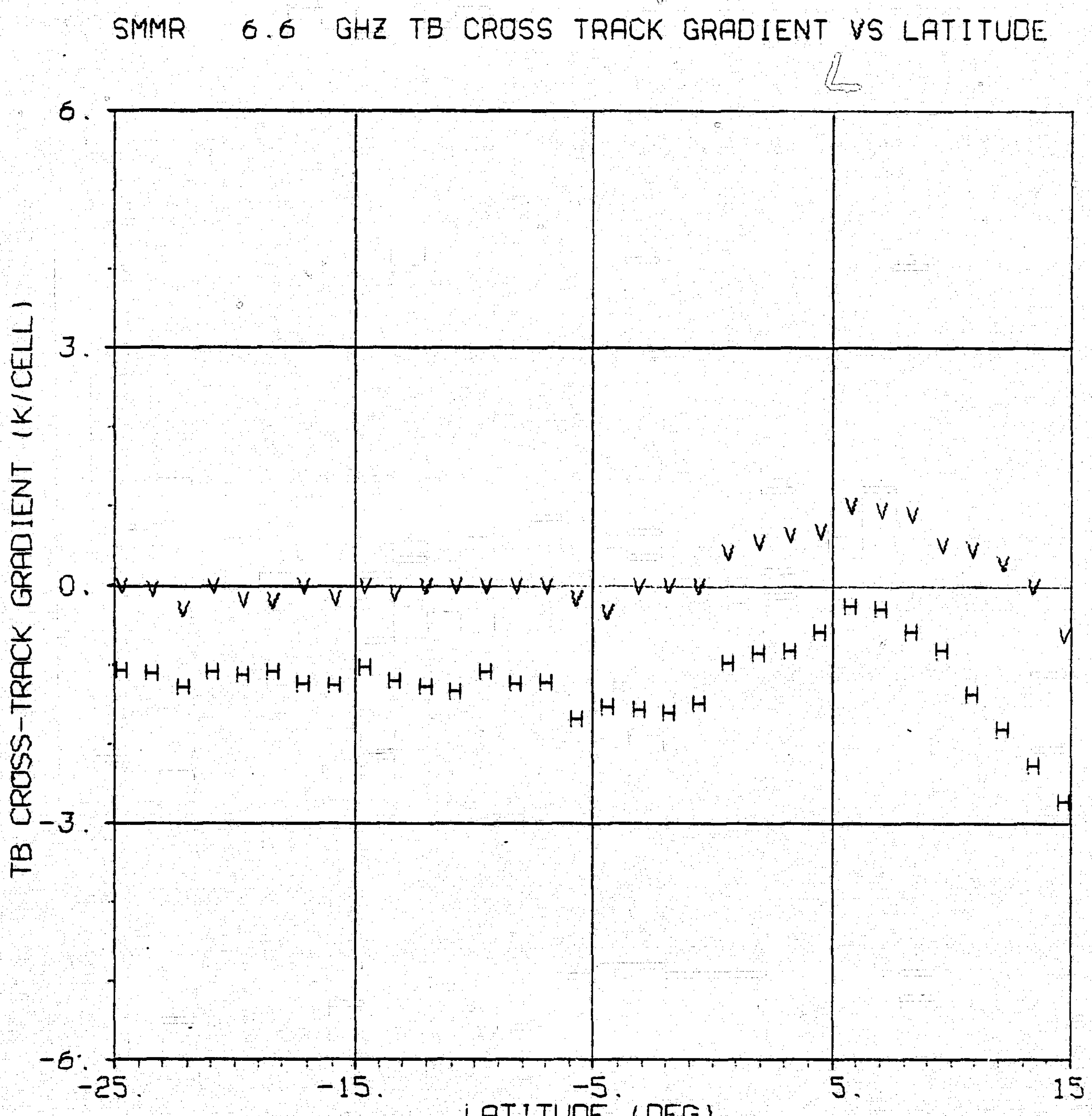

Figure 15.2

Run 9

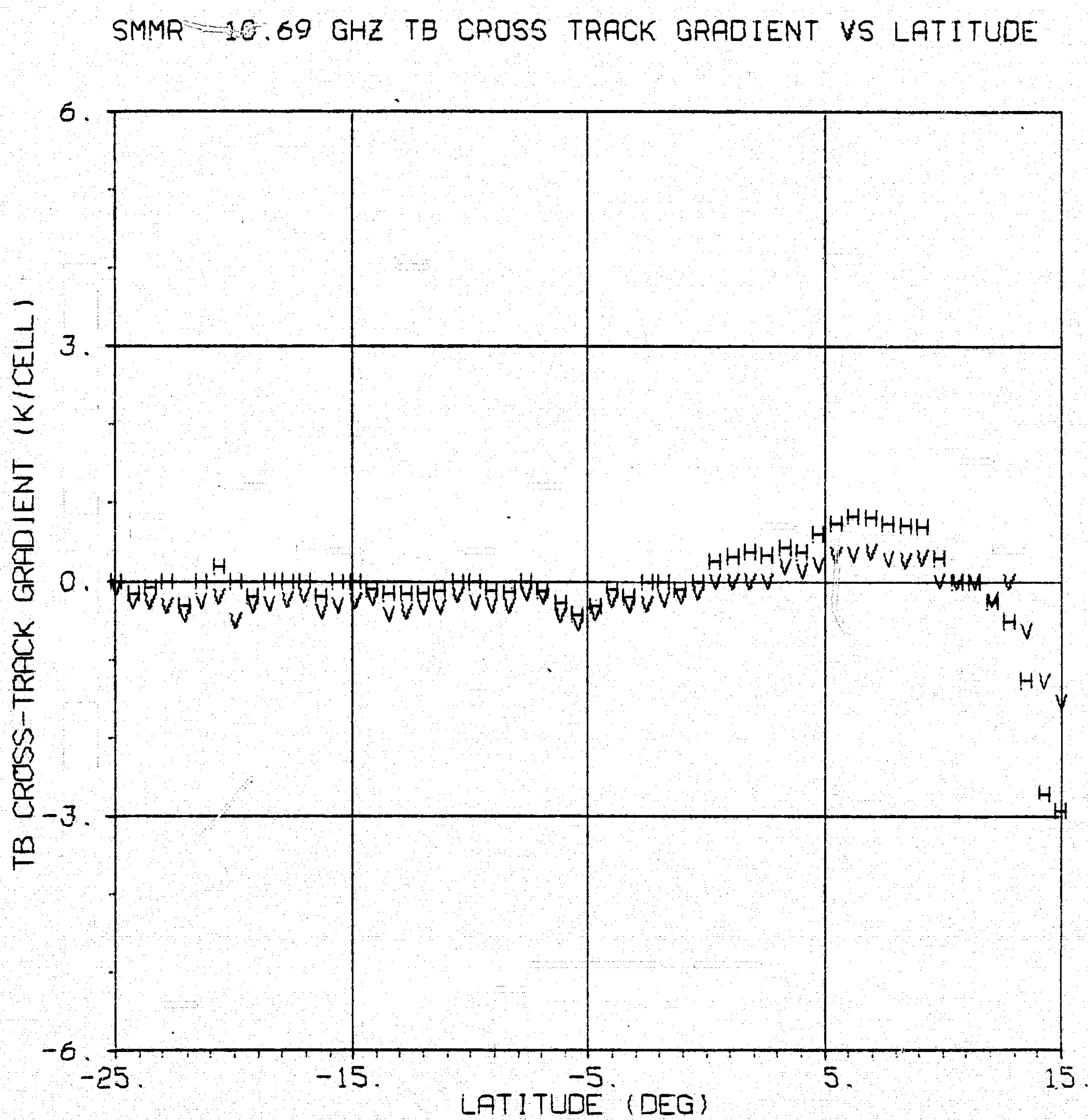

Figure 15.3

Run 9

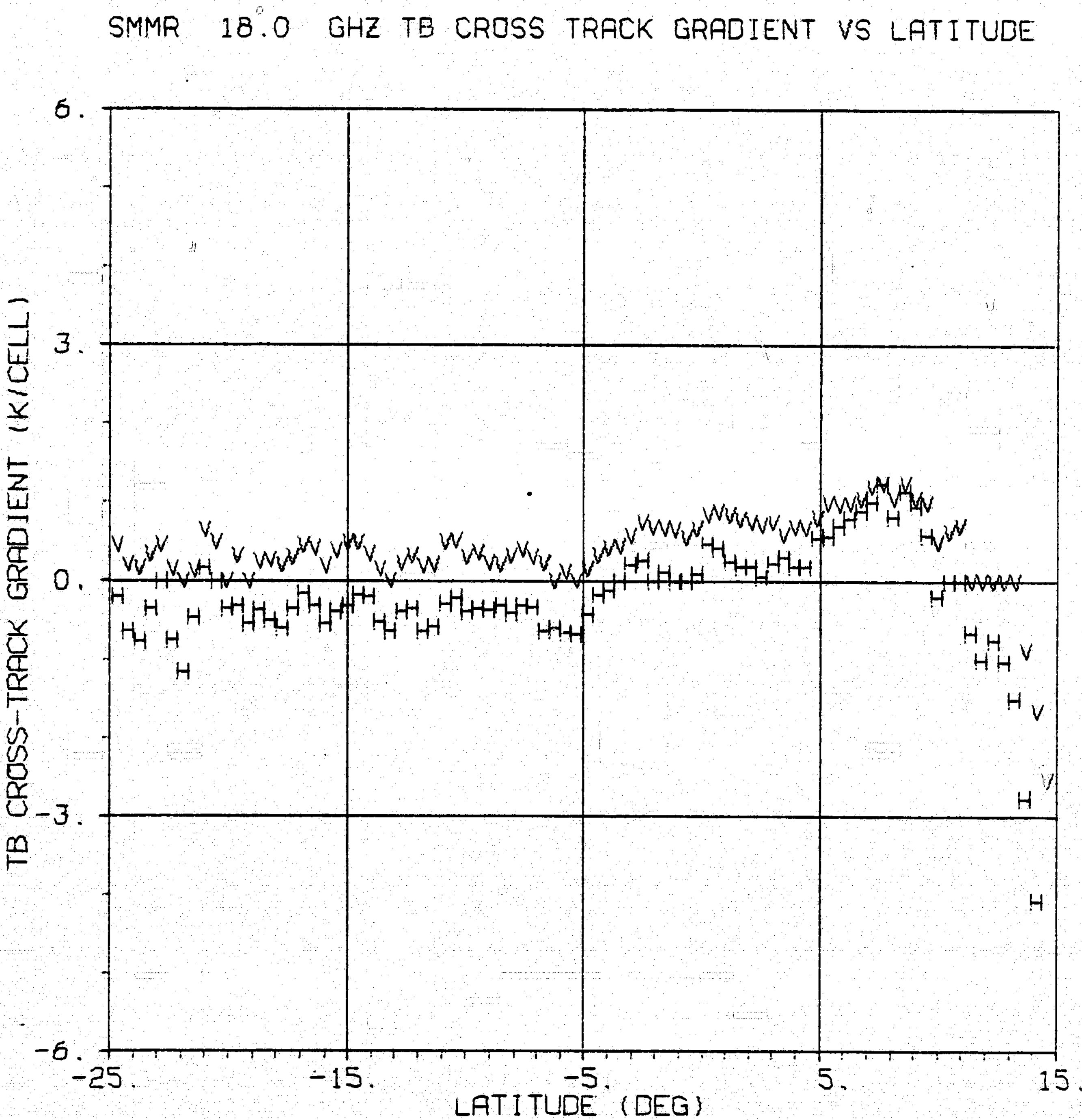

Figure 15.4

Run 9

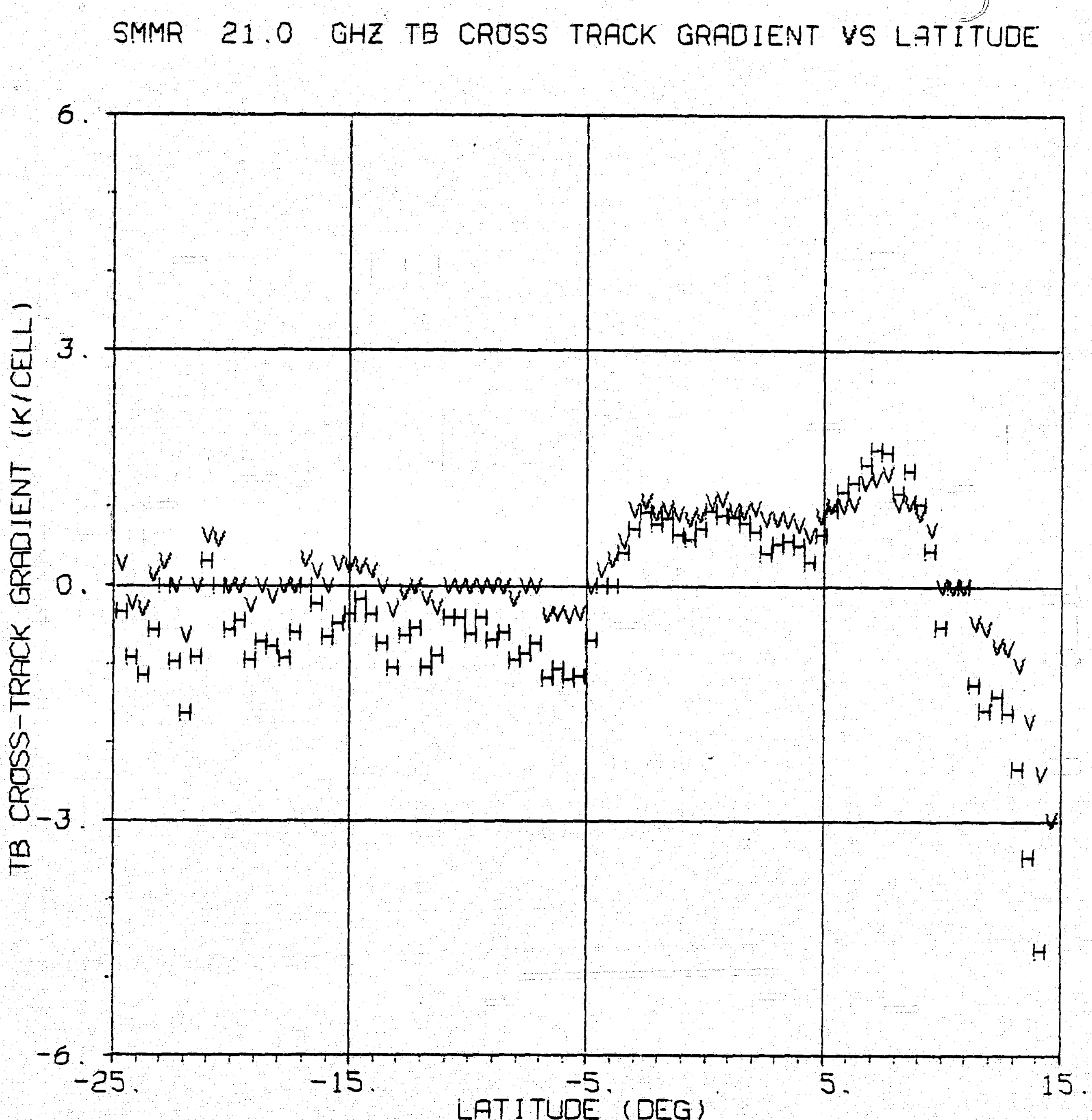

Figure 15.5

Run 9

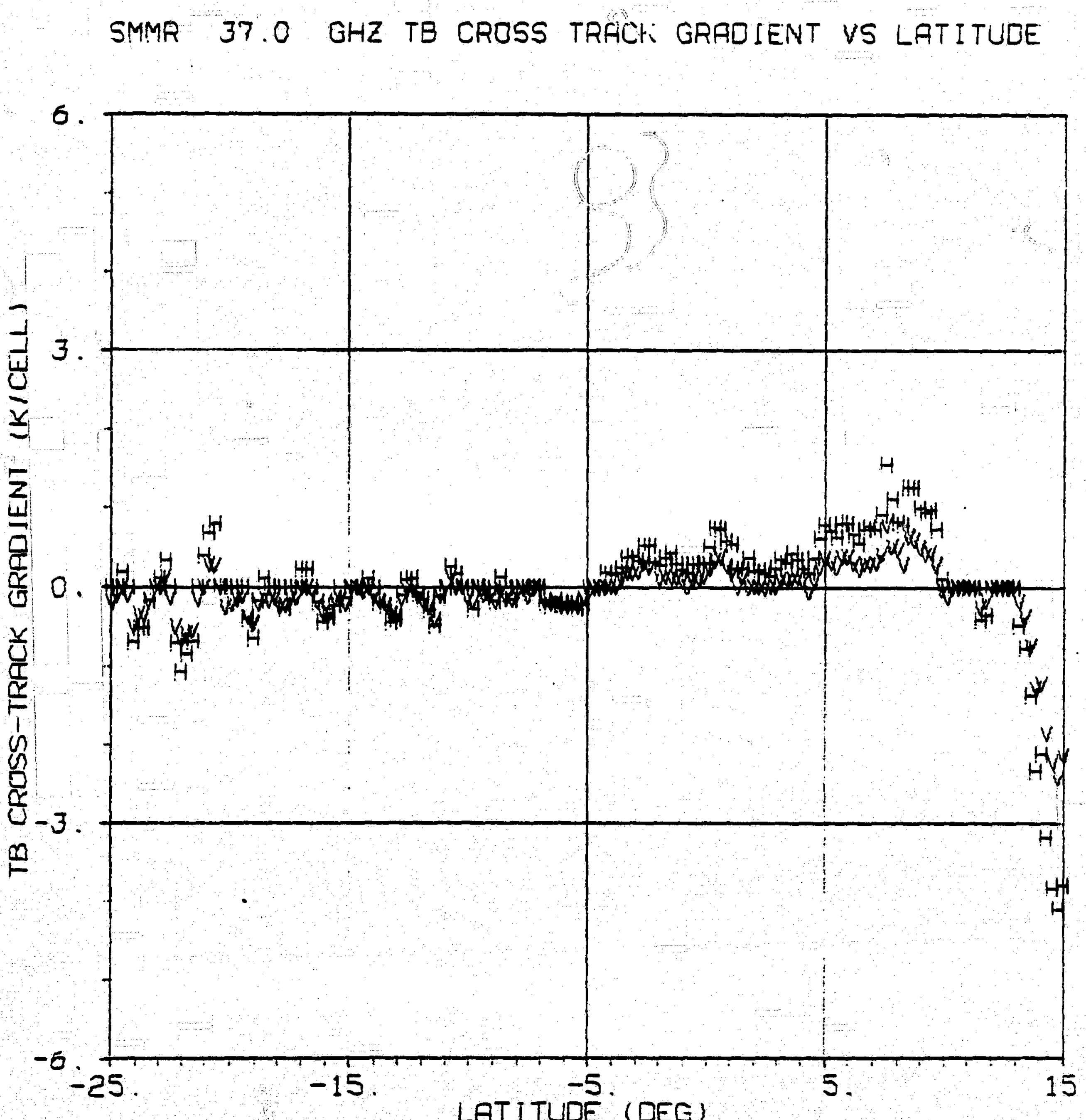

Table 16.1

Run 10

CURVE FITS FOR SMMR 6.6 GHZ T_B VERSUS CELL NUMBER

BLOCK	ROW	AVERAGE LATITUDE	V POL. LINEAR TERM	V POL. CONSTANT TERM	V POL. RMS	H POL. LINEAR TERM	H POL. CONSTANT TERM	H POL. RMS
1	1	47.77	1.201	149.075	.533	.000	89.375	.935
	2	46.55	1.200	149.180	.685	.885	87.205	.726
	3	45.32	1.634	147.940	.621	1.523	85.740	1.306
	4	44.09	1.282	148.405	.437	.933	85.595	.745
2	1	42.86	.858	149.015	.434	.000	86.655	.336
	2	41.61	.664	149.255	.353	-.386	87.180	.385
	3	40.37	.616	149.480	.202	-.874	88.155	.422
	4	39.12	.301	150.900	.311	-.957	88.110	.313
3	1	37.87	.582	150.540	.290	-.754	87.345	.424
	2	36.62	.565	150.565	.284	-.626	86.635	.200
	3	35.37	.489	150.645	.053	-1.124	87.925	.224
	4	34.11	.230	151.695	.096	-1.451	89.635	.224
4	1	32.85	.204	152.545	.103	-1.525	90.965	.304
	2	31.59	.225	153.010	.073	-1.456	91.610	.232
	3	30.32	.285	153.395	.278	-1.525	92.690	.358
	4	29.06	.138	154.370	.140	-1.393	93.560	.189
5	1	27.79	.449	153.935	.406	-1.756	95.010	.763
	2	26.53	.392	153.910	.295	-1.609	94.475	.628
	3	25.26	.525	153.380	.253	-1.546	93.935	.186
	4	23.99	.398	153.855	.136	-1.471	94.125	.290

Table

Run 10

CURVE FITS FOR SMMR 10.69 GHZ TB VERSUS CELL NUMBER

BLOCK	ROW	AVERAGE LATITUDE	V POL. LINEAR TERM	V POL. CONSTANT TERM	V POL. RMS	H POL. LINEAR TERM	H POL. CONSTANT TERM	H POL. RMS
1	1	48.03	.429	160.079	1.117	1.432	97.810	3.066
	2	47.33	.544	159.334	1.158	1.685	96.689	2.551
	3	46.64	.778	158.394	1.237	2.226	94.803	3.594
	4	45.93	.866	158.160	1.603	2.589	93.073	4.370
	5	45.23	1.172	156.971	2.070	3.413	90.281	6.359
	6	44.53	.849	157.490	1.103	2.720	91.774	4.402
	7	43.83	.586	157.876	.629	1.829	93.436	2.294
2	1	43.12	.364	158.170	.713	1.236	94.324	.880
	2	42.41	.226	158.544	.560	.888	94.741	1.114
	3	41.70	.173	158.629	.692	.772	94.829	.698
	4	40.99	.112	158.767	.446	.614	95.027	.846
	5	40.28	.000	159.131	.336	.407	95.766	.613
	6	39.57	.107	158.809	.353	.273	96.264	1.146
	7	38.86	.110	159.204	.491	.312	95.687	1.119
3	1	38.14	.000	160.287	.801	.383	95.871	.796
	2	37.43	.000	160.206	.686	.547	95.010	.561
	3	36.71	.242	159.399	.868	.458	94.601	.433
	4	36.00	.000	160.063	.674	.345	94.350	.775
	5	35.28	.086	159.456	.280	.000	96.134	.837
	6	34.56	.092	159.825	.184	.000	96.840	.602
	7	33.84	-.099	160.944	.317	.000	97.791	.474
4	1	33.12	-.078	161.156	.239	.000	98.436	.584
	2	32.40	-.105	161.873	.196	-.155	99.847	.599
	3	31.68	-.256	162.887	.376	-.131	100.740	.420
	4	30.96	-.123	162.830	.500	-.192	101.581	.427
	5	30.24	.000	162.599	.551	-.137	102.009	.548
	6	29.51	-.216	163.984	.471	-.231	103.311	.773
	7	28.79	.000	163.590	.449	.000	103.766	.732
5	1	28.07	.000	164.550	.731	-.148	105.023	.470
	2	27.34	.000	164.580	.923	.000	104.804	.838
	3	26.62	.000	164.360	1.062	-.183	105.286	.617
	4	25.89	-.209	164.667	.469	-.178	104.421	.447
	5	25.17	-.137	164.604	.494	-.219	104.647	.191
	6	24.44	-.180	164.929	.275	-.325	105.364	.456
	7	23.72	.000	164.491	.917	-.193	105.447	.452

Table [illegible]3

Run 10

CURVE FITS FOR SMMR 18.0 GHZ TB VERSUS CELL NUMBER

			V POL.			H POL.		
BLOCK	ROW	AVERAGE LATITUDE	LINEAR TERM	CONSTANT TERM	RMS	LINEAR TERM	CONSTANT TERM	RMS
1	1	48.16	1.082	171.387	3.739	1.072	123.361	6.911
	2	47.72	1.159	170.488	3.283	1.143	122.296	6.016
	3	47.27	1.315	169.277	3.149	1.587	118.732	6.065
	4	46.83	1.406	168.713	2.863	1.887	116.656	6.703
	5	46.38	1.538	167.177	3.281	2.482	112.807	8.576
	6	45.93	1.515	165.933	2.567	2.539	111.606	7.840
	7	45.49	1.582	165.411	2.419	3.259	107.127	10.693
	8	45.04	1.745	164.452	3.335	3.209	106.747	10.610
	9	44.59	1.543	165.329	2.790	2.648	108.759	7.837
	10	44.14	1.340	165.501	1.564	2.219	109.215	5.357
	11	43.70	1.234	165.690	.920	1.691	110.644	2.614
2	1	43.25	1.151	165.306	1.460	1.358	110.896	1.529
	2	42.80	1.109	165.063	1.074	1.254	110.072	1.336
	3	42.35	.966	165.337	1.179	1.082	110.783	1.600
	4	41.90	.932	165.592	1.432	.817	111.790	1.595
	5	41.44	.896	165.703	1.351	.745	111.995	1.494
	6	41.00	.809	166.321	1.236	.571	112.890	1.470
	7	40.54	.716	166.779	1.184	.272	114.362	1.199
	8	40.09	.639	166.939	1.475	.248	114.649	1.555
	9	39.64	.695	167.105	1.272	.318	114.252	1.950
	10	39.18	.673	167.428	1.429	.287	114.311	2.039
	11	38.73	.683	167.602	1.218	.357	113.896	1.783
3	1	38.27	.715	168.275	1.457	.275	114.971	1.528
	2	37.82	.708	168.446	1.691	.276	115.971	1.846
	3	37.36	.671	168.332	1.643	.360	114.414	2.270
	4	36.91	.804	167.309	1.643	.404	113.119	1.599
	5	36.45	.717	167.082	1.675	.478	111.755	1.702
	6	36.00	.796	165.947	1.321	.297	111.246	1.540
	7	35.54	.863	165.155	.839	.323	110.712	1.351
	8	35.08	.824	165.350	.558	.304	111.233	.990
	9	34.62	.847	165.253	.856	.313	111.914	1.217
	10	34.17	.772	165.917	1.010	.185	113.340	1.404
	11	33.71	.537	167.606	.859	.000	114.649	1.582

Table 16.3 Continued

Run 10

CURVE FITS FOR SMMR 18.0 GHZ TB VERSUS CELL NUMBER

BLOCK	ROW	AVERAGE LATITUDE	V POL. LINEAR TERM	V POL. CONSTANT TERM	V POL. RMS	H POL. LINEAR TERM	H POL. CONSTANT TERM	H POL. RMS
4	1	33.25	.519	167.976	.954	-.213	116.908	1.824
	2	32.79	.361	169.456	1.106	-.435	119.420	2.105
	3	32.34	.333	169.725	.800	-.525	120.623	1.536
	4	31.88	.181	171.425	.645	-.542	120.920	1.141
	5	31.42	.000	172.866	.854	-.739	123.234	1.445
	6	30.96	.199	172.157	1.480	-.245	120.071	1.322
	7	30.50	.475	170.171	1.263	.000	119.308	1.599
	8	30.04	.431	170.419	.751	-.297	121.510	1.490
	9	29.58	.158	173.092	1.344	-.895	127.211	2.661
	10	29.12	.354	173.586	1.304	.000	124.497	3.302
	11	28.66	.754	172.702	.612	.460	123.555	1.882
5	1	28.20	.570	175.215	1.328	-.241	130.093	2.113
	2	27.74	.623	175.575	.915	.000	129.103	1.039
	3	27.28	.438	176.794	1.823	.000	129.297	2.081
	4	26.81	.472	176.808	1.755	.000	129.771	2.479
	5	26.35	.371	176.722	1.664	-.310	130.571	1.825
	6	25.89	.212	177.126	1.179	-.536	131.120	1.263
	7	25.43	.146	178.161	1.031	-.642	132.485	.948
	8	24.97	.207	177.935	.604	-.527	132.104	1.140
	9	24.51	.207	178.094	.915	-.652	132.899	.495
	10	24.05	.000	180.152	.669	-.760	134.872	.868
	11	23.58	.000	181.426	1.791	-.722	135.837	1.492

Table 5.4

Run 10

CURVE FITS FOR SMMR 21.0 GHZ TB VERSUS CELL NUMBER

BLOCK	ROW	AVERAGE LATITUDE	V POL. LINEAR TERM	V POL. CONSTANT TERM	V POL. RMS	H POL. LINEAR TERM	H POL. CONSTANT TERM	H POL. RMS
1	1	48.16	.984	201.708	3.486	1.103	170.295	7.976
	2	47.72	.916	201.549	2.941	1.255	168.438	6.854
	3	47.27	1.186	199.275	2.919	1.784	164.872	6.492
	4	46.83	1.411	197.593	2.597	2.121	161.380	6.571
	5	46.38	1.617	195.456	3.069	2.680	157.275	7.337
	6	45.93	1.619	194.043	2.015	2.838	154.487	6.899
	7	45.49	1.968	190.973	2.581	3.656	148.666	9.295
	8	45.04	1.874	190.789	2.626	3.912	145.835	9.864
	9	44.59	1.822	189.925	2.251	3.372	147.060	8.060
	10	44.14	1.723	190.000	1.338	2.872	143.093	5.053
	11	43.70	1.779	188.545	1.189	2.726	146.569	2.837
2	1	43.25	1.653	188.523	1.218	2.494	145.606	2.195
	2	42.80	1.619	187.344	1.002	2.328	145.080	1.867
	3	42.35	1.333	188.635	.937	1.958	146.004	2.046
	4	41.90	1.336	188.551	1.655	1.645	147.174	2.329
	5	41.44	1.239	188.857	1.458	1.276	149.023	2.472
	6	41.00	.732	192.089	1.527	1.044	150.051	1.741
	7	40.54	.715	192.154	1.569	.686	151.954	1.947
	8	40.09	.695	192.738	1.777	.580	152.883	1.977
	9	37.64	.799	192.306	1.538	.529	153.770	2.472
	10	39.18	.715	193.339	1.742	.521	154.034	2.532
	11	33.73	.601	194.105	1.588	.508	154.490	2.605
3	1	38.27	.778	194.047	1.975	.442	156.135	2.166
	2	37.82	.716	195.220	2.203	.451	157.154	2.834
	3	37.36	.623	195.137	2.654	.573	154.788	2.887
	4	36.91	.823	193.021	2.481	.649	152.699	2.291
	5	36.45	.903	191.549	2.240	.528	151.389	2.764
	6	36.00	.858	191.035	1.998	.665	148.883	2.247
	7	35.54	1.035	188.641	1.418	.752	147.181	1.932
	8	35.08	1.046	188.489	1.409	.724	147.138	1.534
	9	34.62	.923	189.337	1.229	.889	146.170	2.511
	10	34.17	.809	189.985	1.703	.512	149.263	2.683
	11	33.71	.533	191.641	1.343	.000	153.072	3.159

Table 16.4 Continued

Run 10

CURVE FITS FOR SMMR 21.0 GHZ TB VERSUS CELL NUMBER

BLOCK	ROW	AVERAGE LATITUDE	V POL. LINEAR TERM	V POL. CONSTANT TERM	V POL. RMS	H POL. LINEAR TERM	H POL. CONSTANT TERM	H POL. RMS
4	1	33.25	.303	193.754	1.650	-.528	156.787	3.588
	2	32.79	.000	196.765	1.991	-1.080	162.188	4.304
	3	32.34	.000	197.132	1.381	-1.163	163.862	2.855
	4	31.88	.000	197.698	1.507	-1.124	164.174	1.792
	5	31.42	-.332	200.858	1.057	-1.320	167.443	2.584
	6	30.96	.000	198.429	1.492	-.445	161.151	2.264
	7	30.50	.617	194.668	1.581	.000	158.728	2.206
	8	30.04	.390	196.031	1.192	.000	159.426	1.804
	9	29.58	.000	199.929	2.338	-.855	167.005	3.369
	10	29.12	.000	202.672	2.945	.000	166.469	5.534
	11	28.66	.795	201.135	1.267	.628	167.394	3.006
5	1	28.20	.375	206.323	1.714	.000	175.740	2.633
	2	27.74	.701	204.792	1.280	.292	174.684	1.418
	3	27.28	.391	206.519	2.363	.000	176.310	2.875
	4	26.81	.289	207.698	2.207	.000	177.558	2.212
	5	26.35	.182	207.613	1.693	-.518	179.902	1.897
	6	25.89	.000	208.798	1.546	-.710	179.514	1.568
	7	25.43	-.150	210.382	1.371	-.995	182.727	1.809
	8	24.97	.000	209.960	1.111	-.870	183.252	1.311
	9	24.51	.000	210.389	1.526	-.849	183.823	.761
	10	24.05	.000	211.340	1.303	-.869	184.917	.788
	11	23.58	.000	212.303	2.005	-.713	185.663	1.833

Table 16.5

Run 10

CURVE FITS FOR SMMR 37.0 GHZ TB VERSUS CELL NUMBER

			V POL.			H POL.		
BLOCK	ROW	AVERAGE LATITUDE	LINEAR TERM	CONSTANT TERM	RMS	LINEAR TERM	CONSTANT TERM	RMS
1	1	48.27	.000	209.279	8.284	.753	163.738	13.956
	2	48.05	.441	204.157	7.577	.966	161.114	13.850
	3	47.83	.315	205.309	7.037	.886	161.194	12.800
	4	47.61	.336	204.338	6.103	.834	160.827	11.328
	5	47.38	.522	202.230	6.330	1.188	156.666	11.818
	6	47.16	.558	200.806	6.053	1.299	154.464	11.000
	7	46.94	.616	200.590	6.245	1.411	152.689	11.020
	8	46.71	.690	199.126	5.986	1.432	152.059	10.663
	9	46.50	.716	198.382	6.898	1.619	148.976	11.666
	10	46.27	.818	196.659	6.779	1.698	147.096	11.868
	11	46.05	.778	195.717	5.588	1.696	145.782	10.413
	12	45.82	.765	195.695	5.089	1.561	145.649	8.680
	13	45.60	.875	193.711	5.919	1.691	143.664	9.558
	14	45.38	.955	193.037	6.825	1.914	141.051	11.463
	15	45.15	.926	193.753	6.926	1.838	141.881	11.546
	16	44.93	.820	194.803	7.435	1.708	143.462	11.784
	17	44.71	.754	195.700	7.207	1.632	143.534	11.703
	18	44.48	.674	195.825	5.625	1.420	145.589	9.700
	19	44.26	.609	196.437	4.577	1.366	145.148	7.877
	20	44.03	.517	196.435	3.427	1.290	144.463	6.525
	21	43.81	.443	196.606	2.721	1.183	144.534	4.555
	22	43.58	.441	196.384	2.537	1.098	144.995	4.623

Table 16.5 Continued

Run 10

CURVE FITS FOR SMMR 37.0 GHZ TB VERSUS CELL NUMBER

			V POL.			H POL.		
BLOCK	ROW	AVERA E LATITUDE	LINEAR TERM	CONSTANT TERM	RMS	LINEAR TERM	CONSTANT TERM	RMS
2	1	43.36	.415	196.454	2.617	1.077	144.178	4.241
	2	43.14	.392	196.088	2.368	.998	144.075	4.678
	3	42.91	.352	195.690	2.462	.942	143.059	4.296
	4	42.68	.362	195.218	1.959	.933	142.173	3.468
	5	42.46	.310	195.347	2.136	.889	142.081	3.161
	6	42.23	.267	195.814	2.260	.812	142.794	3.973
	7	42.01	.247	196.137	2.298	.732	143.686	4.315
	8	41.78	.220	196.593	2.740	.732	143.816	4.719
	9	41.56	.230	196.153	2.312	.760	142.779	4.531
	10	41.33	.312	195.342	2.483	.804	142.212	5.035
	11	41.11	.217	196.215	2.574	.815	142.197	4.769
	12	40.88	.141	196.534	1.975	.527	143.516	3.591
	13	40.65	.104	197.169	2.167	.458	144.205	3.483
	14	40.43	.000	198.453	2.391	.349	145.371	3.667
	15	40.20	.000	198.598	2.821	.279	146.805	4.783
	16	39.97	.000	198.930	2.476	.392	146.051	5.476
	17	39.75	.173	197.073	2.881	.465	145.848	4.951
	18	39.52	.124	197.536	2.767	.362	146.648	5.615
	19	39.29	.000	198.896	2.779	.326	146.781	5.571
	20	39.07	.133	197.837	2.722	.419	145.631	5.544
	21	38.84	.187	197.144	2.915	.516	144.674	5.614
	22	38.61	.000	199.175	2.705	.388	145.724	5.483

Table 16.5 Continued

Run 10

CURVE FITS FOR SMMR 37.0 GHZ TB VERSUS CELL NUMBER

			V POL.			H POL.		
BLOCK	ROW	AVERAGE LATITUDE	LINEAR TERM	CONSTANT TERM	RMS	LINEAR TERM	CONSTANT TERM	RMS
3	1	38.39	.148	198.439	2.888	.476	146.378	5.332
	2	38.16	.000	200.660	2.551	.407	147.041	4.252
	3	37.93	.125	200.955	2.840	.494	148.173	5.103
	4	37.70	.000	203.023	4.255	.555	149.313	6.343
	5	37.48	.000	201.463	3.874	.529	146.578	5.385
	6	37.25	.132	198.893	3.225	.518	144.742	4.718
	7	37.02	.161	199.185	3.179	.628	144.069	5.022
	8	36.79	.311	197.208	3.335	.741	142.531	5.032
	9	36.56	.224	197.221	3.322	.637	142.277	4.734
	10	36.34	.187	196.412	2.664	.532	141.352	4.157
	11	36.11	.162	195.834	2.789	.492	140.331	4.914
	12	35.88	.320	193.707	2.279	.593	137.687	4.106
	13	35.65	.333	193.100	1.650	.622	137.039	2.975
	14	35.43	.355	192.647	1.006	.558	137.415	1.891
	15	35.20	.281	193.143	1.529	.630	136.927	2.256
	16	34.97	.332	192.909	1.322	.617	137.210	3.016
	17	34.74	.382	191.636	1.822	.615	137.523	3.280
	18	34.51	.373	192.177	2.418	.554	139.216	4.230
	19	34.28	.324	192.661	2.429	.549	139.938	4.778
	20	34.05	.259	193.475	2.164	.449	141.479	4.204
	21	33.82	.142	194.343	1.934	.280	143.630	3.465
	22	33.59	.184	194.372	2.408	.335	142.939	4.004

Table 16.5 Continued

Run 10

CURVE FITS FOR SMMR 37.0 GHZ TB VERSUS CELL NUMBER

BLOCK	ROW	AVERAGE LATITUDE	V POL. LINEAR TERM	V POL. CONSTANT TERM	V POL. RMS	H POL. LINEAR TERM	H POL. CONSTANT TERM	H POL. RMS
4	1	33.37	.000	196.361	1.964	.204	144.748	4.051
	2	33.14	.000	196.350	2.234	.153	145.452	3.837
	3	32.91	.000	197.232	2.457	.000	148.551	4.901
	4	32.68	.000	197.448	2.627	.000	149.621	4.879
	5	32.45	-.090	198.716	2.231	.000	149.300	4.654
	6	32.22	-.098	198.442	1.875	-.164	151.368	3.607
	7	31.99	-.101	198.508	1.676	-.109	151.444	2.997
	8	31.76	-.127	198.352	1.087	-.152	151.673	2.398
	9	31.53	-.385	203.113	2.068	-.601	159.427	4.059
	10	31.30	-.487	204.773	2.697	-.662	160.974	4.927
	11	31.07	-.228	200.499	3.162	-.312	155.379	5.166
	12	30.84	.000	198.205	2.740	.000	152.078	4.588
	13	30.61	.081	197.318	2.167	.274	148.673	4.529
	14	30.38	.000	198.067	2.313	.178	149.796	3.733
	15	30.15	.000	198.005	1.487	.000	152.069	2.450
	16	29.92	-.113	199.432	1.330	-.129	153.558	2.429
	17	29.69	-.214	201.329	1.237	-.302	156.678	2.725
	18	29.46	-.530	206.508	3.907	-.813	166.465	6.951
	19	29.23	-.292	205.112	4.269	-.513	165.307	7.425
	20	29.00	.151	200.544	3.408	.263	156.270	6.182
	21	28.77	.492	197.868	3.330	.948	150.809	6.099
	22	28.54	.227	201.695	2.606	.527	157.158	3.913

Table 16.5 Continued

Run 10

CURVE FITS FOR SMMR 37.0 GHZ TB VERSUS CELL NUMBER

BLOCK	ROW	AVERAGE LATITUDE	V POL. LINEAR TERM	V POL. CONSTANT TERM	V POL. RMS	H POL. LINEAR TERM	H POL. CONSTANT TERM	H POL. RMS
5	1	28.31	.000	206.410	4.027	.000	166.815	6.461
	2	28.08	.000	207.165	4.024	.000	169.354	7.413
	3	27.85	.000	207.101	3.100	.187	165.870	4.749
	4	27.62	.207	204.221	2.900	.343	162.486	4.856
	5	27.39	.000	206.520	2.885	.000	166.767	5.343
	6	27.16	.000	207.626	4.998	.000	168.911	7.685
	7	26.93	.000	207.475	4.413	.000	169.349	6.879
	8	26.70	.148	205.752	4.076	.274	165.314	5.956
	9	26.47	.000	207.155	4.057	.000	167.880	6.802
	10	26.24	.000	205.054	3.251	.000	164.414	5.201
	11	26.01	.000	204.522	2.651	.000	163.571	4.240
	12	25.78	-.144	206.098	2.622	.000	163.437	4.495
	13	25.55	-.199	207.216	2.196	-.361	168.382	3.802
	14	25.32	-.244	208.708	1.928	-.357	169.451	2.568
	15	25.08	-.079	207.181	1.934	.000	165.705	3.234
	16	24.85	-.202	207.916	1.982	-.202	166.965	3.481
	17	24.62	-.262	208.116	1.828	-.277	167.613	2.910
	18	24.39	-.273	209.550	2.220	-.248	169.098	3.233
	19	24.16	-.210	209.148	2.047	-.312	169.802	3.168
	20	23.93	-.430	212.034	2.027	-.584	174.090	2.736
	21	23.70	-.479	213.998	2.041	-.743	177.900	3.523
	22	23.47	-.257	211.304	4.099	-.429	174.727	6.817

Figure 16.1

Run 10

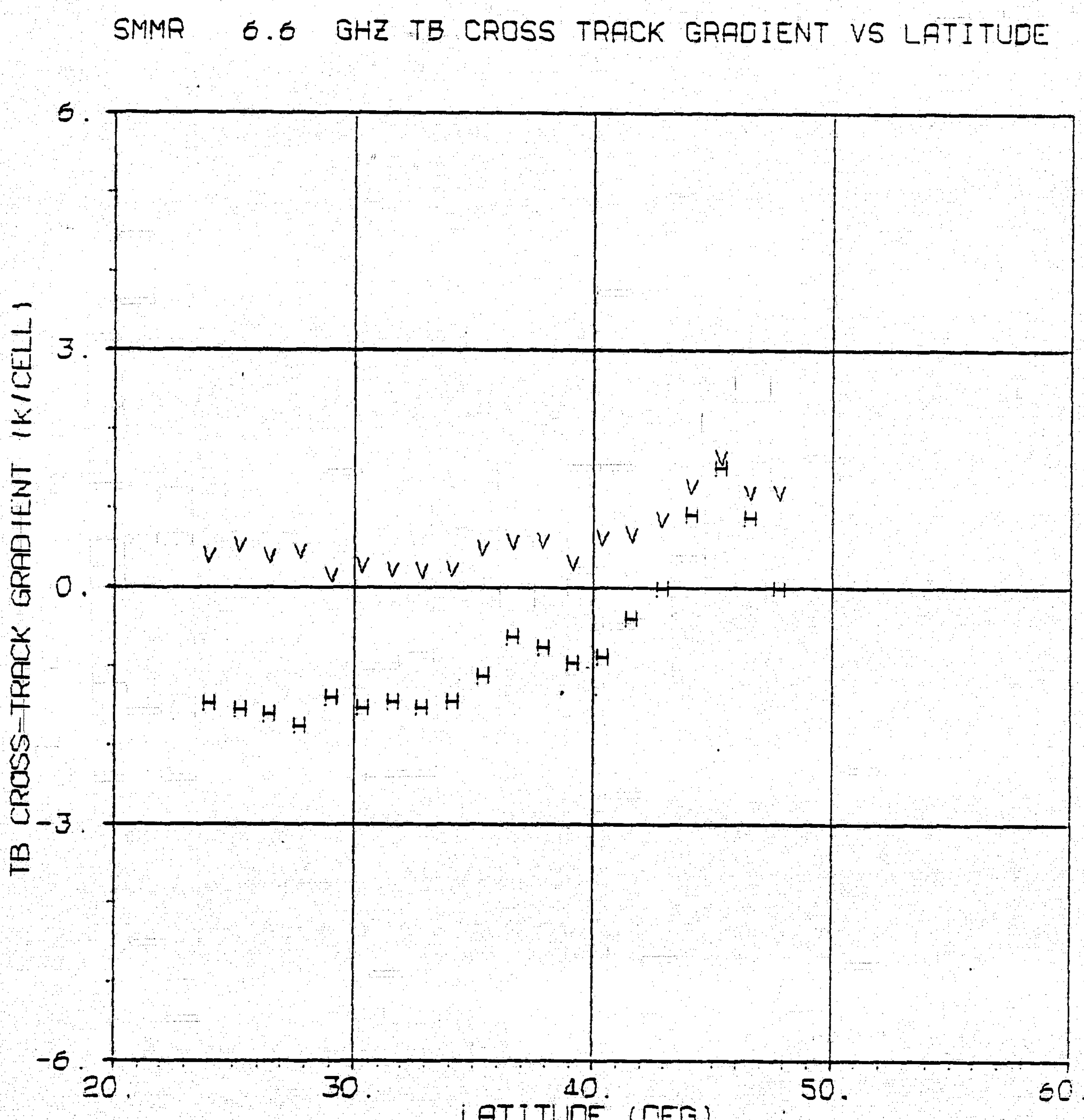

Figure 16.2

Run 10

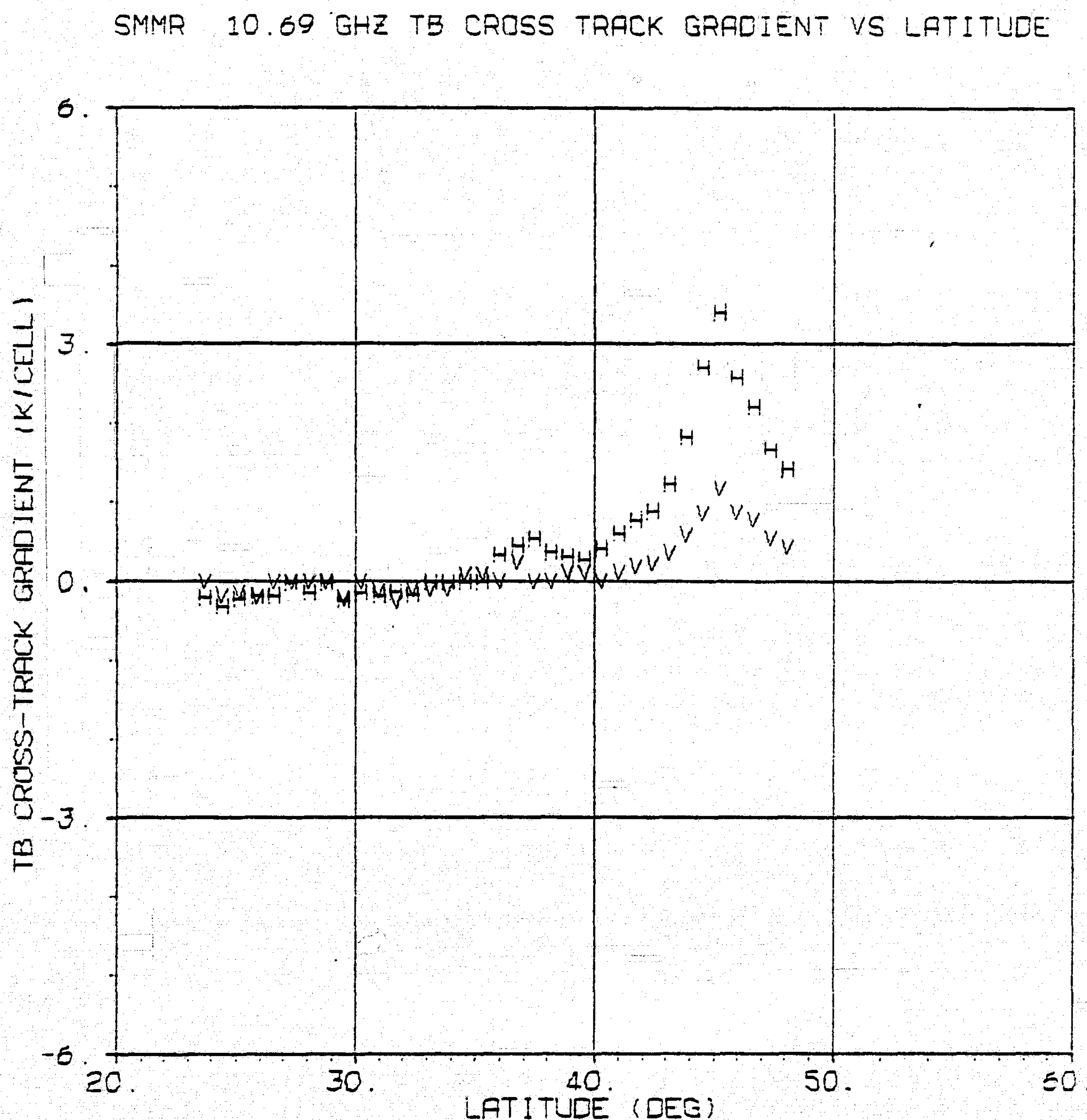

Figure 16.3

Run 10

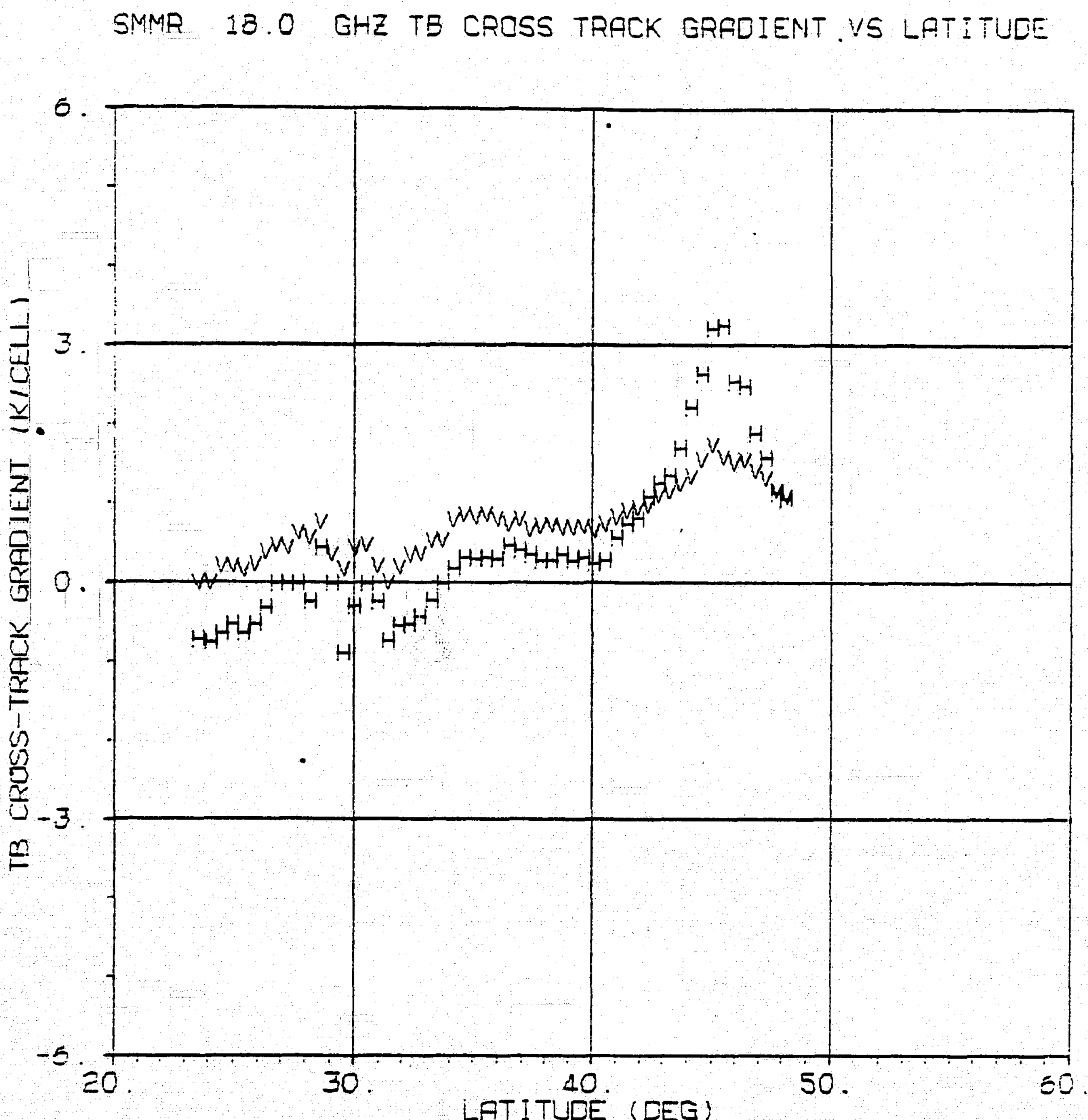

Figure 16.4

Run 10

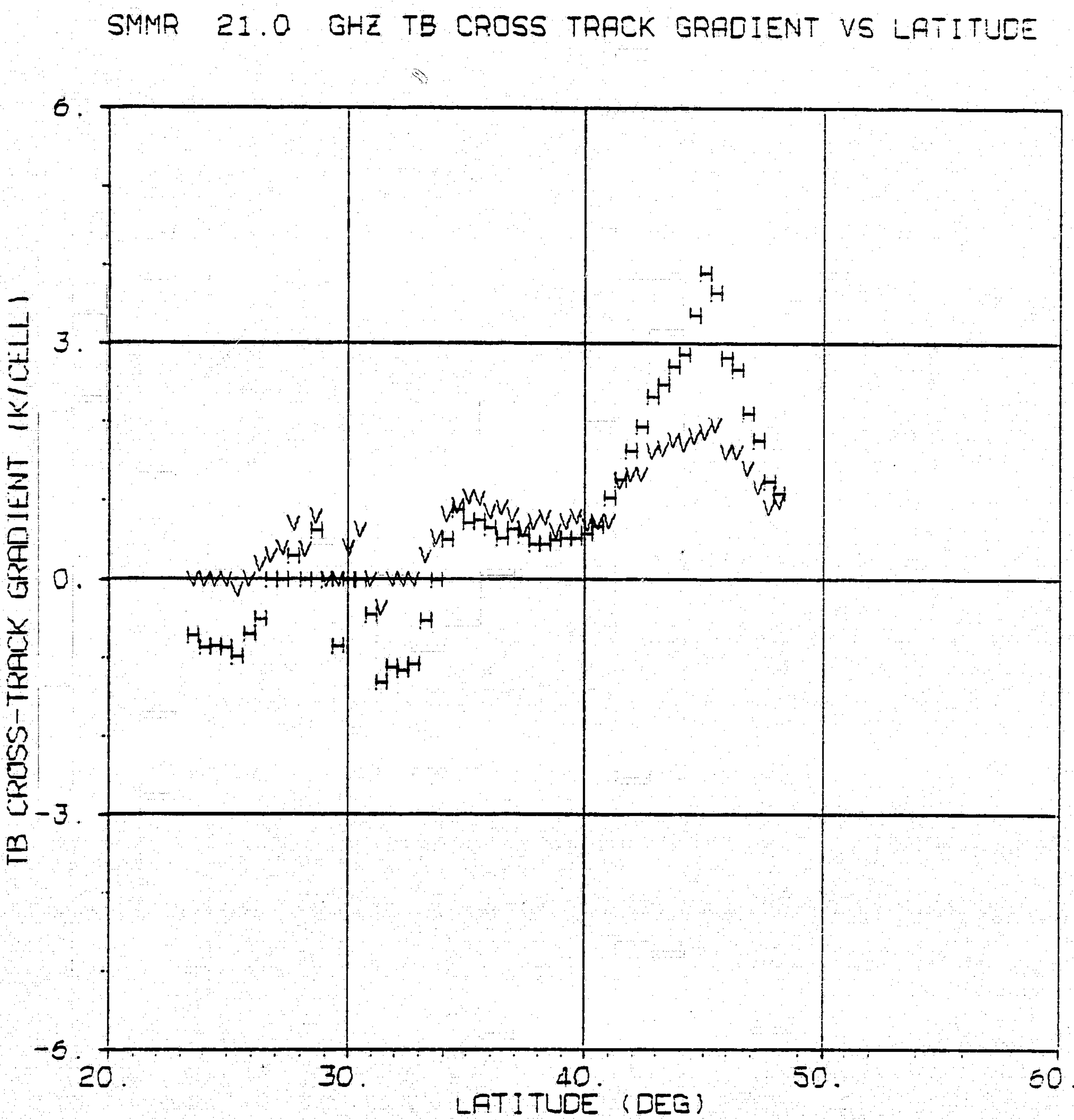

Figure 16.5

Run 10

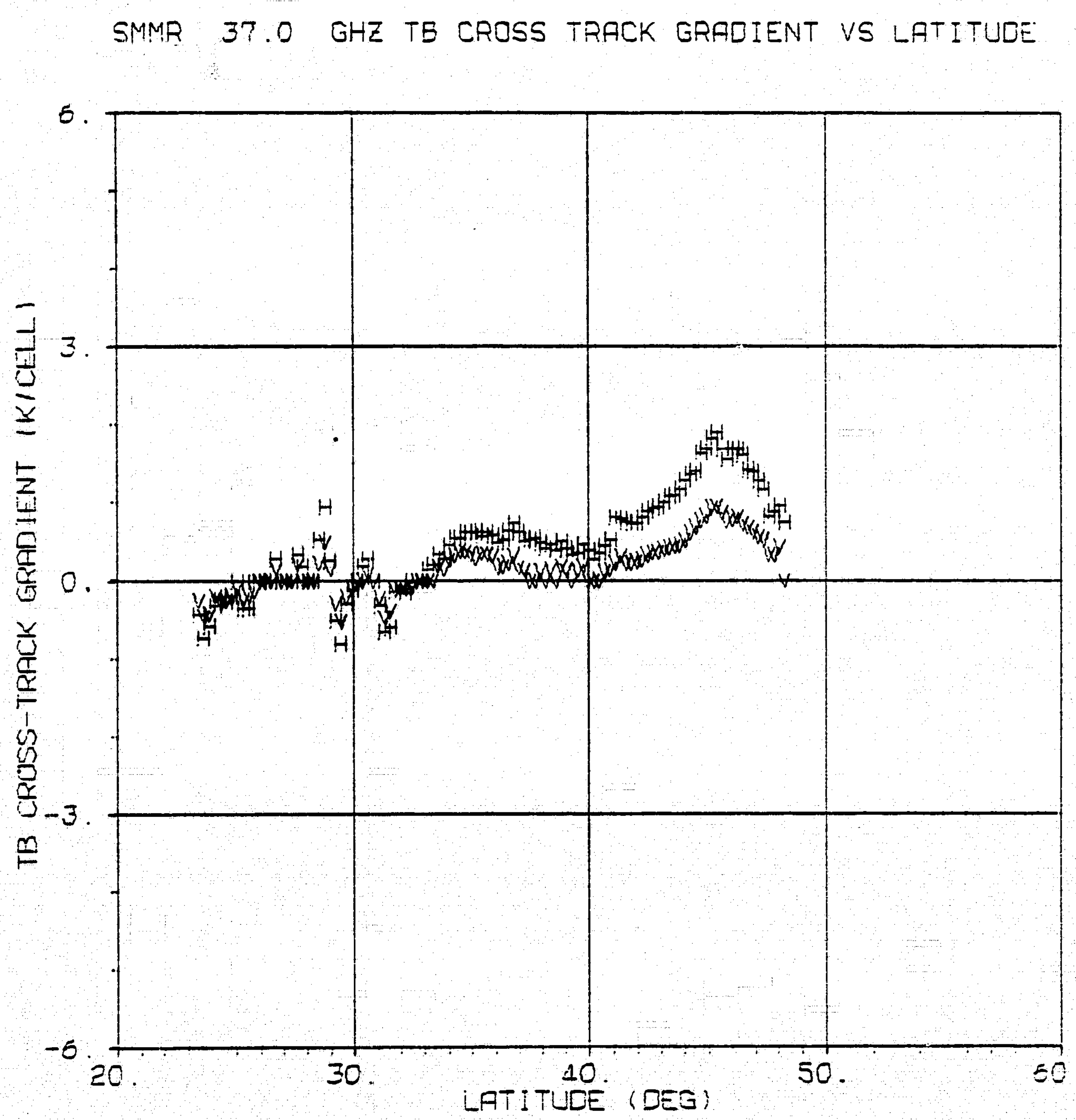

Table 17

Run 11

CURVE FITS FOR SMMR 6.6 GHZ TB VERSUS CELL NUMBER

			V POL.			H POL.		
BLOCK	ROW	AVERAGE LATITUDE	LINEAR TERM	CONSTANT TERM	RMS	LINEAR TERM	CONSTANT TERM	RMS
1	1	26.88	.666	151.335	.063	-.698	88.755	.060
	2	25.62	.732	151.530	.526	-.859	88.910	.276
	3	24.35	.800	151.070	.187	-.880	88.515	.325
	4	23.08	.421	151.[illegible]	.193	-.899	88.935	.307
2	1	21.80	.412	152.[illegible]	.405	-.843	89.395	.726
	2	20.53	.517	152.[illegible]	.288	-1.265	91.315	.580
	3	19.25	.138	154.[illegible]	.158	-1.395	92.065	.466
	4	17.98	.000	155.237	.224	-1.776	93.975	.221
3	1	16.71	.000	156.070	.093	-2.281	95.755	.218
	2	15.43	.000	156.827	.227	-2.895	98.020	.269
	3	14.15	.000	157.455	1.442	-2.724	97.740	1.851
	4	12.88	.000	158.610	2.889	-3.629	102.115	4.514
4	1	11.60	.000	158.187	1.615	-2.461	98.130	2.215
	2	10.32	-.341	158.460	.430	-3.809	100.945	.827
	3	9.05	.337	155.810	.271	-2.349	95.875	.812
	4	7.77	1.150	153.405	.151	-.875	91.995	.099
5	1	6.49	1.108	152.800	.045	-.686	90.365	.392
	2	5.22	1.248	151.555	.380	-.429	88.670	.630
	3	3.94	1.257	150.640	.391	-.690	88.575	.457
	4	2.66	1.055	150.145	.167	-.723	87.860	.048
6	1	1.39	1.102	150.010	.165	-.921	88.530	.198
	2	.12	.725	150.715	.090	-1.326	89.495	.166
	3	-1.15	.000	152.670	.405	-1.620	90.170	.321
	4	-2.43	.000	152.855	.518	-1.489	89.915	.478
7	1	-3.70	.400	151.945	.160	-1.234	89.285	.385
	2	-4.98	.371	152.135	.245	-1.397	89.940	.354
	3	-6.25	.479	151.885	.090	-1.373	89.610	.367
	4	-7.52	.405	152.355	.243	-1.271	89.400	.300
8	1	-8.80	.605	151.795	.038	-1.210	89.560	.329
	2	-10.07	.645	151.800	.062	-.982	89.000	.200
	3	-11.34	1.195	150.660	.146	-.706	88.390	.233
	4	-12.61	1.002	150.955	.277	-.693	88.105	.138

Figure 17.1

Run 11

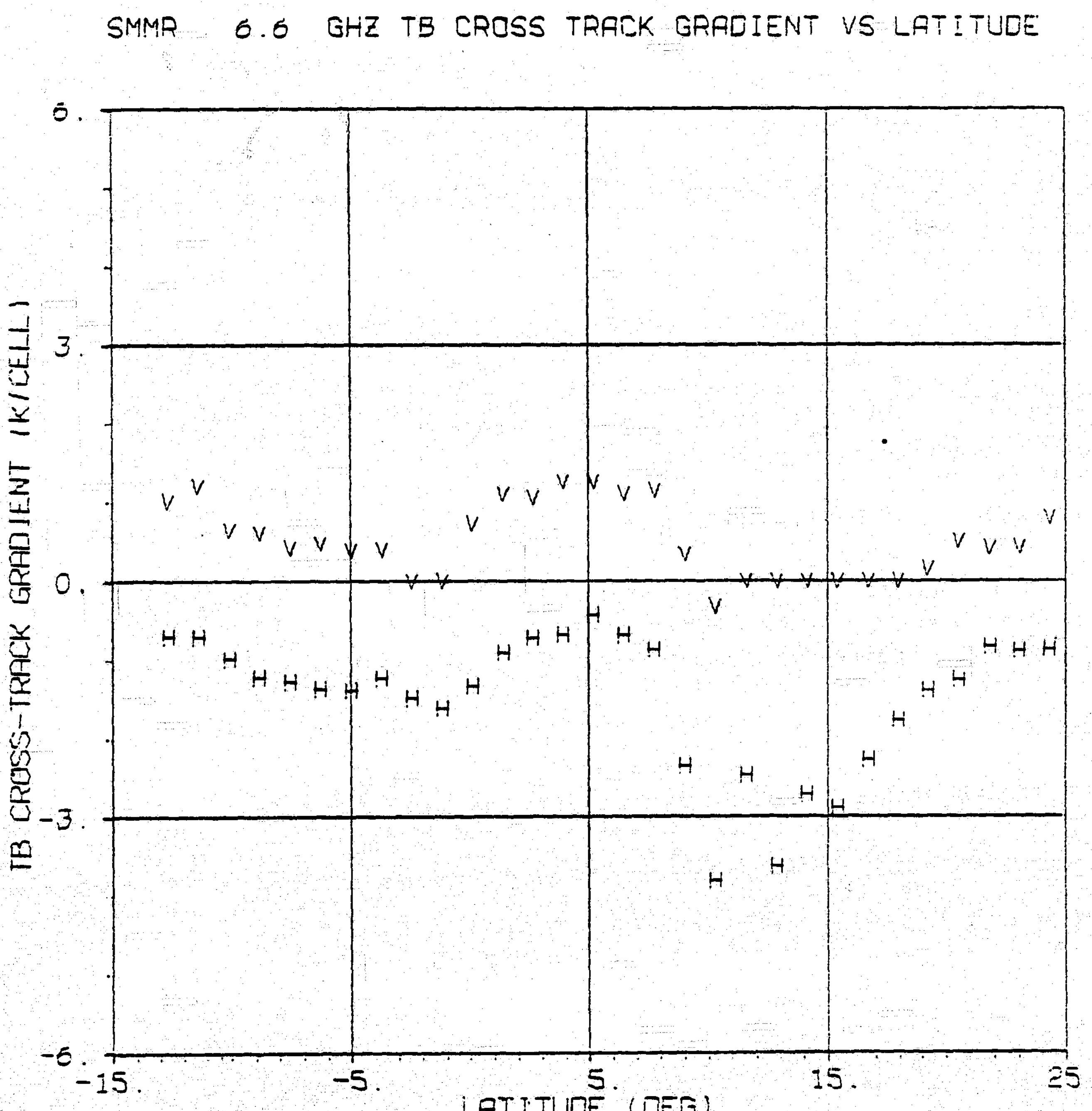

Figure 17.2

Run 11

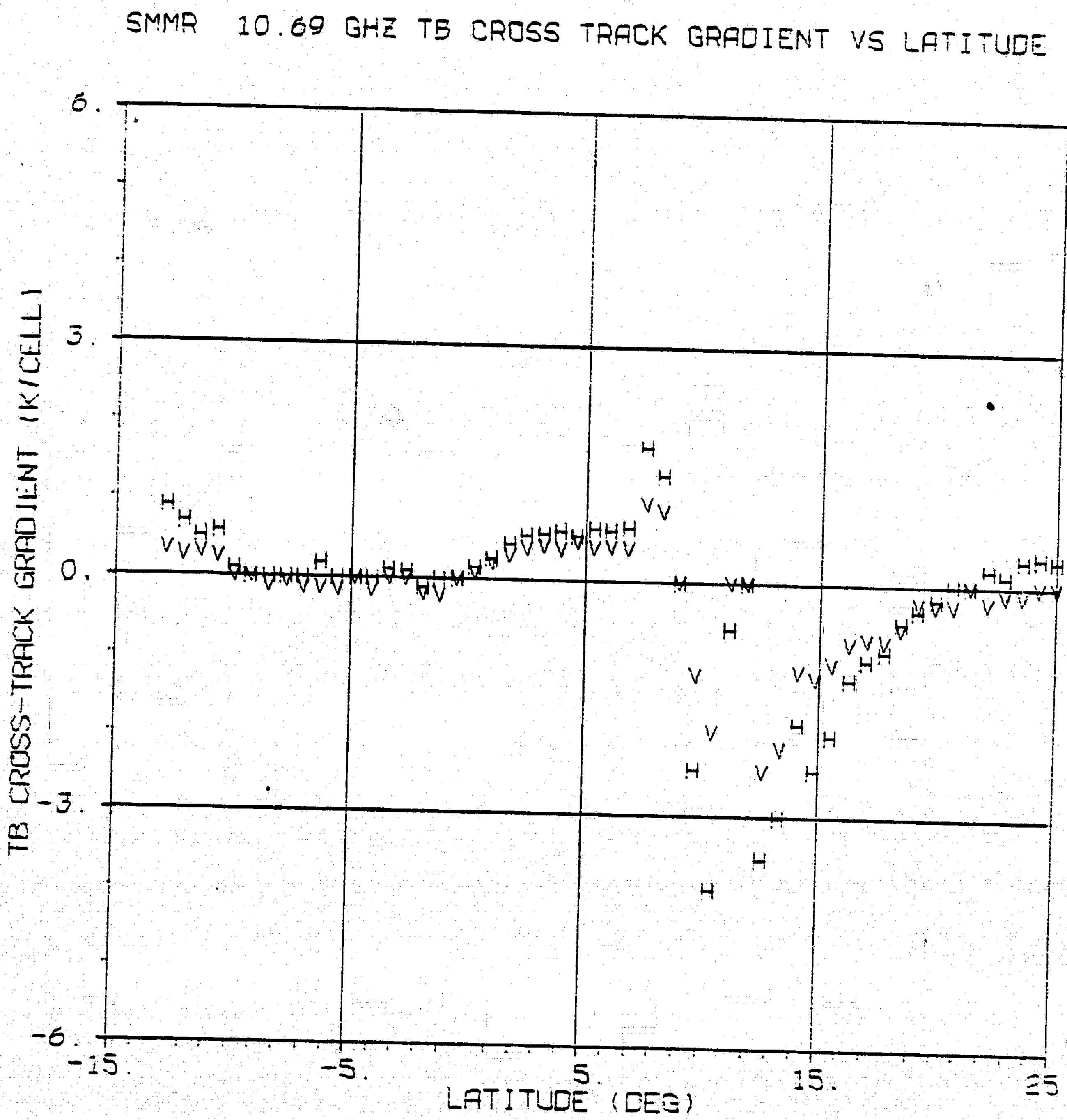

Figure 17.3

Run 11

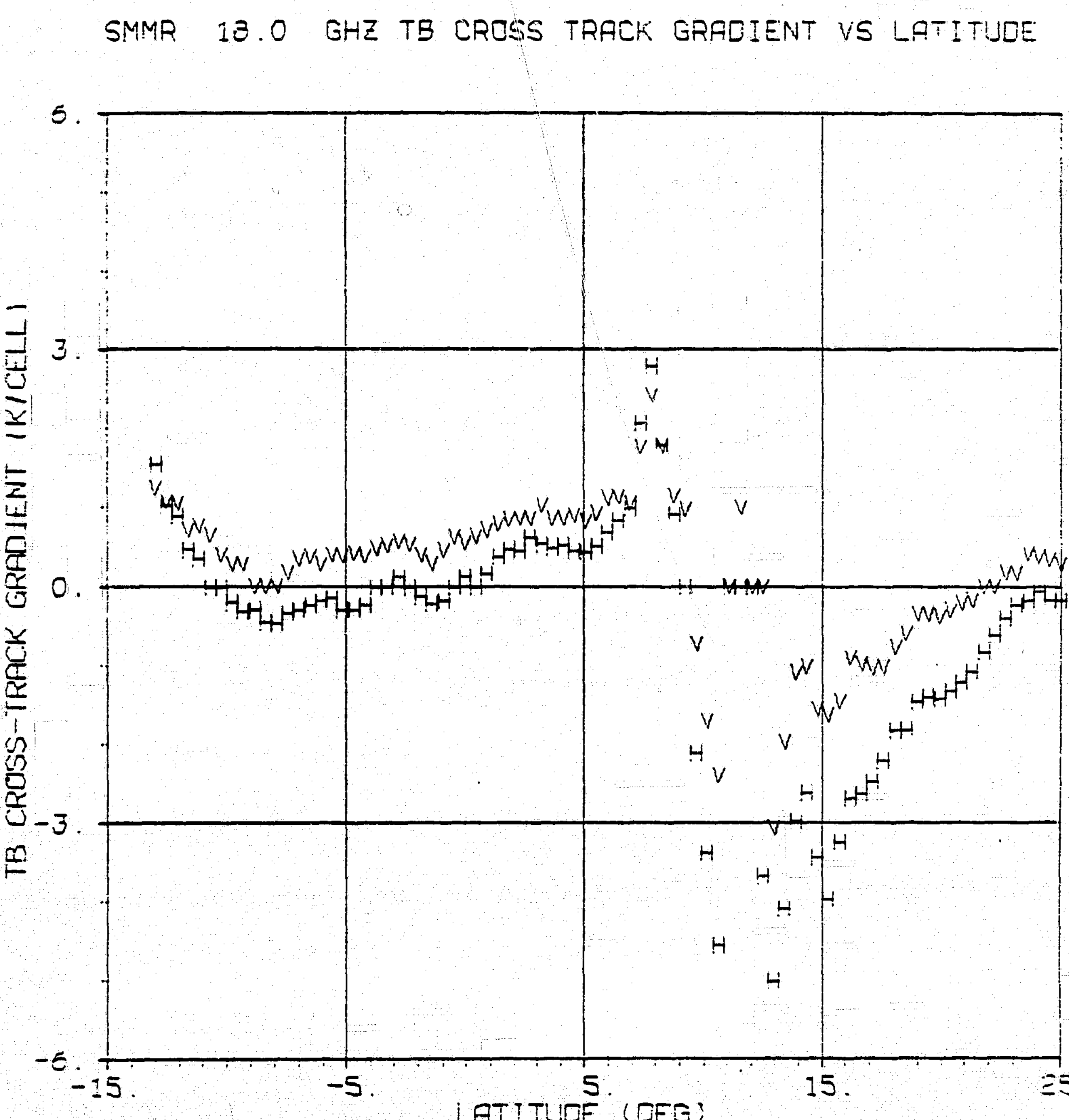

Figure 17.4

Run 11

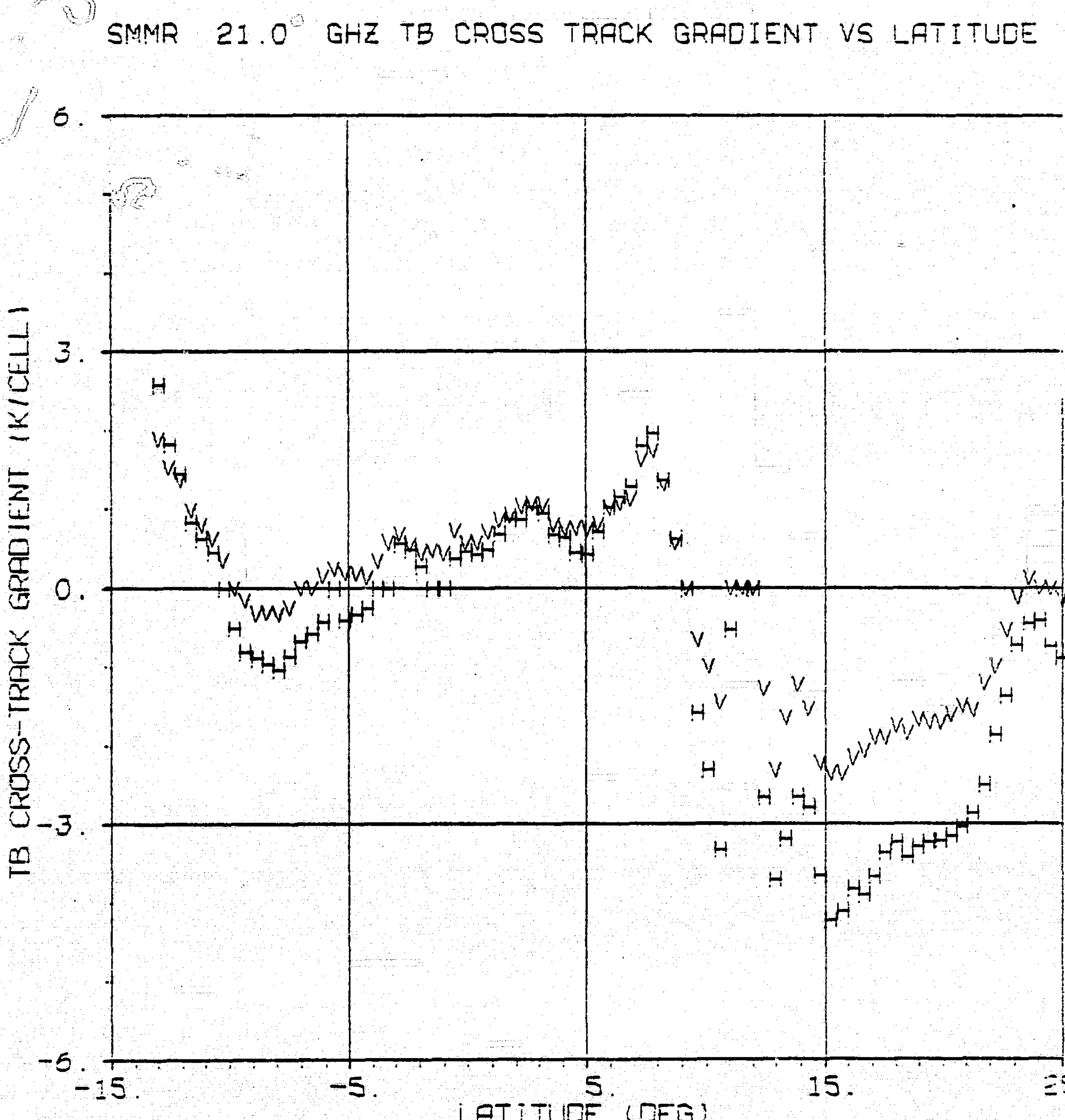

Figure 17.5

Run 11

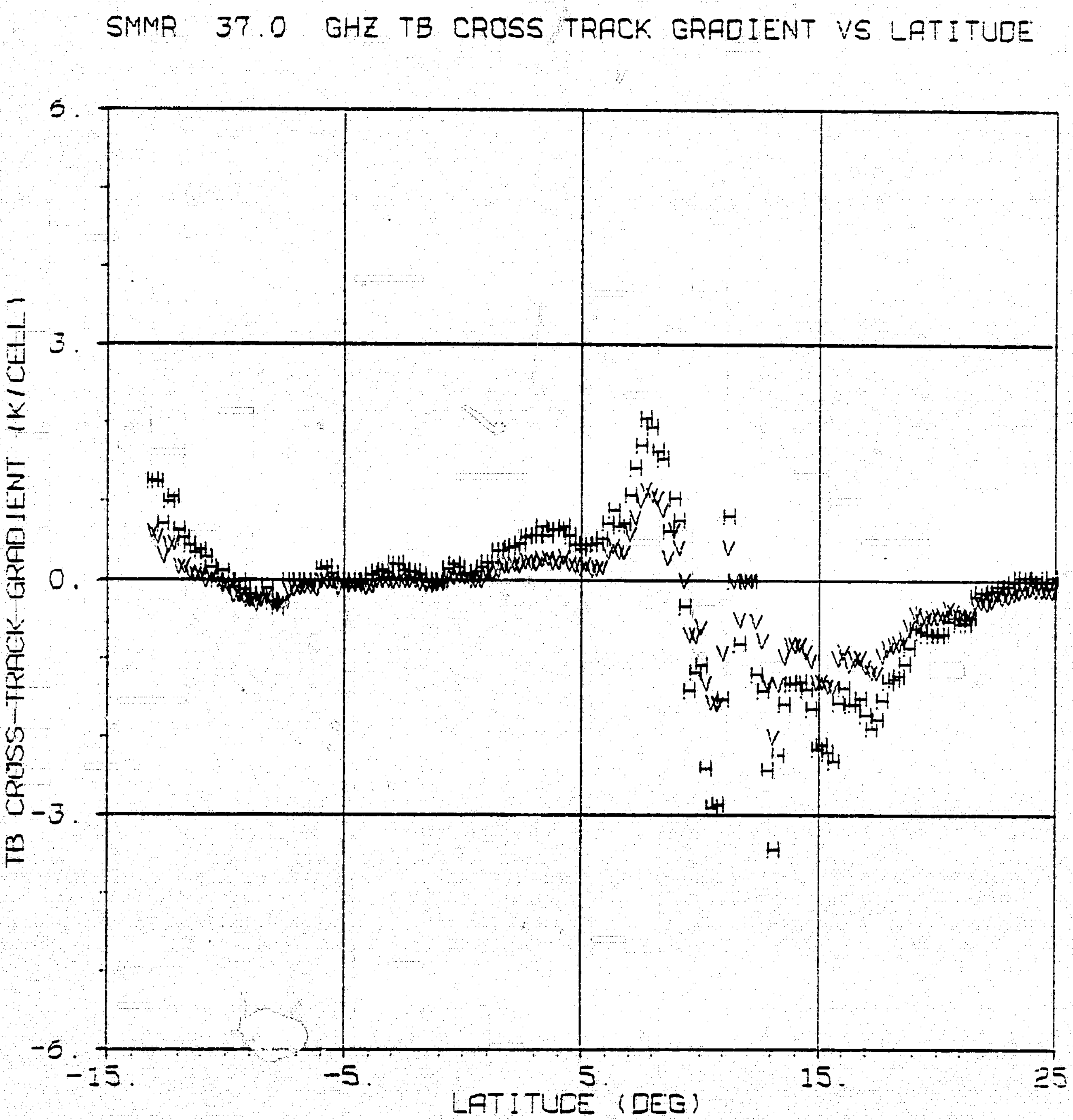

Table 18

Run 12

CURVE FITS FOR SMMR 6.6 GHZ TB VERSUS CELL NUMBER

			V POL.			H POL.		
BLOCK	ROW	AVERAGE LATITUDE	LINEAR TERM	CONSTANT TERM	RMS	LINEAR TERM	CONSTANT TERM	RMS
1	1	-13.22	.190	155.650	.160	-1.208	93.115	.557
	2	-11.95	.264	155.665	.202	-1.227	93.045	.409
	3	-10.68	.000	156.362	.059	-1.173	92.905	.358
	4	-9.41	.124	155.640	.170	-1.122	92.040	.400
2	1	-8.13	.217	155.025	.218	-1.147	91.715	.548
	2	-6.86	.157	154.770	.244	-1.132	91.250	.494
	3	-5.59	.000	154.640	.430	-1.264	91.035	.635
	4	-4.32	.000	154.592	.209	-1.195	90.695	.378
3	1	-3.04	.000	154.445	.208	-1.192	90.625	.335
	2	-1.77	-.237	154.695	.368	-1.249	90.270	.150
	3	-.49	.000	153.760	.100	-1.189	89.965	.280
	4	.78	.369	153.160	.280	-.855	89.305	.380
4	1	2.05	.000	155.340	.650	-.837	90.210	.566
	2	3.33	.736	154.655	.327	-.975	91.785	.658
	3	4.60	.405	156.010	.108	-.971	92.045	.307
	4	5.88	.618	156.410	.186	-.974	93.000	.079
5	1	7.16	.414	157.590	.151	-1.064	93.910	.324
	2	8.44	.000	159.720	.260	-1.720	97.645	.402
	3	9.71	.347	159.270	.441	-.957	96.785	.587
	4	10.99	.000	160.030	.510	-2.681	100.955	1.179
6	1	12.27	.000	159.742	1.086	-3.838	102.945	1.155
	2	13.54	.862	156.390	.390	-.993	94.265	.577
	3	14.82	1.215	155.940	.192	.252	92.025	.388
	4	16.10	1.068	155.850	.196	.000	91.962	.282
7	1	17.37	.798	156.500	.299	-.575	92.765	.472
	2	18.64	1.282	154.240	.249	-.674	91.750	.187
	3	19.92	.841	154.915	.139	-.571	91.240	.191
	4	21.19	.684	155.065	.148	-.378	91.465	.413

Figure 18.1

Run 12

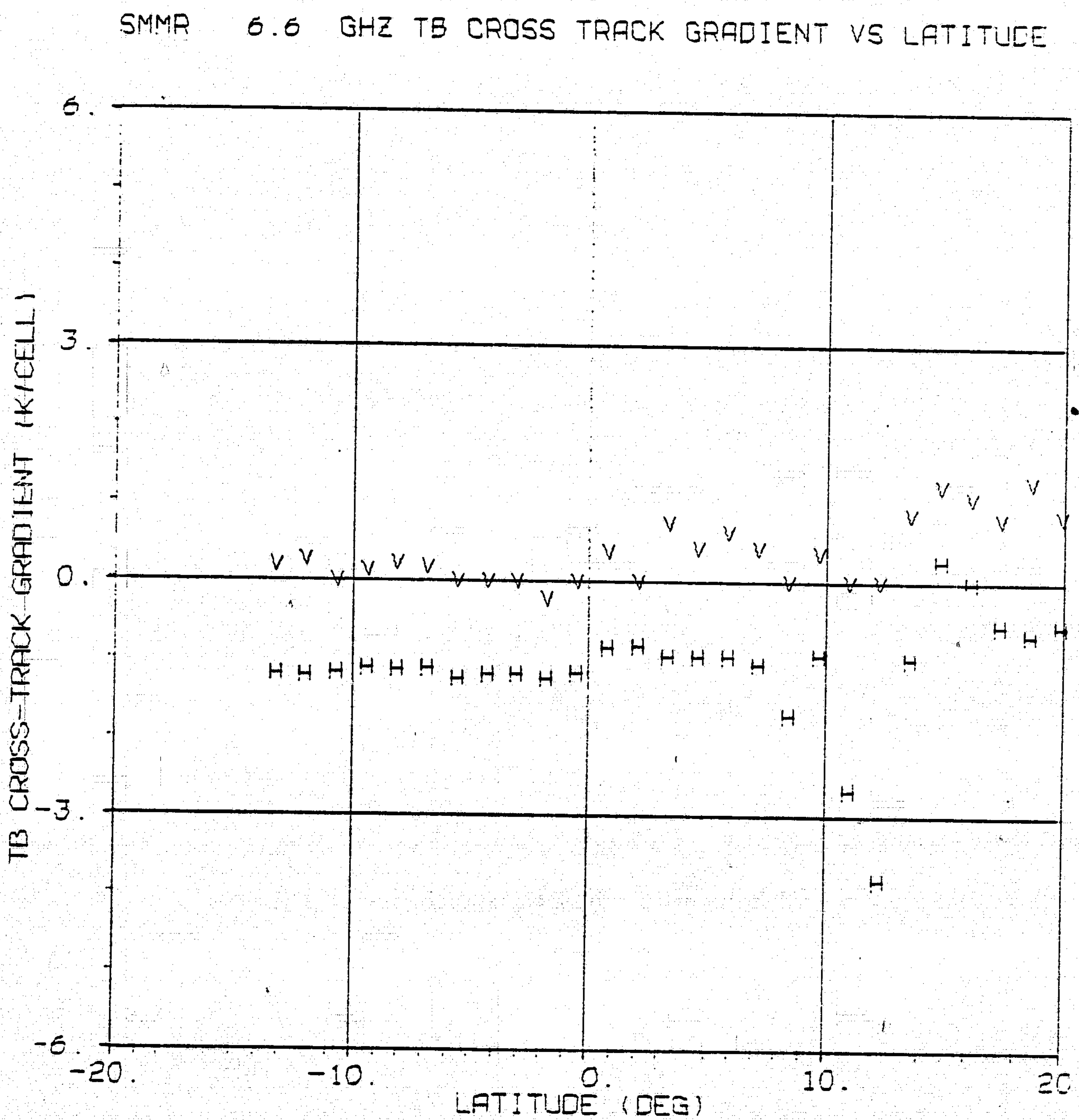

Figure 18.2

Run 12

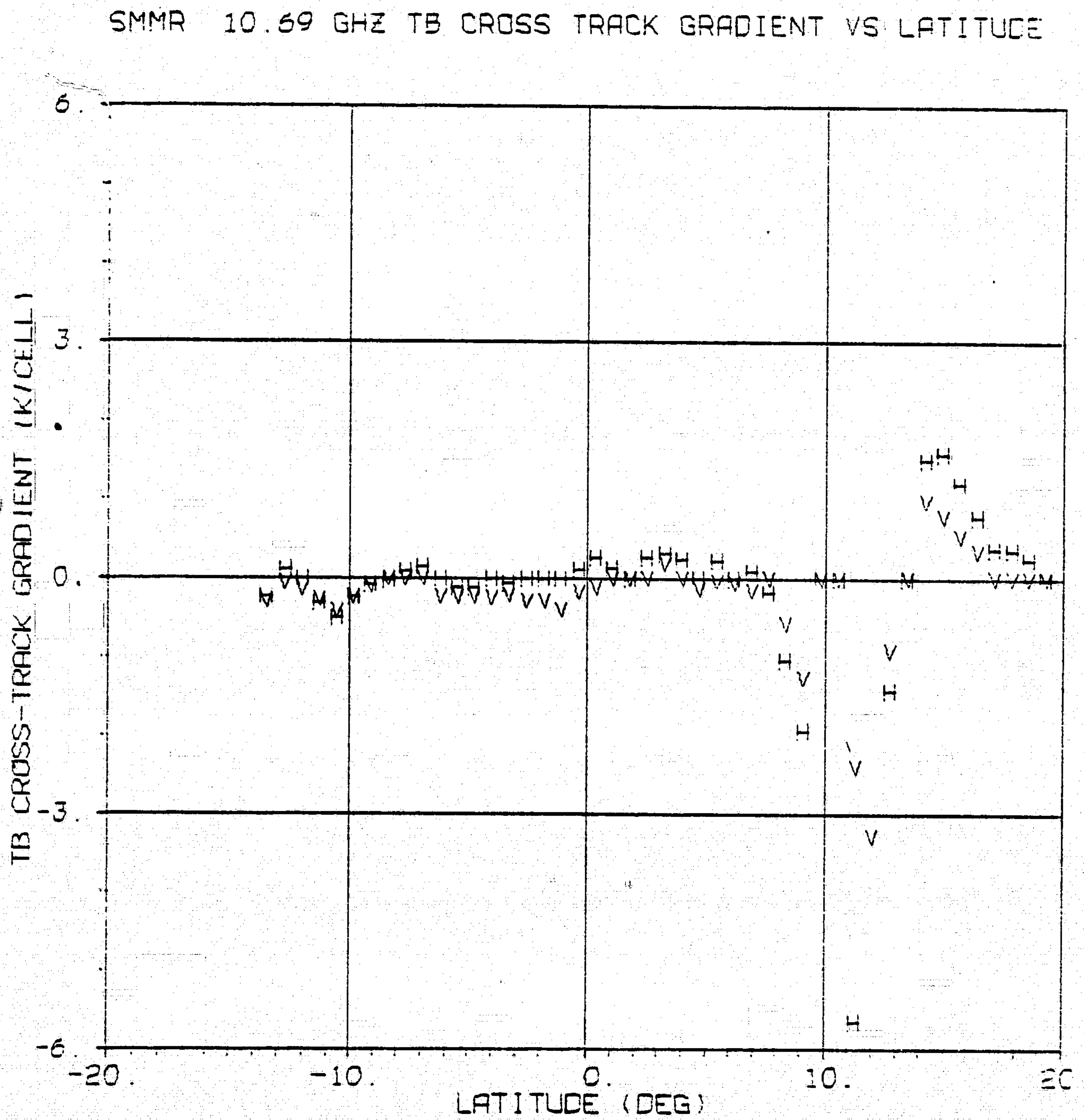

Figure 18.3

Run 12

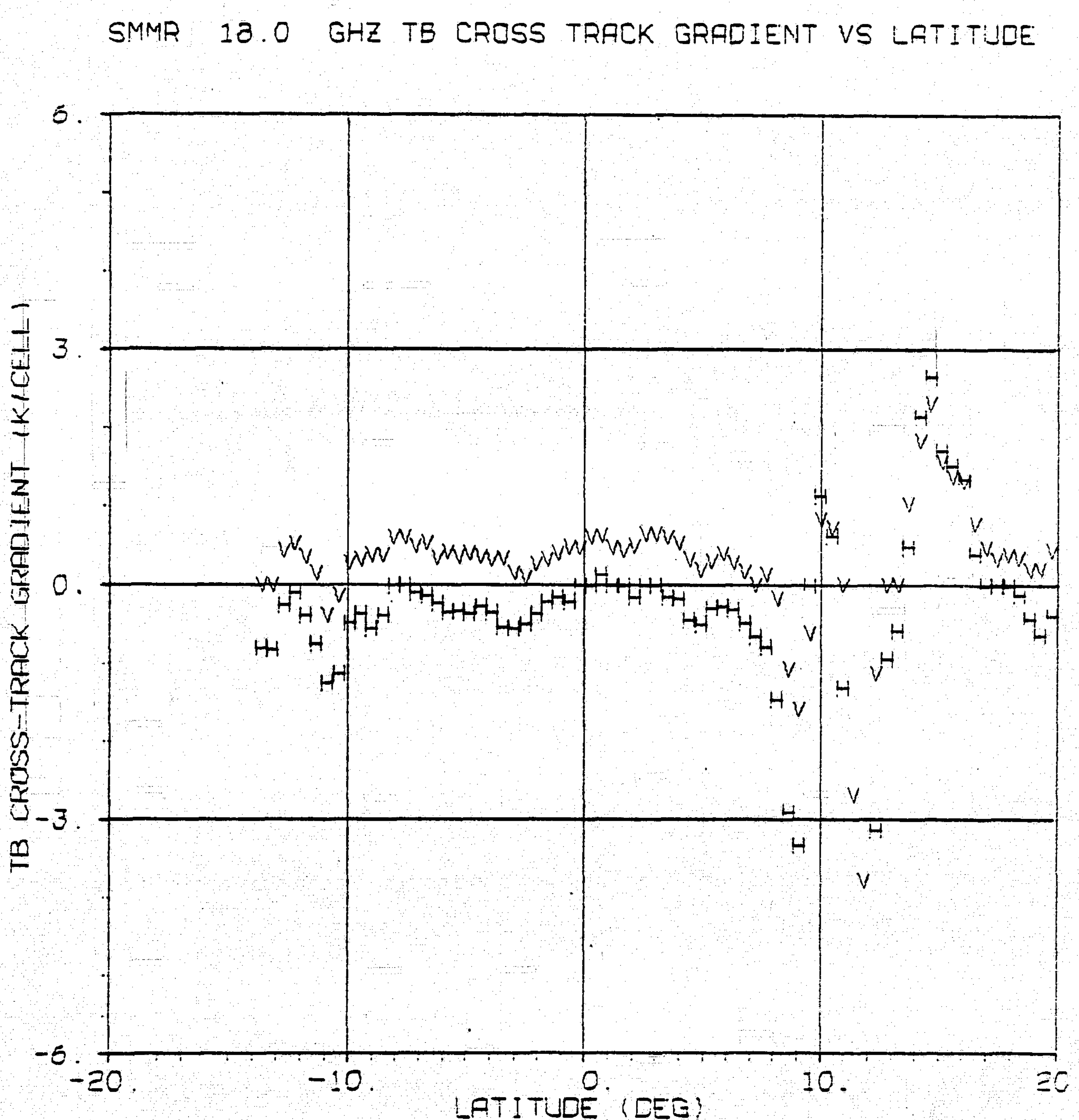

Figure 18.4

Run 12

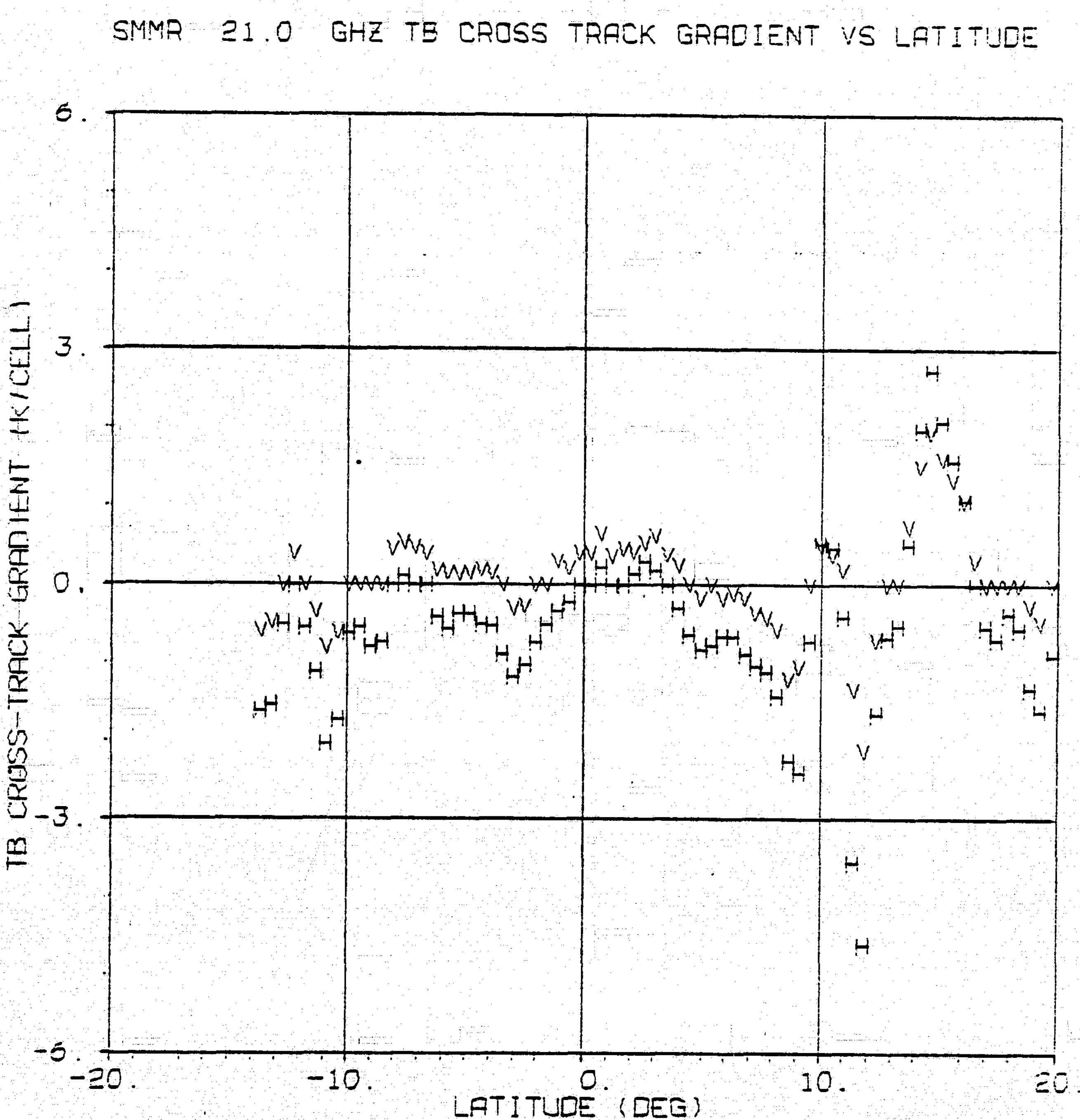

Figure 18.5

Run 12

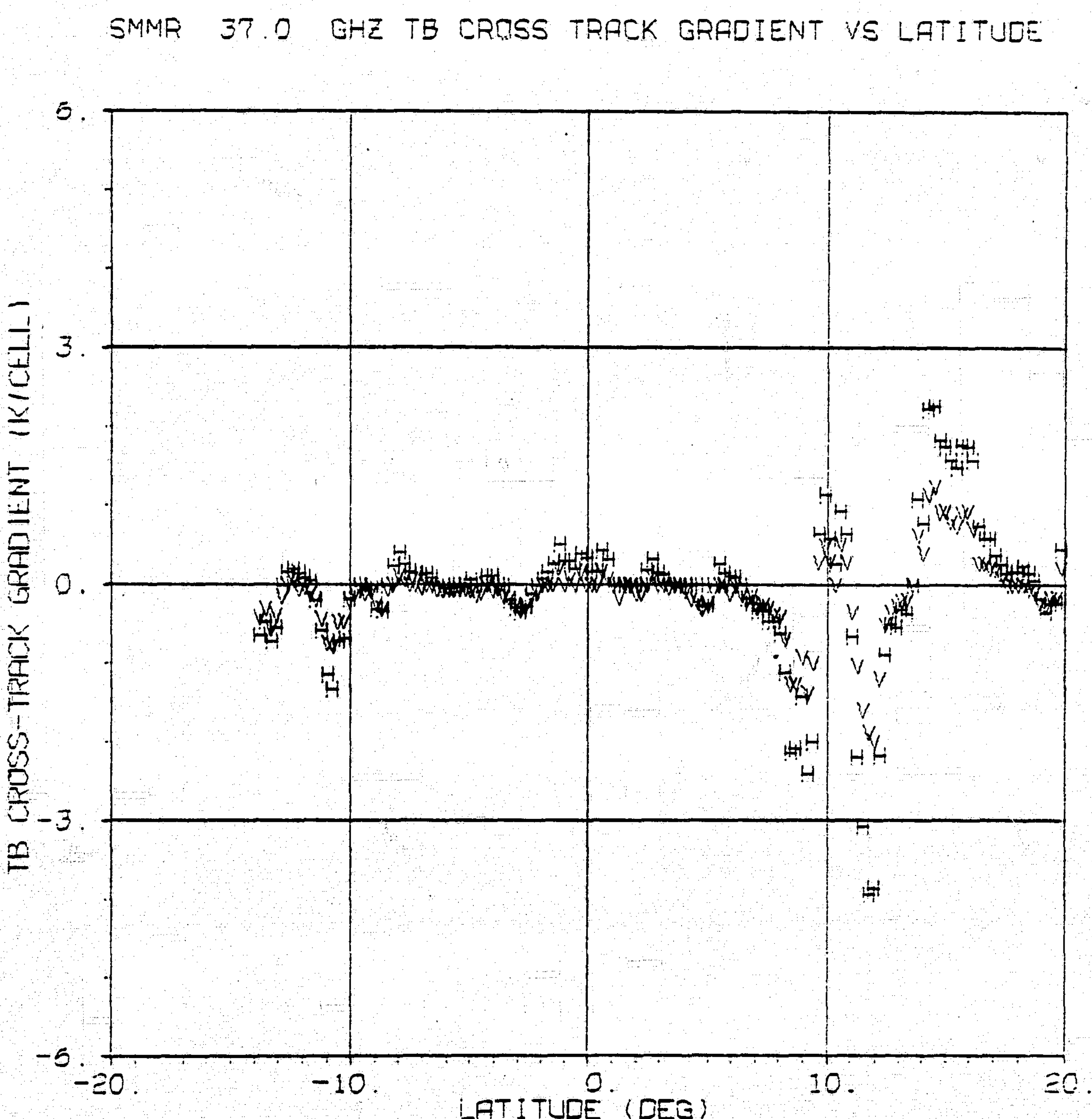

Table 19.1. Mean Cross-Track Gradient Values

		Orbit 1198, -10^o to 0^o Latitude			Orbit 1255, -25^o to -5^o Latitude		
		Mean Slope (K/cell)	Std. Dev. of Slope (K/cell)	Total Variation Across Swath (K)	Mean Slope (K/cell)	Std. Dev. of Slope (K/cell)	Total Variation Across Swath (K)
6.6	V	0.03	0.14	0.12	-0.07	0.10	-0.28
6.6	H	-1.19	0.05	-4.76	-1.20	0.16	-4.80
10.69	V	-0.19	0.12	-1.33	-0.30	0.11	-2.10
10.69	H	-0.02	0.10	-0.14	-0.09	0.13	-0.63
18	V	0.37	0.12	4.07	0.27	0.16	2.97
18	H	-0.30	0.18	-3.30	-0.42	0.23	-4.62
21	V	0.14	0.22	1.54	-0.02	0.25	-0.22
21	H	- 0.47	0.35	-5.17	-0.67	0.38	-7.37
37	V	-0.07	0.12	-1.54	-0.17	0.17	-3.74
37	H	0.05	0.20	1.10	-0.11	0.29	-2.42

Table 19.2. Day/Night Cross-Track Gradient Variations

	Descending (local night)		Ascending (local day)	
Latitude Range:	Orbit 1205 -5° to -10°	Orbit 1206 25° to 30°	Orbit 1198 -10° to 0°	Orbit 1255 -25° to -5°
6.6 V Mean Slope (K/cell)	0.50	0.36	0.03	-0.07
6.6 V Std. Dev. of Slope (K/cell)	0.12	0.15	0.14	0.10
6.6 V Total Variation Across Swath (K)	2.00	1.44	0.12	-0.28
6.6 H Mean Slope (K/cell)	-1.25	-1.57	-1.19	-1.20
6.6 H Std. Dev. of Slope (K/cell)	0.17	0.13	0.05	0.16
6.6 H Total Variation Across Swath (K)	-5.00	-6.28	-4.76	-4.80
Difference between V and H Total Variations (K)	7.00	7.72	4.88	4.52